MARITIME TECHNOLOGY MONOGRAPH

No. 4

The NPL High Speed Round Bilge Displacement Hull Series

by D. Bailey, M.R.I.N.A.

The Royal Institution of Naval Architects

THE NPL HIGH SPEED ROUND BILGE DISPLACEMENT HULL SERIES

Resistance, Propulsion, Manoeuvring and Seakeeping Data

by

D. Bailey, C.Eng. (Member)

National Maritime Institute
(formerly Ship Division, National Physical Laboratory)

CONTENTS

	Page No.
SUMMARY	1
INTRODUCTION	1
THE MODEL SERIES	2
MODEL CONSTRUCTION	3
ARRANGEMENT OF THE MODEL EXPERIMENTS	3
PRESENTATION AND DISCUSSION OF RESULTS	6
FURTHER WORK	12
ACKNOWLEDGEMENTS	12
NOMENCLATURE	13
REFERENCES	15
APPENDICES	16

SUMMARY

A series of high speed model hulls of round bilge shape designed for operation in the Froude number range, F_N = 0.3 - 1.2 has been tested at NPL. This monograph presents data which can be used at the early design stages of marine vessels such as heavily loaded work boats, fast patrol craft and small naval ships.

Resistance and propulsion data are presented in a simple form enabling predictions to be made of the calm water speed and power requirements for a given design and a worked example is appended. Stability underway, manoeuvring and seakeeping characteristics are discussed in the light of model test results obtained from a representative selection of designs based on the series.

1. INTRODUCTION

Resistance data for high speed round bilge forms obtained at NPL were originally presented in 1969 [1] . The purpose at the time was to add to the limited information that was then available for this type of vessel. The response from industry was large and further work was put in hand to extend the work and to vary some of the hull parameters in order to examine the effect of resistance in calm water. In addition propulsion, manoeuvring and seakeeping data have been obtained and this monograph presents all of the information collected from the series of models tested.

Other relevant calm water resistance data include a small model series reported by Nordström [2] , data based on a collection of random round bilge designs [3] and the American series 64 [4] which is exclusively concerned with slender hull forms. None of the foregoing comprehensively cover the range into which round bilge designs can fall and the original NPL data [1] attempted to do this. There still existed a gap, however, between these and series 64, and the NPL series as now presented includes data obtained from three additional models of length to beam ratio 7.5 which approach the lowest L/B ratio (8.45) covered by series 64.

Fast displacement type vessels fall into two categories, the relatively slow round bilge sectioned type and the faster planing craft. Underway, both experience lift due to the action of dynamic forces. In the former this is slight and the forces are only fully exploited by planing craft whose underwater sections are characteristically flat. Fully developed planing demands speed in excess of F_N = 1.1, whereas the very large number of vessels designed within the speed range F_N = 0.4 - 1.1 do not plane and

ideally have rounded underwater sections, It is this type of hull that is covered by the NPL series.

The data presented enable the resistance of any proposed design to be calculated through diagrams of residuary resistance derived from the model experiment results. In optimising a given form within the limitations of its dimensions the effect on resistance of changing the position of the longitudinal centre of buoyancy is shown, and refinements such as the addition of transom wedges and spray rails are examined. Propulsion and ship-model correlation data are also included, and although limited in quantity do enable the required power for a specified ship speed to be assessed with some confidence. Data relating to the manoeuvring qualities of such craft are provided and also information concerning their motions in irregular head seas of coastal water type.

2. THE MODEL SERIES

The models that comprise the series are derivatives of a parent form typical of the round bilge hull which is characterised by straight entrance waterlines, rounded afterbody sections and straight buttock lines terminating sharply at a transom. The longitudinal centre of buoyancy, LCB of the hull was chosen to be in the afterbody, since from resistance considerations, this was known to be advantageous.

The parent model was numbered 100A. Its principal dimensions are given in Table 1, offsets in Tables 2 and 3 and body sections and endings are shown in Figs 1A, B and C. Models deriving from the parent cover length-beam ratios, L/B of 3.33 - 7.5 and length displacement ratio, $\textcircled{M}$ 4.47 - 8.3. $\textcircled{M}$ values are equivalent to displacement-length ratios of 50, 80, 100, 150, 200, 250 and 320 and these simpler numbers were used as prefixes when identifying each model. Beginning with the parent ($L/B = 6.25$), three wider models of the same displacement were derived at $L/B = 5.41$ (model 100B), 4.54 (model 100C) and 3.33 (model 100D) and also a fourth, narrower model at $L/B = 7.5$ (model 100Z). Hence five models of constant displacement but varying beam were created. To maintain constant displacement the draught of each new model was changed in proportion to its change in beam. These five models were then used to vary $\textcircled{M}$, the draught of each model in turn

being increased or decreased to derive a further model. Thus, for example, from the parent model, models 50A (Ⓜ = 8.3), 80A (Ⓜ =7.1) and 150A (Ⓜ = 5.76) were created, each of constant $L/_B$. Altogether 21 models were derived from the parent.

The geometric variations introduced concern beam and draught only. Thus each model retains constant coefficients of fineness and LCB. Model particulars are listed in Table 4 and the range of $L/_B$ and $B/_T$ represented pictorially in Fig 2. The wetted area of each model hull at rest can be read from Fig 3.

The hull offsets of a given design can be derived from Tables 2 and 3 following the procedure outlined in Appendix 1.

Arising from the results obtained from these models came the desire to investigate the effect of altering the position of the LCB. Ten additional models were produced each stemming from a selected model from the series. The principal dimensions were unchanged and by "swinging" the area curve concerned a new LCB position was produced. For example, model 80Z was taken and its LCB changed to 2% L aft amidships from 6.4% L aft and the new model was designated number 80Z (1). Particulars of the additional ten models are given in Table 5.

3. MODEL CONSTRUCTION

All models were made of wood or polyurathane with a painted surface, and had a constant waterline length of 2.54 m. For the purposes of the resistance experiments they were finished as bare hulls without keels or any kind of appendage. To stimulate turbulent flow over the surface of the model, studs 3 mm in diameter were fitted near the bow profile. They projected 2.5 mm and were spaced 25 mm apart.

4. ARRANGEMENT OF THE MODEL EXPERIMENTS

4.1 Resistance experiments in calm water

Each model was ballasted to its required displacement and set to a

level trim at rest.

The models were tested in No 3 Tank, Ship Division and towed in calm water over a speed range F_N = 0.3 - 1.19. For some of the heavily loaded models, speeds above F_N = 1.0 were thought to be unrealistic and in these cases the top speed tested was somewhat lower.

During each experiment, model speed, resistance and running attitude were measured and photographs were taken some of which are reproduced in Figs 4 and 5.

4.2 Loll experiments

At the higher speeds tested in the resistance experiments, some models experienced transverse instability which developed into a loll angle which increased with speed.

To investigate the phenomenon, selected models were further tested using a flexible towing rod designed to reduce as far as possible any restraint in the loll tendency. Also, by re-arranging the position of the ballast weights inside the model, a range of model transverse GM was examined. The results of this work are described in [5] .

4.3 Propulsion experiments

The propulsion data included in this monograph have been collected from experiments conducted on specific ship designs which were based on the model series and whose leading particulars thus fall within the range of parameters covered by the series. These individual designs were propelled by twin propellers. Shafting arrangements differed, shaft slopes ranging from 5 - 12½ degrees. Also some were fitted with A bracket supports, others having I or P bracket arrargements.

The range of speed and displacement investigated depended on each design, but in general, F_N = 0.3 - 1.05 and (M) 5.0 - 7.0 have been covered. Model thrust and torque were measured on conventional mechanical

dynamometers and propeller revolutions by an electric tachometer.

4.4 Manoeuvring experiments

These were conducted on one model only (model 100B). The model was propelled by twin propellers and rudders, details of the latter being given in Fig 48. The model was remotely controlled from the shore by radio link. A speed range of F_N 0.2 - 0.5 was covered at the design displacement; higher speeds were not possible due to limitations in the control system. The model's response to the rudder during the various manoeuvres conducted was charted by a camera mounted overhead.

4.5 Seakeeping experiments

As in the propulsion experiments, seakeeping data have been collected from specific twin screw ship designs that were based on the series. In all cases irregular head seas as defined by Darbyshire [6] for coastal waters were reproduced in the towing tank. Their energy spectra are given by Darbyshire as follows:-

$$\text{Wave energy density, } S(f) = 1.49 \left(h_{\frac{1}{3}}\right)^2 y \exp - \left[\frac{y^2(f-fo)^2}{0.085\{y(f-fo)+P.042\}}\right]^{\frac{1}{2}}$$

where $h_{\frac{1}{3}}$ is significant wave height $= \left(y^{3/2}\, W^{3/2}\right) \times 0.023$ m

y is fetch parameter $= \dfrac{x^3+3x^2+65x}{x^3+12x^2+260x+80}$

where x is fetch in nautical miles

W is wind speed in knots

f is wave frequency in Hz

$$fo = \frac{1}{1.55y^{\frac{3}{4}}W^{\frac{1}{2}}} \quad \text{Hz} \qquad (1/_{fo} \text{ is modal period})$$

For the purposes of the experiments x was taken as 100 nautical miles and W varied from 7 - 25 knots through the familiar Beaufort wind scale. Full scale values for $h\frac{1}{3}$ equivalent to those present during the experiments are tabulated in Table 6 together with the maximum wave heights to be expected for a given sample of 500 waves.

Models spanning (M) = 5.76 - 7.1 were tested and a speed range F_N = 0.4 - 1.2 has been covered. The radius of gyration in pitch was selected as 0.25 L for all models.

During each experiment, model speed and propeller revolutions were measured together with pitch and heave motions and the vertical acceleration at two points on the hull, one forward and one aft.

5. PRESENTATION AND DISCUSSION OF RESULTS

5.1 RESISTANCE EXPERIMENTS

5.1.1 Resistance experiment data

At each speed tested the frictional resistance, R_F of each model has been calculated following th 1957 ITTC skin friction formulation. The wetted surface of the hull at rest was used in the calculation. The residuary resistance, R_R was thus obtained by subtracting R_F from the total measured resistance and curves of $^{R}R/_{\Delta}$ against (M) and F_∇ have been drawn for each $L/_B$ group of models (Figs 6-10). Total resistance coefficient, C_T is plotted against F_N in Figs 11 - 15 for LWL = 30.5 m. The measurements of the running attitude of each model have been converted to running trim angle, τ and the rise or fall of the model at its LCG. Figs 16 - 25 present these data in terms of (M) and F_∇.

These data can be used in estimating the effective power requirements of a given design and Appendix 2 outlines the procedure with a worked example.

If the displacement of the ship when built exceeds the design figure then the ship resistance will be greater than that anticipated

at the design stage. Models 80A, 100A and 150A were each tested over a range of draught and the effect on resistance of a change of displacement from the designed figure can be seen. These results are given in Figs 26 - 31 in the form of total resistance coefficient, C_T for LWL = 30.5 m against F_N within the range 60 - 240%Δ. C_T is seen to vary linearly with %Δ.

5.1.2 Effect of hull roughness on resistance

Ideally the hull of a new ship will have a perfectly smooth finish but this is rarely achieved and roughness will exist, its degree being a matter of individual judgement. $\delta C_F = 0.0002$ is generally accepted as an average increment to C_F. Fig 32 shows that the effect of increasing roughness on the effective power, P_E for a given design. This can clearly be significant and $\delta C_F = 0.0004$ produces a 10% increase in P_E at $F_N = 1.0$ and hulls operating in tropical waters where rapid marine growth will increase roughness should be carefully considered when estimating P_E.

5.1.3 Use of spray rails

A spray rail if fitted on each side of the forebody above the DWL will restrict the growth of the thin "bow wave", or sheet of water that develops with speed and allows the hull, particularly if it is a full form, to run more cleanly. The rails deflect the sheet of water and also change the running trim of the craft slightly and there is some evidence that in doing this the resistance is reduced in certain cases.

The size and positioning of the rail is not critical and it need only extend over half the length of the craft. Its underside should be fitted parallel to the water surface at rest. Fig 33 shows typical arrangements, and photographs reproduced in Fig 34 show how effective such rails can be.

5.1.4 Influence of the transom wedge

The resistance of a high speed craft is importantly linked with its running trim and the transom wedge is a simple device that can be

fitted and which, if properly selected, will reduce both running trim and resistance.

Three models, 100A, 150C and 250D were taken and fitted with wedges 0.015 L long which extended over the whole width of the transom. The models were tested at their designed displacement over a range of speed. Figs 35 - 37 show the results obtained which can be summarised as follows:-

(i) Running trim, τ, reduces with increase of wedge angle. This can be taken too far (see Fig 36 where negative τ occurs with a 15^{o} wedge fitted). Although hull resistance continues to be reduced at low τ it would be unacceptable to operate a ship at high speed in this attitude to the sea.

(ii) Optimum values of resistance occur when τ = 1 - 1.5 degrees, and although τ varies with speed there is every indication that a specific design speed should be associated with τ between 1 and 1½ degrees. Thus, from Fig 35, model 250D would operate best at F_{∇} = 2.0 with a 10^{o} wedge fitted, but for the same F_{∇}, a 5^{o} wedge is superior to a 10^{o} wedge in model 100A (Fig 37).

(iii) Wedges appear to operate most successfully in terms of reducing hull resistance in the region of the main resistance hump (F_N = 0.5) and the reductions become greater as Ⓜ decreases. Wedges offer no advantages at F_{∇} <1.2 .

5.1.5 Transverse instability underway

The resistance data presented were all obtained in the absence of any transverse instability in the models. When loll occurred this was eliminated by lowering weights inside the model thereby stiffening it due to the increased transverse GM. The results of the loll experiments, carried out separately, are summarised in Fig 38 and further details can be found in [5] .

5.1.6 Position of LCB

The variation in LCB tested in the ten additional models selected ranged from 2 - 5.2% L aft amidships. The ten models stemmed from models 80Z, 150B, 150C, 200B and 200C and thus covered a (M) range of 5.23 - 7.1. The results of the tests indicate:-

(a) There is no advantage in selecting a position for the LCB which is further forward than that adopted in the series, ie 6.4% L aft amidships. Figs 39 - 42 show percentage increases in $R_R/_\Delta$ over the range of LCB position tested and in only one instance (at (M) = 7.1) does the resistance reduce for an alternative LCB position and this reduction is very small and occurs at low values of F_∇.

The optimum position of the LCB is thus about 6% L aft of amidships and in most cases tested an increase in resistance can be expected for LCB positions further forward of about 4% L aft of amidships.

(b) The influence of (M) is most noticeable at higher F_∇ values where percentage increases in resistance are less for lower (M) values.

(c) The wetted surfaces of the hulls did not change significantly as the LCB varied.

(d) As was to be expected the running trim of the ten models tested differed from that of the series models from which they were derived, but changes were never more than about ½ degree.

5.2 PROPULSION EXPERIMENTS

5.2.1 Propulsion data

The models tested did not have identical stern arrangements and it is thus not surprising to see the large scatter in t , η_H and η_R as shown in

Figs 44 and 45. Values of the wake fraction, W_T are fairly constant at about zero, and this is to be expected for clear sterns having reasonably straight buttock flow beneath them.

Propulsive elements interact in a complicated way and it is clear that for any design, propeller-hull clearance, slope of shafting and the relative position of rudder and propeller will influence performance. It is thus extremely difficult to suggest accurate values of t ,η_H and η_R for a particular design without recourse to specific model experiments. The values given in Figs 44 and 45 have been meaned and the curves drawn should be regarded as average values which can be applied to round-bilge craft.

Some models were fitted with transom wedges and an attempt has been made to show their influence but there is insufficient information available for positive conclusions to be drawn.

5.2.2 Ship-model correlation factors

Current values of the propulsion prediction factor, $(1+_x)$ and propeller revolutions factor, k_2 are given in Figs 46 and 47. These have been determined from separate ship-model correlation studies carried out at NPL for round bilge craft. The values have been obtained from measured-mile trials conducted at sea on completed vessels having reasonably smooth hulls and corresponding model experiments the analyses of which included zero roughness allowances. $(1+_x)$ and k_2 will be the subject of continual review as further data become available.

5.3 MANOEUVRING EXPERIMENTS

Round bilge hulls fitted with a skeg, twin propellers and rudders should not present major manoeuvring problems except perhaps at very low ship speeds. Close attention should be paid to rudder design however and relatively small rudders can be used since when fitted they are in close proximity to flat hull sections which effectively increase the aspect ratio of the rudder. The ratio produced is approximately double the geometric aspect ratio . Rudder area can be significant and a total

area ratio should be near to 1/30. Details of the rudders fitted in the manoeuvring experiments, which are regarded as ideal for designs based on the series, are given in Fig 48.

The results from the manoeuvring experiments have been obtained from model 100B only and are given in Figs 49 -55. Undoubtedly differences would have been detected had other models from the series been tested, but the most important characteristics, that of no instability at low rudder angles (Figs 49 and 53) is thought to be reproducible throughout the series.

5.4 SEAKEEPING EXPERIMENTS

The results obtained have been analysed to provide significant values of motion and vertical acceleration. The data are not very extensive being obtained from five models lying within the range $L/_B$ = 4.54 - 6.25 and $\nabla^{\frac{1}{3}}/_B$ = 5.76 - 7.1 , and there is no apparent trend with either $L/_B$ or $\nabla^{\frac{1}{3}}/_B$. The results shown in Figs 56 and 57 therefore contain meaned values of pitch, heave and acceleration. They are plotted against $h_{\frac{1}{3}}/_B$, $h_{\frac{1}{3}}$ being the significant wave height of the particular Darbyshire sea state selected in the experiments.

The results reveal the following:-

(i) Pitch and heave reduce with ship speed for a given $h_{\frac{1}{3}}/_B$ (Fig 56).

(ii) Vertical acceleration increases with ship speed for a given $h_{\frac{1}{3}}/_B$ (Fig 57).

(iii) Deck wetness observed during the experiments increased with speed for a given $h_{\frac{1}{3}}/_B$. It is difficult to suggest a limiting condition for safe operation, but each of the models tested appeared capable of F_N = 1.0 within the range of $h_{\frac{1}{3}}/_B$ tested.

6. FURTHER WORK

C_B has been kept constant at 0.397 throughout the series and in certain designs it may be difficult to hold this value. Further tests on models having C_B up to say 0.55 will provide useful information on the effect of greater fullness on calm water resistance. Alternatively, C_B could be varied.

Further propulsion experiments are needed in which the nature and disposition of various stern arrangements can be systematically varied. The effect on propulsion efficiency of changes in the inclination of propeller shafts (and hence line of thrust) could usefully be studied.

Information on the performance of the round bilge hull in waves is extremely limited. To date designs are best assessed individually from model tests conducted in irregular waves. The data obtained can be used statistically and a spectral analysis will yield motion response operators which up to $F_N = 0.4$ can be applied linearly to provide motion data at higher sea states. However at $F_N > 0.4$ the fast hull no longer contours each wave it meets but jumps from wave crest to wave crest ignoring the smaller waves present in the irregular system. The model running at high speed therefore does not react to all of the waves it meets and it would be incorrect to apply the results linearly to higher sea states. Similarly theoretical approaches which are in current use (such as the Frank close-fit program) are invalid at $F_N > 0.4$.

There is thus ample scope for both theoretical and model studies to improve existing knowledge of the performance of high speed craft in waves.

7. ACKNOWLEDGEMENTS

The author is grateful to the many individuals who assisted him during the course of this work. Mr R Jacob was responsible for the manoeuvring and seakeeping experiments and Mr C Pettite was involved with the later resistance experiments and the subsequent analysis required.

The Canadian Department of Supply and Services commissioned

resistance experiments on three of the models tested and the results from these are published by permission of that Department.

8. NOMENCLATURE

			UNITS
A	Wetted surface of hull at rest		m^2
B	Breadth or beam of hull on DWL		m
C	Mean chord length of rudder		m
C_B	Block coefficient	)	
C_P	Prismatic coefficient	) coefficients of fineness	
C_M	Max section area coefficient	)	
C_F	Specific fictional resistance coefficient		
C_T	Total resistance coefficient		
DWL	Designed waterline		m
F_N	Froude number	$F_N = 0.1643\ V/\sqrt{L}$	V in knots L in m
F_∇	Volumetric Froude number	$F_\nabla = 0.165\ V/\nabla^{\frac{1}{6}}$	V in knots
	(Note:	$F_\nabla = \sqrt{M} \times F_N = \frac{1}{2\sqrt{\pi}} \quad K$)	∇ in tonnes
$f_{\frac{1}{3}}$	Significant acceleration		g
GM	Transverse metacentric height		m
$h_{\frac{1}{3}}$	Significant wave height		m
L	Length		m
LOA	Length overall		m
LWL	Length on DWL		m
LCB	Longitudinal centre of buoyancy		
LCG	Longitudinal centre of gravity		
M	Froude length constant	$M = 1.0083\ L/\nabla^{\frac{1}{3}}$	L in m ∇ in tonnes
OPC	Overall propulsion coefficient		
P	Propulsive factor	$P = \eta_H \times \eta_R$	
P_E	Effective power		kW
P_S	Shaft power		kW
R	Resistance, generally		
R_N	Reynolds number	$R_N = VL/\nu$	V in m/sec L in m
		$= VL/1.1883 \times 10^{-6}$	for salt water at 15° C

R_F	Frictional resistance	Newton
R_R	Residuary resistance	Newton
R_T	Total resistance of bare hull	Newton
$R_{R/\Delta}$	Residuary resistance displacement ratio*	
Ⓢ	Froude wetted surface constant	
T	Draught at DWL (to lowest part of bare hull)	m
t	Thrust deduction	
$V/\sqrt{L}$	Speed length ratio $V/\sqrt{L} = 6.086\ F_N$ **	V in knots L in m
W_T	Taylor wake fraction -	
Δ	Displacement mass	tonnes
δ	Displacement mass of model	kg
∇	Displacement volume	m^3
ρ	Mass density of salt water $\rho = 1025.9\ kg/m^3$ $= 1.0259\ tonnes/m^3$ at 15°C	
ν	Kinematic viscosity of salt water $\nu = 1.18831 \times 10^{-6}\ m^2/sec$ at 15°C	
τ	Running trim angle	deg
η_H	Hull efficiency	
η_0	Propeller open water efficiency	
η_R	Relative rotative efficiency	
$2\ \Theta_{\frac{1}{3}}$	Significant pitch amplitude	deg
$2\ Z_{\frac{1}{3}}$	Significant heave amplitude	m

*Residuary resistance has been expressed in terms of force per unit mass of displacement. This quantity which strictly has the dimensions of an acceleration has been plotted in Figs 6-10 and 35-37 as a number indicating the resistance force in kilonewtons per tonne of craft mass.

**$V/\sqrt{L}$ is conveniently expressed in knot and feet units. If these are preferred then $V/\sqrt{L} = 3.36\ F_N$.

9. REFERENCES

1 MARWOOD, W.J. and BAILEY, D. "Design data for high speed displacement hulls of round bilge form", NPL Ship Report 99 (1969)

2 NORDSTRÖM, H.F. "Some tests with models of small vessels", Swedish Tank Publication 19 (1951).

3 MARWOOD, W.J. and SILVERLEAF, A. "Design data for high speed displacement-type hulls and a comparison with hydrofoil craft", 3rd Symposium on Naval Hydrodynamics - High performance ships, ONR ARC-65 (1960)

4 YEH, Hugh Y.H. "Series 64 Resistance experiments on high speed displacement forms", Marine Technology (July, 1965).

5 MARWOOD, W.J. and BAILEY, D. "Transverse instability of round-bottomed high speed craft under way", NPL Ship Report 98 (1968).

6 DARBYSHIRE, J. "The one dimensional wave spectrum in the Atlantic Ocean and in coastal waters", Ocean wave spectra, pp 27-39, New Jersey: Prentice-Hall Inc. (1963).

7 HOERNER, S.F. "Fluid dynamic drag", published by the author, USA (1965).

8 GAWN, R.W.L. "Effect of pitch and blade width on propeller performance", Trans. RINA (1953).

9 GAWN, R.W.L. and BURRILL, L.C. "Effect of cavitation on the performance of a series of 16 in model propellers", Trans. RINA (1957).

10. APPENDICES

APPENDIX 1

Determination of dimensions for a proposed design

Suppose a 38 m ship displacing 190 tonnes is to be designed for 30 knots ie :

LOA = 38 m
LWL = 35 m say
DWL = 35 m
Δ = 190 tonnes (in salt water at 15°C)
V = 30 knots (alternatively 30 x 0.5148 m/sec)
then, ∇ Δ/ρ = 190/1.0259 = 185.37 m^3

$$F_{\nabla} = 0.165\ V/\Delta^{1/6} \qquad \ldots (1)$$

$$= \frac{0.165 \times 30}{(190)^{1/6}} = 2.064$$

$$\text{(M)} = 1.0083\ L/\Delta^{1/3} \qquad \ldots (2)$$

$$= \frac{1.0083 \times 35}{(190)^{1/3}} = 6.14$$

Hull resistance will reduce with beam and if we assume that a DWL beam of 6 m is the lowest practical figure that can be accepted, then

$$L/B = 35/6 = 5.83$$

The block coefficient will be that of the model series, 0.397 and for Δ = 190,

$$0.397 = \frac{\nabla}{LBT} = \frac{185.37}{35 \times 6 \times T} \quad \text{and} \quad T = 2.223 \text{ m}$$

Summarising, the principal dimensions of the design become:

LWL	=	35 m
B	=	6 m
T	=	2.223 m
Δ	=	190 tonnes
C_B	=	0.397
LCB	=	5.4% aft amidships
(M)	=	6.14
F_∇	=	2.064 (for V = 30 knots)

The hull offsets can be derived from those of the parent hull of the series given in Table 2. The ship dimensions are first reduced to correspond to those of the parent model. Thus:

L (parent model) = 2.54 m

L (ship design) = 35 m

Scale = $2.54/35$ = $1/13.7795$

The reduced ship dimensions become:

L = 2.54 m

B = $6/13.7795$ = 0.4354 m

T = $2.223/13.7795$ = 0.1613 m

The offsets and waterline heights can now be calculated from those of the parent model given in Table 2 using a ratio determined by the relative sizes of the parent and the reduced ship dimensions. Thus,

$$\text{Waterline ratio} = \frac{0.1613}{0.14} = 1.1523$$

where 0.14 m is the draught of the parent model

$$\text{Offset ratio} = \frac{0.4354}{0.4064} = 1.0714$$

where 0.4064 m is the beam on DWL of the parent model

Using these ratios we arrive at

L = 2.54 m				L = 35 m	
WATERLINE		OFFSET AT STN 2		SHIP DIMENSIONS AT STN 2	
PARENT	SHIP DESIGN	PARENT	SHIP DESIGN	WATERLINE	OFFSET
50 mm	57.62 mm	22.4 mm	24 mm	793.97 mm	330.7 mm
60 mm	69.14 mm	62.9 mm	67.4 mm	952.71 mm	928.7 mm

and so on

The height of the underside of hull at the centreline above the base for each station can be calculated from those of the parent model given in Table 3.

The designer is free to add any reasonable deck line and freeboard above the DWL to the underwater hull dimensions obtained.

Sufficient information is now available for the preparation of a lines plan. If problems exist such as finding sufficient space for the accommodation of engines, etc some hull sections will have to be modified leading to a different LCB position. This is best done using conventional area curves and the final LCB position noted.

APPENDIX 2

Estimation of effective power for a given design

Effective power, P_E at a speed V is given by:

$$P_E = R_T V$$

and $$R_T = R_F + R_R$$

The residuary resistance, R_R for the example considered in Appendix 1 is obtained by interpolation of Figs 8 and 9 for the design values of $L/_B = 5.83$, $F_\nabla = 2.064$ and $\textcircled{M} = 6.14$.

ie for $L/_B = 5.41$ (Fig 8), $R_{R/_\Delta} = 0.664$ at $F_\nabla = 2.064$ and $M = 6.14$

and for $L/_B = 6.25$ (Fig 9), $R_{R/_\Delta} = 0.627$

from which at $L/_B = 5.83$, $R_{R/_\Delta} = 0.644$

Therefore $R_R = 190 \times 0.644 = 122.4$ kN

The frictional resistance, R_F is dependent on the skin friction correlation adopted. The 1957 ITTC formulation was used in analysing experiment data from the model series and calculations of R_F must therefore be based on the same formulation in which the specific frictional resistance coefficient is defined as:

$$C_F = \frac{0.075}{(\log_{10} R_N - 2)^2} \qquad \ldots (3)$$

To calculate R_F we proceed as follows:

For $F_\nabla = 2.064$, (M) $= 6.14$ and $L/_B = 5.83$

wetted surface of ship's hull at rest, from Fig 3 is:

$$\left(\frac{35}{2.54}\right)^2 \times 1.163 = 220.82 \text{ m}^2$$

In equation (3), R_N is given by $VL/_\nu$

ie $R_N = \frac{(30 \times 0.5148) \times 35}{1.18831} \times 10^6$ for salt water at 15^0C

$= 4.542 \times 10^8$

from which, following equation (3)

$$C_F = \frac{0.075}{[\log_{10}(4.542\times10^8)-2]^2} = \frac{0.075}{(6.6572)^2} = 0.00169$$

and $C_F = R_F/\frac{1}{2}\rho AV^2$

where ρ is mass density of salt water at 15°C (1025.9 kg/m^3)
A is wetted area of hull at rest (m^2)
V is ship speed (m/sec)
and R_F will be in kgm/sec^2 or Newtons

Therefore $R_F = C_F \times \frac{1}{2}\rho AV^2$

$$= 0.00169 \times \tfrac{1}{2} \times 1025.9 \frac{kg}{m^3} \times 220.82\ m^2 \times (30\times0.5148 \frac{m}{sec})^2$$

$$= 45658\ kgm/sec^2$$

$$= 45658\ N = 45.658\ kN$$

The total ship resistance at 30 knots is thus

$$R_F + R_R = 45.658 + 122.4 = 168.058\ kN$$

and $P_E = 168.058 \times (30\times0.5148)\ kNm/sec = 2595.48\ kNm/sec = \underline{2595.48\ kW}$

The running trim of the ship underway can be estimated from Figs 11-15. In our example, (M) = 6.14, L/B = 5.83 and F_∇ = 2.064., the running trim at 30 knots will be approximately 2.6 degrees (Figs 18 and 19) and the hull will rise by about $35 \times \frac{0.05}{100}$ m = 0.0175 m at its LCG (Figs 23 and 24).

The above calculations, repeated at different speeds, will give curves of P_E, τ and rise over a chosen range of ship speed.

Notes

1. The C_F value of 0.00169 obtained will be related to a perfectly smooth hull surface. If the hull is expected to be abnormally rough then δC_F of say 0.0005 should be included in the C_F value to bring it to 0.00219.

2. If when arriving at the final hull shape the position of the LCB is different to that of the model series, then use of Figs 39-42 will allow a correction to $R_{R/\Delta}$ to be made. A small change in LCB will not affect the wetted surface, but if the LCB change is large then an independent calculation of the hull wetted surface should be made and included in the calculation of R_F.

3. The estimate of P_E made in this Appendix will apply to the bare hull only. The underwater fittings that will be fitted will increase P_E and the effect of individual items such as shafts and brackets should be assessed separately following Appendix 3 and added to the value of P_E obtained above to give the effective power of hull and appendages at the speed considered.

4. Values of ρ and ν over a range of temperature for both fresh and salt water are given in Tables 7 and 8.

APPENDIX 3

Estimation of the resistance of hull appendages

In model experiments the resistance of hull appendages such as propeller shafting and brackets can be measured and expressed as a percentage of the bare hull resistance. However, these percentages cannot be successfully applied to any design and if model data are not available then the resistance of the individual appendages for a specific ship design are best calculated following the formulae given below:

(a) Centreline keels and skegs

Resistance, $R = \frac{1}{2} \rho A V^2 C_f$ ... (4)

where A is wetted area of both sides of keel

V is ship speed

C_f is obtained through equation (3), L in R_N being taken as the length of the keel in the direction of the flow.

ρ is the mass density of water

(b) Rudders and struts

LEMG

Hoerner [7] gives a formula for aerofoil sections which is in good agreement with measured resistances obtained for rudders and struts of NACA section. Hence:

$$R = \tfrac{1}{2} \rho S_R V^2 \left[2 C_f \{1+2t/c+60(t/c)^4\} \right] \quad \ldots (5)$$

where S_R is profile area of rudder or strut as seen from one side

t/c is section thickness-chord ratio and other symbols as for equation (4)

(c) Propeller shafting and strut bossings

These appendages are subject to cross flow conditions and again Hoerner [7] gives:

$$R = \tfrac{1}{2} \rho l d V^2 (1.1 \sin^3 \varepsilon + \pi C_f) \quad \ldots (6)$$

where l is the length of shaft or bossing

d is diameter of shaft or bossing

ε is angle of flow striking the appendage (the flow is assumed parallel to the underside of hull)

and other symbols as for equation (4)

(d) Bilge keels

$$R = 1.67 (\tfrac{1}{2} \rho S_B V^2 C_f) \quad \ldots (7)$$

where S_B is total wetted surface of bilge keels less area of ship's hull masked by the keels

and other symbols as for equation (4)

The resistance of all the hull appendages will be the sum of the individual items, from which the effective power due to them can be calculated.

APPENDIX 4

Estimation of power required at ship's propeller

This will involve a propeller design and in estimating the power absorbed at the ship's propellers from model experiment data, the total shaft power for a given ship speed is given by:

$$\text{Shaft power, } P_S = \frac{P_E}{OPC} \qquad \ldots (8)$$

where P_E is effective power of hull and appendages

OPC is the overall propulsive coefficient

For a ship driven by marine propellers the OPC is made up as follows:

$$OPC = \frac{\eta_o \times P}{(1+x)} \qquad \ldots (9)$$

where η_o is the open water propeller efficiency

P is the product of hull and relative rotative efficiencies (see Fig 45). In Fig 45,

$$F_N = 0.1643\, V/\sqrt{L} = \frac{0.1643 \times 30}{\sqrt{35}} = 0.83,$$

for example given in Appendix 1.

(1+x) is a propulsion prediction factor

It is necessary to introduce (1+x) into the calculation to take account of differences that exist between actual ship power and that predicted from a corresponding model test.

An assumed value for P_S is taken initially, obtained through equation (8) taking OPC = 0.5. From P_S a ship's engine can be selected and the propeller torque to be absorbed at the particular ship speed calculated. The blade area of the propeller is selected using a safe blade loading of, for

example 0.7 kgf/cm^2, and conventional propeller design charts used to determine the best combination of propeller diameter and pitch which will match the characteristics of the engine. The process is iterative over a range of propeller diameter and an optimum η_o is ultimately determined. OPC is then calculated through equation (9) where values of P and $(1+x)$ are obtained from Figs 45 and 46. If OPC differs significantly from 0.5, the value taken initially, then the whole calculation is repeated beginning with the new OPC until equality is achieved, and an accurate value for P_S obtained.

Notes

1. The Gawn propeller data [8] are preferred in the case of high speed craft which do not demand extreme loading or rotational speeds. Gawn used relatively large propeller models which help to reduce scale effect and his data cover blade area ratios up to 1.1, these higher values being inevitably required to minimise propeller cavitation.

2. Once a propeller has been selected a cavitation check should be made using the Gawn and Burrill data [9] and if the indicated degree of cavitation is severe an increase in propeller blade area will help but the calculation process has to be repeated to provide a final η_o.

3. For the same reasons that $(1+x)$ is required in equation (9), a propeller revolutions prediction factor, k_2, is needed in determining ship propeller rotation, N_S, where

$$N_S = N_m \times k_2$$

N_m being ship propeller rotation equivalent to model rate of rotation

Values for k_2 are given in Fig 47.

TABLE 1 PRINCIPAL PARTICULARS OF PARENT MODEL

Designation	100 A
Length on designed waterline (LWL)	2.54 m
Beam on designed waterline (B)	0.4064 m
Draught of designed waterline (T)	0.140 m
Displacement (Δ)	57.33 kg
Block coefficient (C_B)	0.397
Prismatic coefficient (C_p)	0.693
Max section area coefficient (C_m)	0.573
Maximum section	40% LWL from transom
Longitudinal centre of buoyancy (LCB)	43.6% LWL from transom (6.4% LWL aft &)
Half angle of entrance of DWL	11 degrees
Deadrise at transom	12 degrees
Length-beam ratio ($L/_B$)	6.25
Beam-draught ratio ($B/_T$)	2.90
Froude length constant (M)	6.59
Froude wetted surface constant (S)	7.17

STATION	Base Line	10mm WL	20mm WL	30mm WL	40mm WL	50mm WL	60mm WL	70mm WL	80mm WL	90mm WL	100mm WL	110mm WL	120mm WL	130mm WL	140mm WL	150mm WL	160mm WL	180mm WL	200mm WL	220mm WL	240mm WL	260mm WL
0(AP)	-	-	-	-	-	-	-	19.7	65.2	102.6	131.6	150.5	159.1	164.5	166.6	167.8	168.4	169.1	169.5	169.9	170.5	170.
½	-	-	-	-	-	-	-	40.0	82.4	117.2	140.5	155.4	164.6	170.5	173.9	176.1	177.2	178.0	178.2	178.7	179.2	179.
1	-	-	-	-	-	-	16.9	59.6	98.4	131.7	151.0	163.9	172.4	177.6	180.6	182.4	183.6	184.9	185.6	186.4	187.0	187.
1½	-	-	-	-	-	-	44.3	79.4	115.8	141.3	158.7	170.0	177.3	182.5	186.2	188.6	190.3	191.8	192.9	193.7	194.6	195.
2	-	-	-	-	-	22.4	62.9	98.5	130.6	153.5	168.9	179.4	184.9	189.2	192.2	194.3	195.9	198.3	199.6	200.6	201.5	202.
3	-	-	-	-	23.1	58.4	92.3	121.5	148.7	168.3	180.2	187.5	192.5	196.7	199.5	201.9	203.6	206.5	208.4	210.0	211.3	212.
4	-	-	-	25.3	58.2	88.0	115.2	137.4	156.7	172.2	183.3	190.9	196.2	200.3	203.2	205.4	207.2	210.4	213.0	214.9	216.6	218.
5	-	-	22.3	48.0	74.2	97.3	117.3	134.8	149.1	161.2	171.3	179.6	186.5	192.0	196.6	200.4	203.9	207.7	212.4	215.7	218.8	221.
6	-	14.8	34.0	52.5	70.0	86.3	101.7	115.7	127.9	139.1	149.0	158.4	165.6	172.1	178.0	183.1	187.9	195.7	202.9	208.8	214.5	220.
7	3.4	16.4	29.4	41.8	54.0	65.0	76.0	86.4	96.0	105.4	114.1	122.6	130.3	137.8	144.7	151.5	157.6	169.4	181.3	192.2	203.1	213.
8	3.4	11.0	19.0	26.9	34.4	41.7	48.9	56.0	62.7	69.6	76.4	83.0	89.6	96.1	102.6	119.2 *	115.7	128.6	143.1	157.5	173.1	189.
8½	-	8.4	13.7	19.0	24.6	29.7	35.0	40.4	45.5	51.0	56.4	61.9	67.2	72.6	78.4	84.1	90.1	102.2	116.5	131.7	149.0	167.
9	-	4.3	7.7	11.3	14.7	17.4	22.0	25.6	29.3	33.3	37.2	41.4	45.5	49.7	54.3	57.7	63.8	74.0	86.5	100.4	117.0	135.
9½	-	-	-	-	4.4	6.8	9.3	11.6	14.0	16.4	18.9	21.4	24.2	28.0	29.9	33.3	36.9	44.4	53.7	64.5	78.1	94.
10(FP)	-	-	-	-	-	-	-	-	-	-	-	-	-	-	3.4	5.6	8.2	13.4	19.6	26.8	36.0	46.

* 109,2

Length on designed waterline = 2540 mm

TABLE 2 OFFSETS OF PARENT MODEL

STATION	DISTANCE X (mm)	STATION	DISTANCE X (mm)
0	67	4	23
1/2	62	5	12·4
1	56	6	3·5
1 1/2	50	7 and 8	0
2	45	9	7·6
3	34	9 1/2	35
		10	140

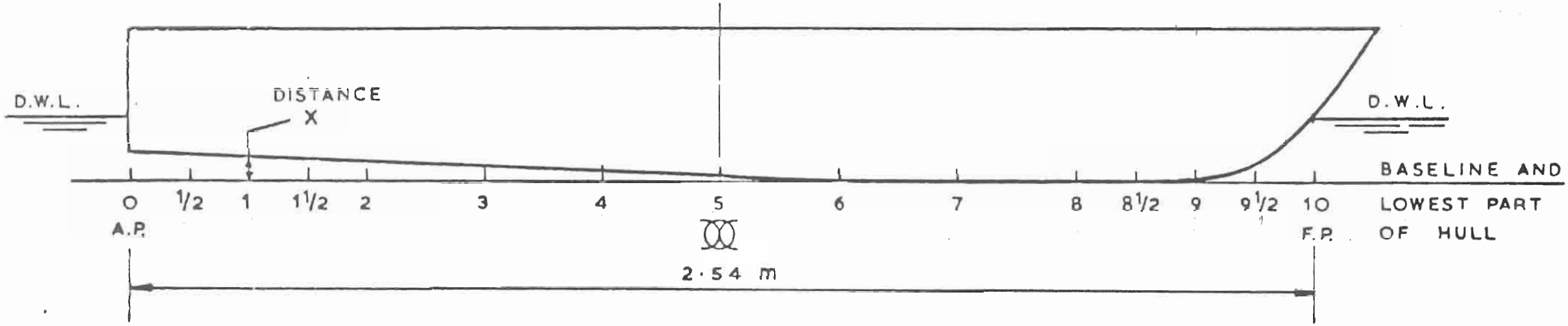

TABLE.3. CENTRELINE PROFILE OF PARENT MODEL

MODEL DIMENSIONS

Model Number	Length on DWL, L (m)	Beam on DWL, B (m)	Draught of DWL, T (m)	Displacement (kg)	L/B	B/T	(M)	LCB %L aft ⊠
50 Z	2.54	0.338	0.084	28.67	7.50	4.02	8.3	6.4
50 A	"	0.406	0.070	"	6.25	5.80	"	"
80 Z	"	0.338	0.134	45.86	7.50	2.51	7.1	"
80 A	"	0.406	0.112	"	6.25	3.63	"	"
80 B	"	0.470	0.097	"	5.41	4.86	"	"
80 C	"	0.559	0.081	"	4.54	6.87	"	"
100 Z	"	0.338	0.168	57.33	7.50	2.01	6.59	"
100 A	"	0.406	0.140	"	6.25	2.90	"	"
100 B	"	0.470	0.121	"	5.41	3.88	"	"
100 C	"	0.559	0.102	"	4.54	5.49	"	"
100 D	"	0.762	0.075	"	3.33	10.21	"	"
150 A	"	0.406	0.210	86.0	6.25	1.93	5.76	"
150 B	"	0.470	0.181	"	5.41	2.59	"	"
150 C	"	0.559	0.152	"	4.54	3.67	"	"
150 D	"	0.762	0.112	"	3.33	6.80	"	"
200 B	"	0.470	0.242	114.66	5.41	1.94	5.23	"
200 C	"	0.559	0.204	"	4.54	2.75	"	"
200 D	"	0.762	0.149	"	3.33	5.10	"	"
250 C	"	0.559	0.254	143.33	4.54	2.19	4.86	"
250 D	"	0.762	0.187	"	3.33	4.08	"	"
320 C	"	0.559	0.326	183.46	4.54	1.72	4.47	"
320 D	"	0.762	0.239	"	3.33	3.19	"	"

TABLE 4 DETAILS OF MODELS COMPRISING THE SERIES

MODEL DIMENSIONS

Model Number	Length on DWL, L (m)	Beam on DWL, B (m)	Draught on DWL, T (m)	Displacement (kg)	L/B	B/T	(M)	LCB %L aft ⊠
80 Z(1)	2.54	0.338	0.134	45.86	7.5	2.51	7.1	2.0
80 Z(2)	"	"	"	"	"	"	"	3.8
80 Z(3)	"	"	"	"	"	"	"	5.2
150 B(1)	"	0.47	0.181	86.0	5.41	2.59	5.76	2.0
150 C(1)	"	0.559	0.152	"	4.54	3.67	"	2.0
150 C(2)	"	"	"	"	"	"	"	3.8
200 B(1)	"	0.47	0.242	114.66	5.41	1.94	5.23	2.0
200 B(2)	"	"	"	"	"	"	"	3.8
200 C(1)	"	0.559	0.204	"	4.54	2.75	"	2.0
200 C(2)	"	"	"	"	"	"	"	3.8

TABLE 5 DETAILS OF MODELS USED IN INVESTIGATING POSITION OF LCB

TABLE 6 Full scale wave amplitudes for coastal waters as defined by Darbyshire

Beaufort Number	$h_{\frac{1}{3}}$ (m)	Max wave height expected in a sample of 500 waves (m)
3	0.55	0.99
4	0.95	1.71
5	1.52	2.74
6	2.35	3.9

TABLE 7 VALUES OF MASS DENSITY, p FOR FRESH AND SALT WATER AGAINST TEMPERATURE IN DEGREES CELSIUS VALUES ARE IN kg/m^3

FRESH WATER

C	p	C	p
0	999.8	16	998.9
1	999.8	17	998.7
2	999.9	18	998.5
3	999.9	19	998.3
4	999.9	20	998.1
5	999.9	21	997.9
6	999.9	22	997.7
7	999.8	23	997.4
8	999.8	24	997.2
9	999.7	25	996.9
10	999.6	26	996.7
11	999.5	27	996.4
12	999.4	28	996.2
13	999.3	29	995.9
14	999.1	30	995.6
15	999.0		

SALT WATER, SALINITY 3.5%

C	p	C	p
0	1028.0	16	1025.7
1	1027.9	17	1025.4
2	1027.8	18	1025.2
3	1027.8	19	1025.0
4	1027.7	20	1024.7
5	1027.6	21	1024.4
6	1027.4	22	1024.1
7	1027.3	23	1023.8
8	1027.1	24	1023.5
9	1027.0	25	1023.2
10	1026.9	26	1022.9
11	1026.7	27	1022.6
12	1026.6	28	1022.3
13	1026.3	29	1022.0
14	1026.1	30	1021.7
15	1025.9		

TABLE 8 VALUES OF KINEMATIC VISCOSITY FOR FRESH AND SALT WATER AGAINST TEMPERATURES IN DEC. CELSIUS.

VALUES ARE IN CENTISTOKES cSt = $10^{-6} m^2 / s$

Fresh Water

C	0.0	0.1	0.2	0.3	0.4	0.5	0.6	0.7	0.8	0.9
0.	1.78667	1.78056	1.77450	1.76846	1.76246	1.75648	1.75054	1.74461	1.73871	1.73285
1.	1.72701	1.72121	1.71545	1.70972	1.70403	1.69837	1.69272	1.68710	1.68151	1.67594
2.	1.67040	1.66489	1.65940	1.65396	1.64855	1.64316	1.63780	1.63247	1.67217	1.62190
3.	1.61665	1.61142	1.60622	1.60105	1.59591	1.59079	1.58570	1.58063	1.57558	1.57057
4	1.56557	1.56060	1.55566	1.55074	1.54585	1.54098	1.53616	1.53131	1.52651	1.52173
5	1.51698	1.51225	1.50754	1.50286	1.49820	1.49356	1.48894	1.48435	1.47978	1.47523
6	1.47070	1.46619	1.46172	1.45727	1.45285	1.44844	1.44405	1.43968	1.43533	1.43099
7	1.42667	1.42238	1.41810	1.41386	1.40964	1.40543	1.40125	1.39709	1.39294	1.38882
8	1.38471	1.38063	1.37656	1.37251	1.36848	1.36445	1.36045	1.35646	1.35249	1.34855
9.	1.34463	1.34073	1.33684	1.33298	1.32913	1.32530	1.32149	1.31769	1.31391	1.31015
0.	1.30641	1.30268	1.29897	1.29528	1.29160	1.28794	1.28430	1.28067	1.27706	1.27346
1.	1.26988	1.26632	1.26277	1.25924	1.25573	1.25223	1.24874	1.24527	1.24182	1.23838
2.	1.23495	1.23154	1.22815	1.22478	1.22143	1.21809	1.21477	1.21146	1.20816	1.20487
3.	1.20159	1.19832	1.19508	1.19184	1.18863	1.18543	1.18225	1.17908	1.17592	1.17278
4.	1.16964	1.16651	1.16340	1.16030	1.15721	1.15414	1.15109	1.14806	1.14503	1.14202
5.	1.13902	1.13603	1.13304	1.13007	1.12711	1.12417	1.12124	1.11832	1.11542	1.11254
6	1.10966	1.10680	1.10395	1.10110	1.09828	1.09546	1.09265	1.08986	1.08708	1.08431
7.	1.08155	1.07880	1.07606	1.07334	1.07062	1.06792	1.06523	1.06254	1.05987	1.05721
8.	1.05456	1.05193	1.04930	1.04668	1.04407	1.04148	1.03889	1.03631	1.03375	1.03119
9.	1.02865	1.02611	1.02359	1.02107	1.01857	1.01607	1.01359	1.01111	1.00865	1.00619
0.	1.00374	1.00131	0.99888	0.99646	0.99405	0.99165	0.98927	0.98690	0.98454	0.98218
1.	0.97984	0.97750	0.97517	0.97285	0.97053	0.96822	0.96592	0.96363	0.96135	0.95908
2.	0.95682	0.95456	0.95231	0.95008	0.94786	0.94565	0.94345	0.94125	0.93906	0.93688
3	0.93471	0.93255	0.93040	0.92825	0.92611	0.92397	0.92184	0.91971	0.91760	0.91549
4	0.91340	0.91132	0.90924	0.90718	0.90512	0.90306	0.90102	0.89898	0.89595	0.89493
5	0.89292	0.89090	0.88889	0.88689	0.88490	0.88291	0.88094	0.87897	0.87702	0.87507
6	0.87313	0.87119	0.86926	0.86734	0.86543	0.86352	0.86162	0.85973	0.85784	0.85596
7	0.85409	0.85222	0.85036	0.84851	0.84666	0.84482	0.84298	0.84116	0.83934	0.83752
8	0.83572	0.83391	0.83212	0.83033	0.82855	0.82677	0.82500	0.82324	0.82148	0.81973
9	0.81798	0.81625	0.81451	0.81279	0.81106	0.80935	0.80765	0.80596	0.80427	0.80258
0	0.80091	0.79923	0.79755	0.79588	0.79422	0.79256	0.79090	0.78924	0.78757	0.78592

TABLE 8: VALUES OF KINEMATIC VISCOSITY FOR FRESH AND SALT WATER AGAINST TEMPERATURES IN DEC. CELSIUS.

VALUES ARE IN CENTISTOKES cSt = $10^{-6} m^2/s$

Salt water salinity 3.5%

DEG.C	0.0	0.1	0.2	0.3	0.4	0.5	0.6	0.7	0.8	0.9
0.	1.82844	1.82237	1.81633	1.81033	1.80436	1.79842	1.79251	1.78662	1.78077	1.77494
1.	1.76915	1.76339	1.75767	1.75199	1.74634	1.74072	1.73513	1.72956	1.72403	1.71853
2.	1.71306	1.70761	1.70220	1.69681	1.69145	1.68612	1.68082	1.67554	1.67030	1.66508
3.	1.65988	1.65472	1.64958	1.64446	1.63938	1.63432	1.62928	1.62427	1.61929	1.61433
4.	1.60940	1.60449	1.59961	1.59475	1.58992	1.58511	1.58032	1.57556	1.57082	1.56611
5.	1.56142	1.55676	1.55213	1.54752	1.54294	1.53838	1.53383	1.52930	1.52479	1.52030
6.	1.51584	1.51139	1.50698	1.50259	1.49823	1.49388	1.48956	1.48525	1.48095	1.47667
7.	1.47242	1.46818	1.46397	1.45978	1.45562	1.45147	1.44735	1.44325	1.43916	1.43506
8.	1.43102	1.42698	1.42296	1.41895	1.41498	1.41102	1.40709	1.40317	1.39927	1.39539
9.	1.39152	1.38767	1.38385	1.38003	1.37624	1.37246	1.36870	1.36496	1.36123	1.35752
10.	1.35383	1.35014	1.34647	1.34281	1.33917	1.33555	1.33195	1.32837	1.32481	1.32126
11.	1.31773	1.31421	1.31071	1.30722	1.30375	1.30030	1.29685	1.29343	1.29002	1.28662
12.	1.28324	1.27987	1.27652	1.27319	1.26988	1.26658	1.26330	1.26003	1.25677	1.25352
13.	1.25028	1.24705	1.24384	1.24064	1.23745	1.23428	1.23112	1.22798	1.22484	1.22172
14.	1.21862	1.21552	1.21244	1.20938	1.20632	1.20328	1.20027	1.19726	1.19426	1.19128
15.	1.18831	1.18534	1.18239	1.17944	1.17651	1.17359	1.17068	1.16778	1.16490	1.16202
16.	1.15916	1.15631	1.15348	1.15066	1.14786	1.14506	1.14228	1.13951	1.13674	1.13399
17.	1.13125	1.12852	1.12581	1.12309	1.12038	1.11769	1.11500	1.11232	1.10966	1.10702
18.	1.10438	1.10176	1.09914	1.09654	1.09394	1.09135	1.08876	1.08619	1.08363	1.08107
19.	1.07854	1.07601	1.07350	1.07099	1.06850	1.06601	1.06353	1.06106	1.05861	1.05616
20.	1.05372	1.05129	1.04886	1.04645	1.04405	1.04165	1.03927	1.03689	1.03452	1.03216
21.	1.02981	1.02747	1.02514	1.02281	1.02050	1.01819	1.01589	1.01360	1.01132	1.00904
22.	1.00678	1.00452	1.00227	1.00003	0.99780	0.99557	0.99336	0.99115	0.98895	0.98676
23.	0.98457	0.98239	0.98023	0.97806	0.97591	0.97376	0.97163	0.96950	0.96737	0.96526
24.	0.96315	0.96105	0.95896	0.95687	0.95479	0.95272	0.95067	0.94862	0.94658	0.94455
25.	0.94252	0.94049	0.93847	0.93646	0.93445	0.93245	0.93046	0.92847	0.92649	0.92452
26.	0.92255	0.92059	0.91865	0.91671	0.91478	0.91286	0.91094	0.90903	0.90711	0.90521
27.	0.90331	0.90141	0.89953	0.89765	0.89579	0.89393	0.89207	0.89023	0.88838	0.88654
28.	0.88470	0.88287	0.88105	0.87923	0.87742	0.87562	0.87383	0.87205	0.87027	0.86849
29.	0.86671	0.86494	0.86318	0.86142	0.85966	0.85792	0.75619	0.85446	0.85274	0.85102
30.	0.84931	0.84759	0.84588	0.84418	0.84248	0.84079	0.83910	0.83739	0.83570	0.83400

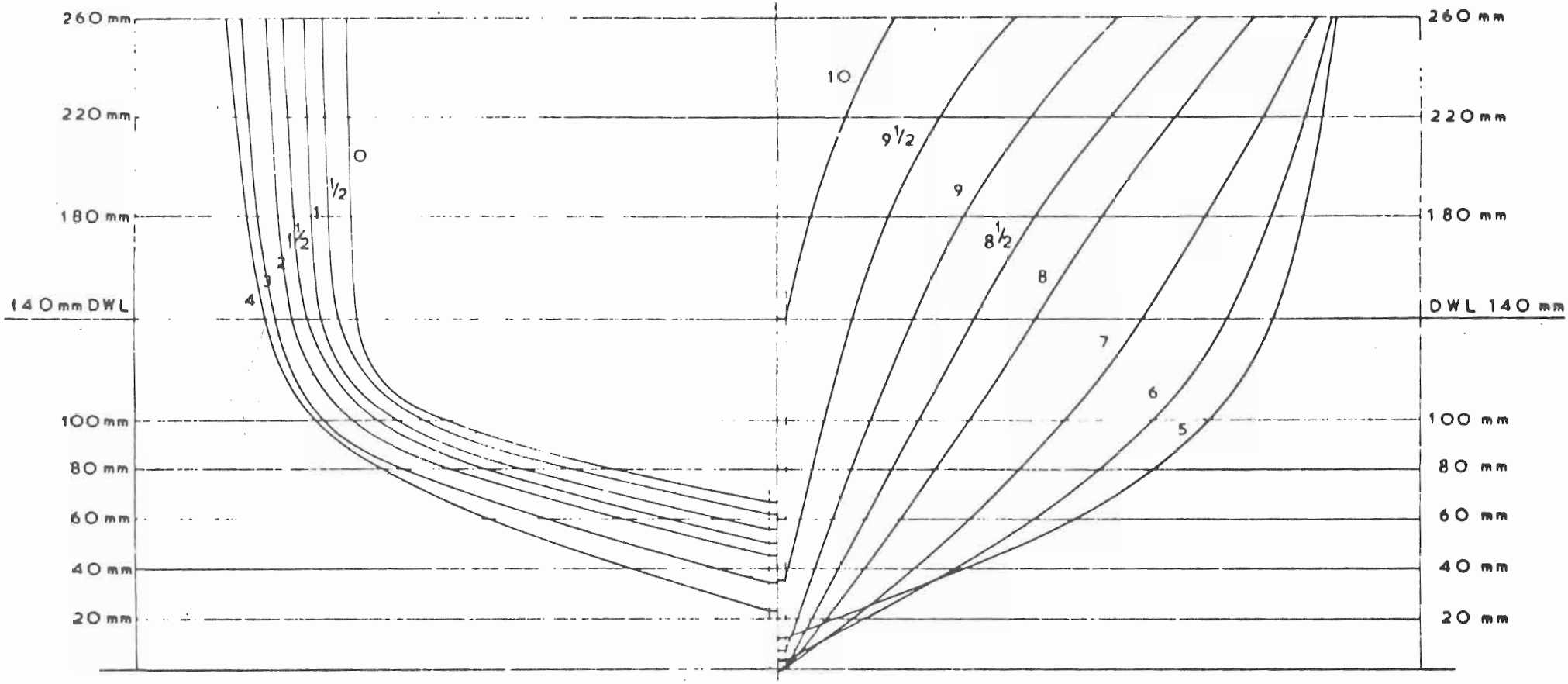

FIG. 1 A. BODY SECTIONS OF PARENT MODEL

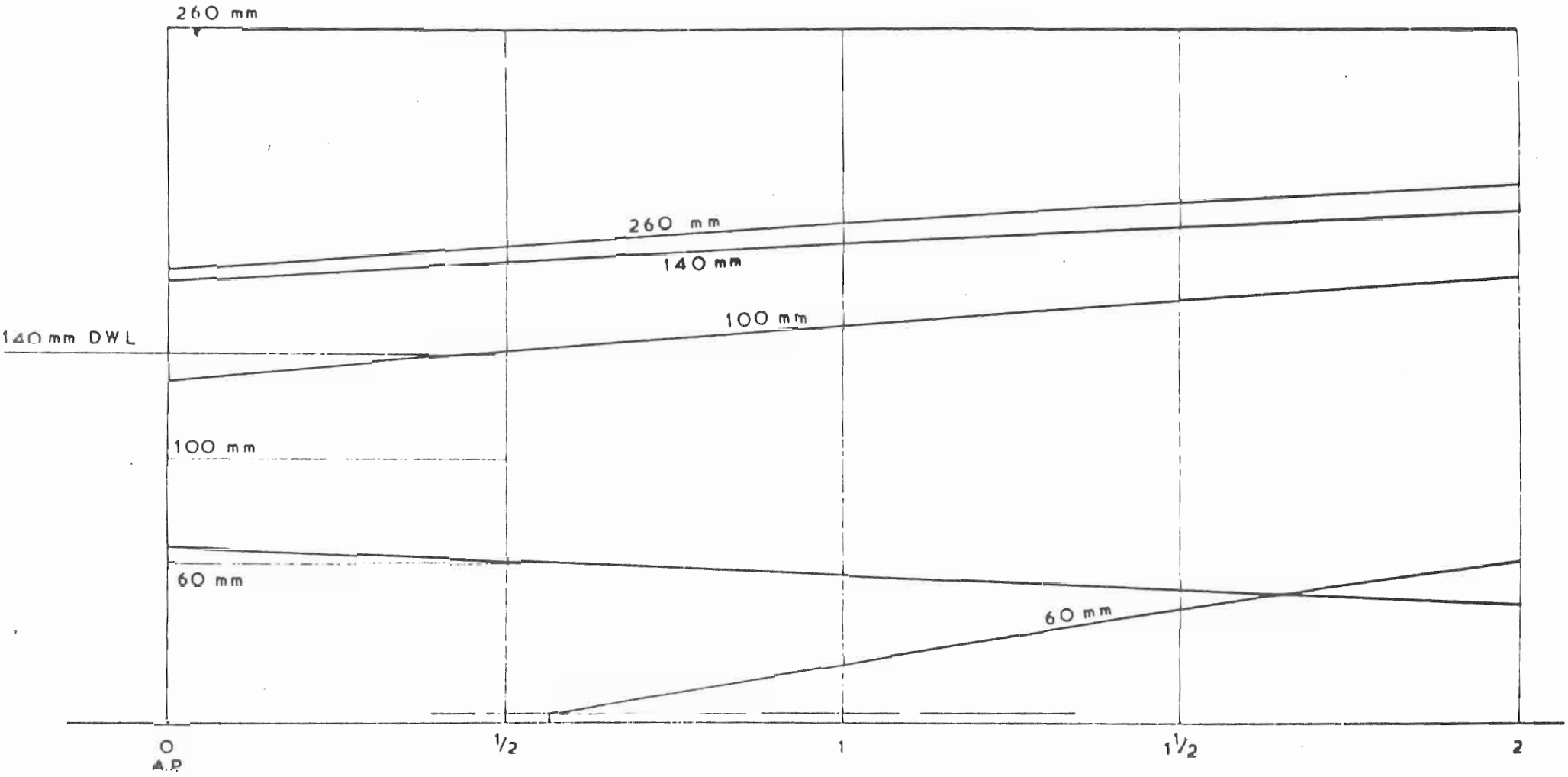

FIG. 1 B. STERN CONTOUR AND WATERLINE ENDINGS OF PARENT MODEL

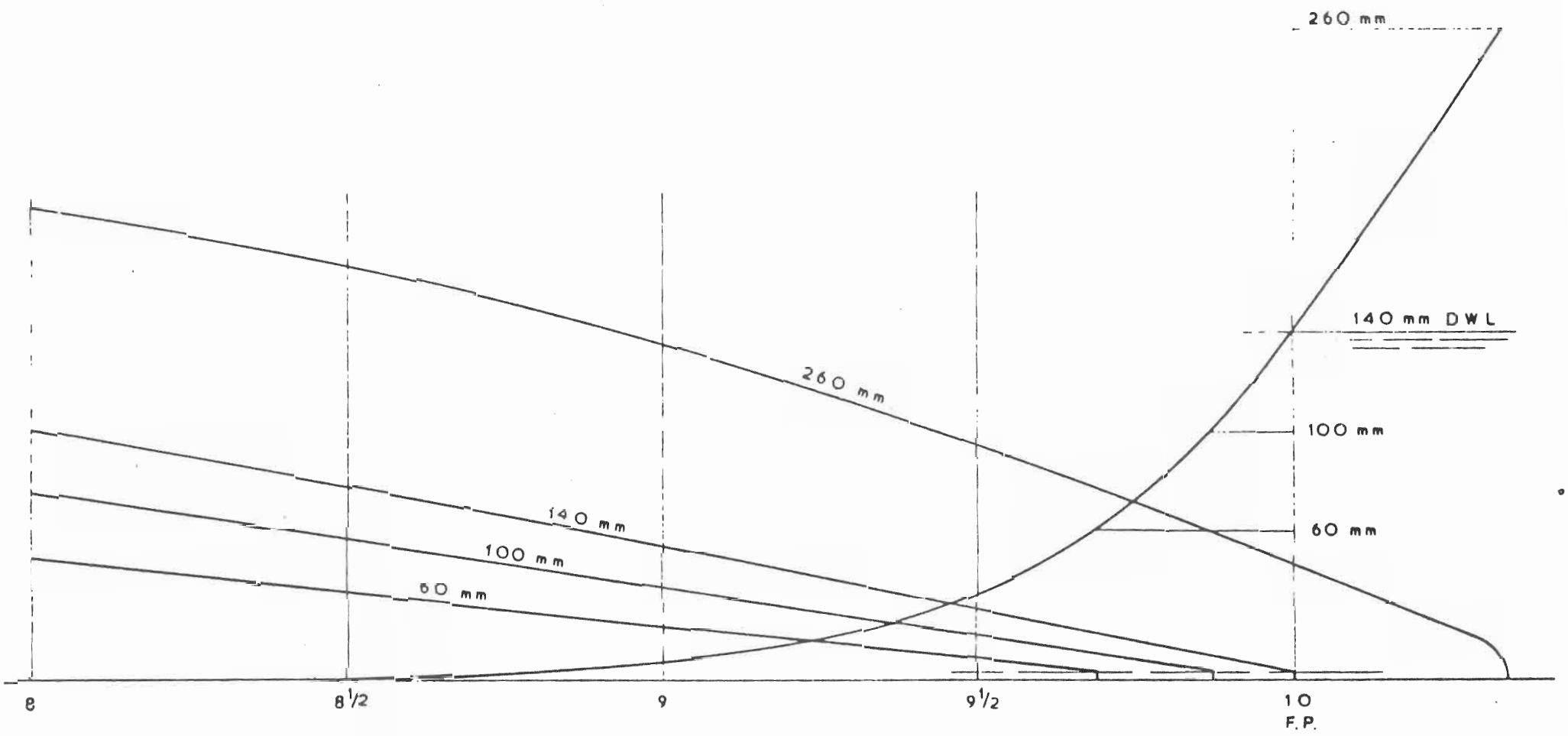

FIG. 1 C. BOW CONTOUR AND WATERLINE ENDINGS OF PARENT MODEL

FIG. 2.

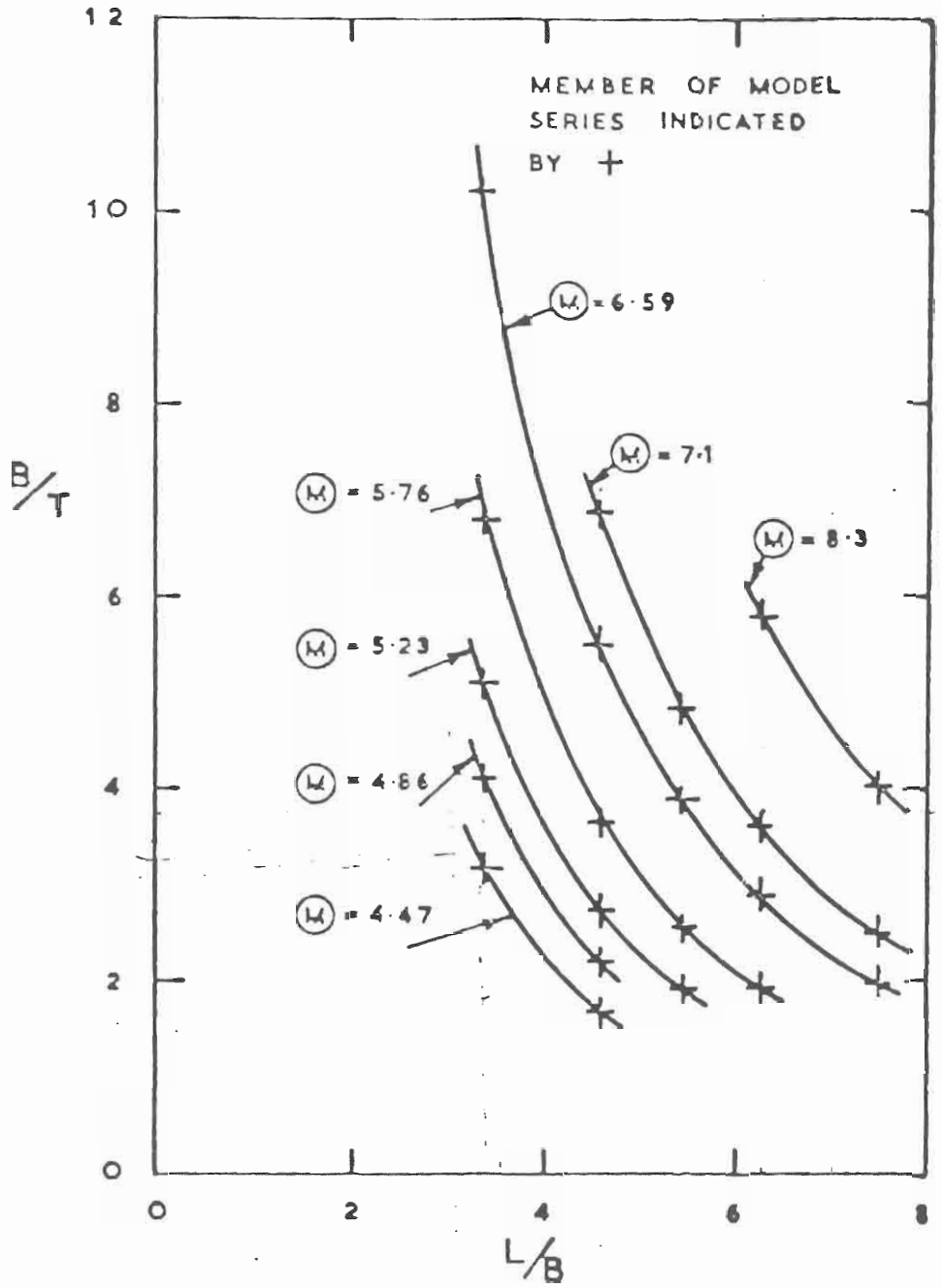

RANGE OF PARAMETERS COVERED IN MODEL SERIES

FIG. 3.

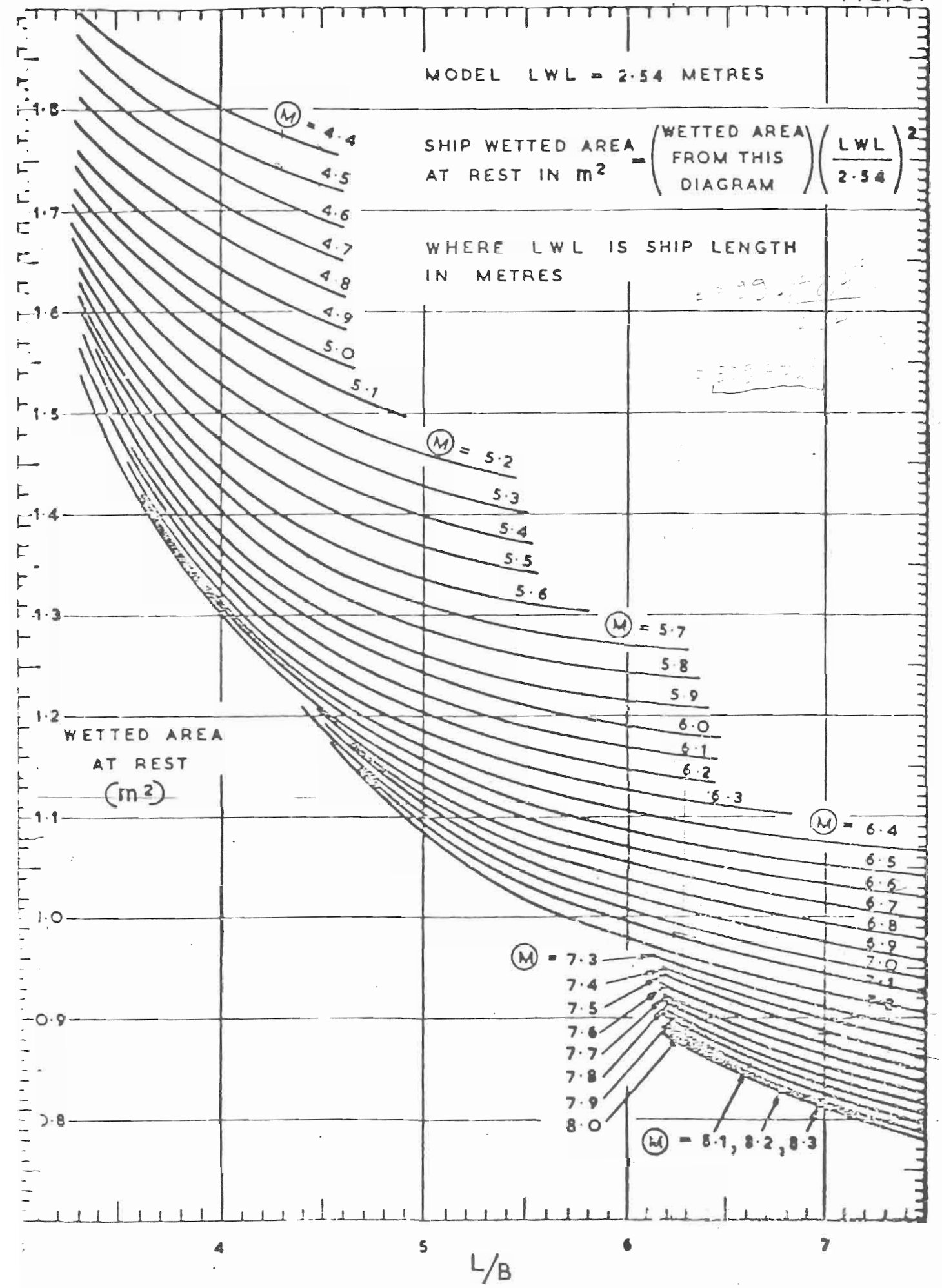

WETTED AREA OF HULL AT REST

FIG. 4.

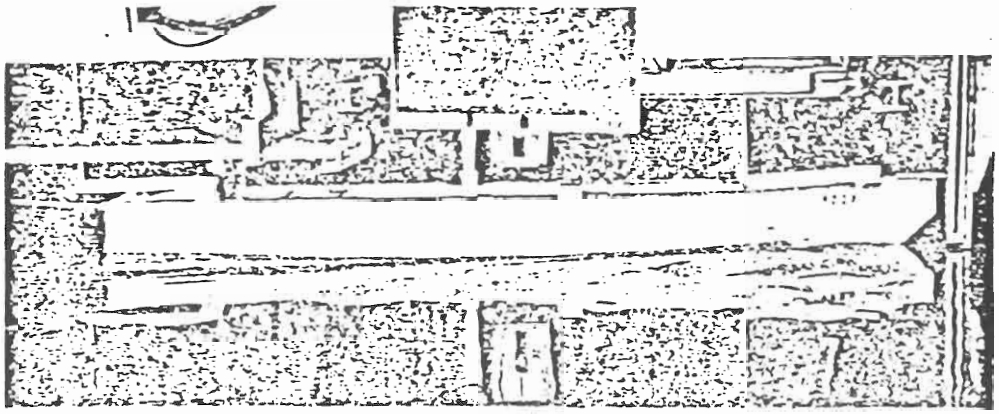

$F_N = 0.6$

$F_N = 1.19$

MODEL Nº 50 Z

$L/B = 7.5$

$(M) = 8.3$

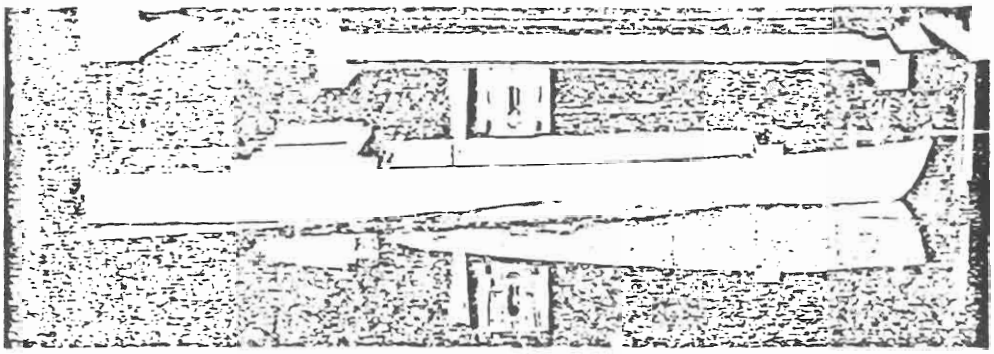

$F_N = 0.7$

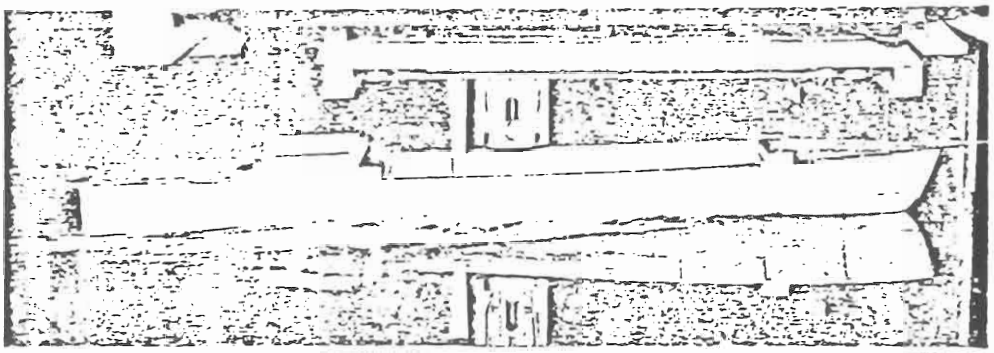

$F_N = 1.05$

MODEL Nº 100B

$L/B = 5.41$

$(M) = 6.59$

CALM WATER RESISTANCE EXPERIMENTS

FIG. 5.

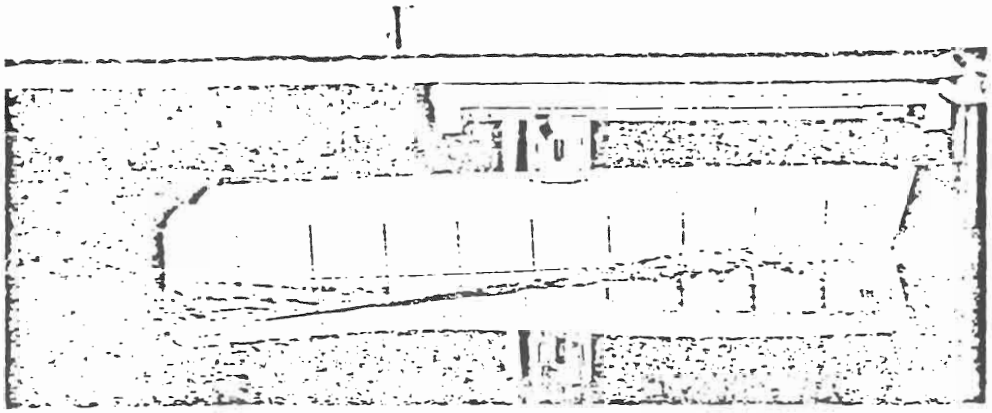

$F_N = 0.33$

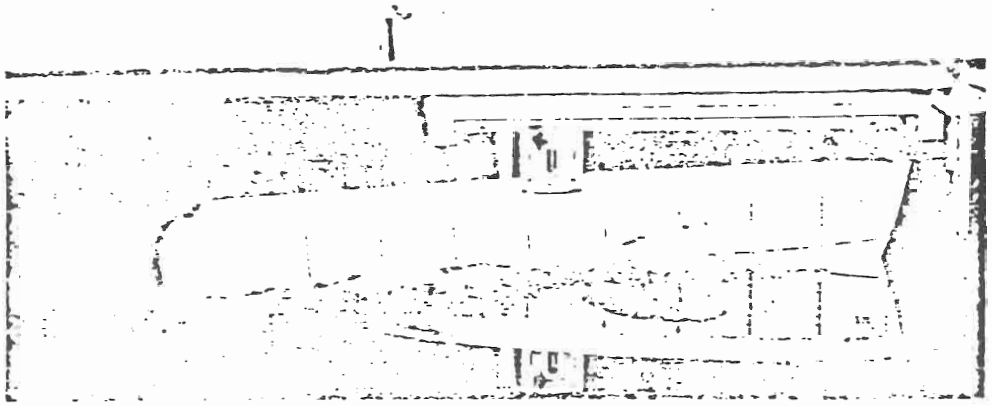

$F_N = 0.77$

MODEL Nº 250C

$L/B = 4.54$

(M) = 4.86

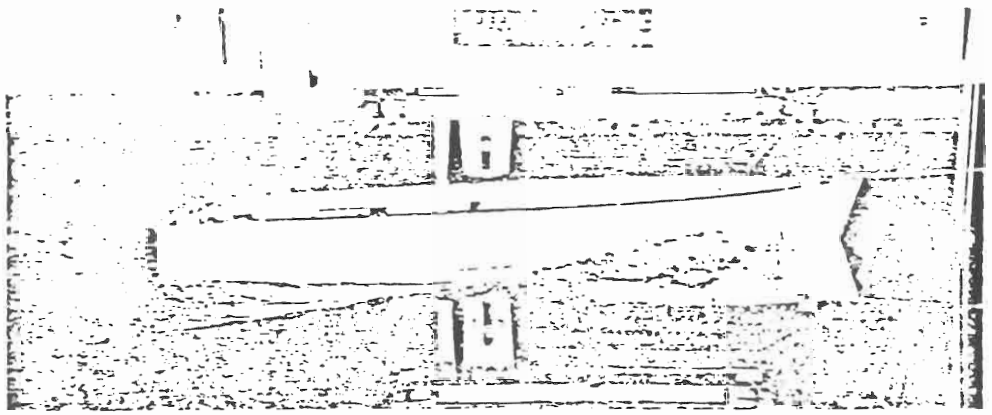

$F_N = 0.48$

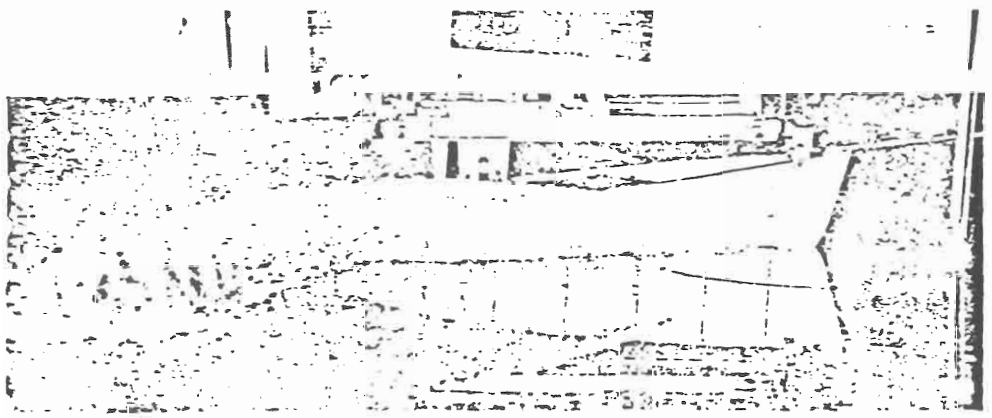

$F_N = 1.1$

MODEL Nº 320 D

$L/B = 3.33$

(M) = 4.47

CALM WATER RESISTANCE EXPERIMENTS

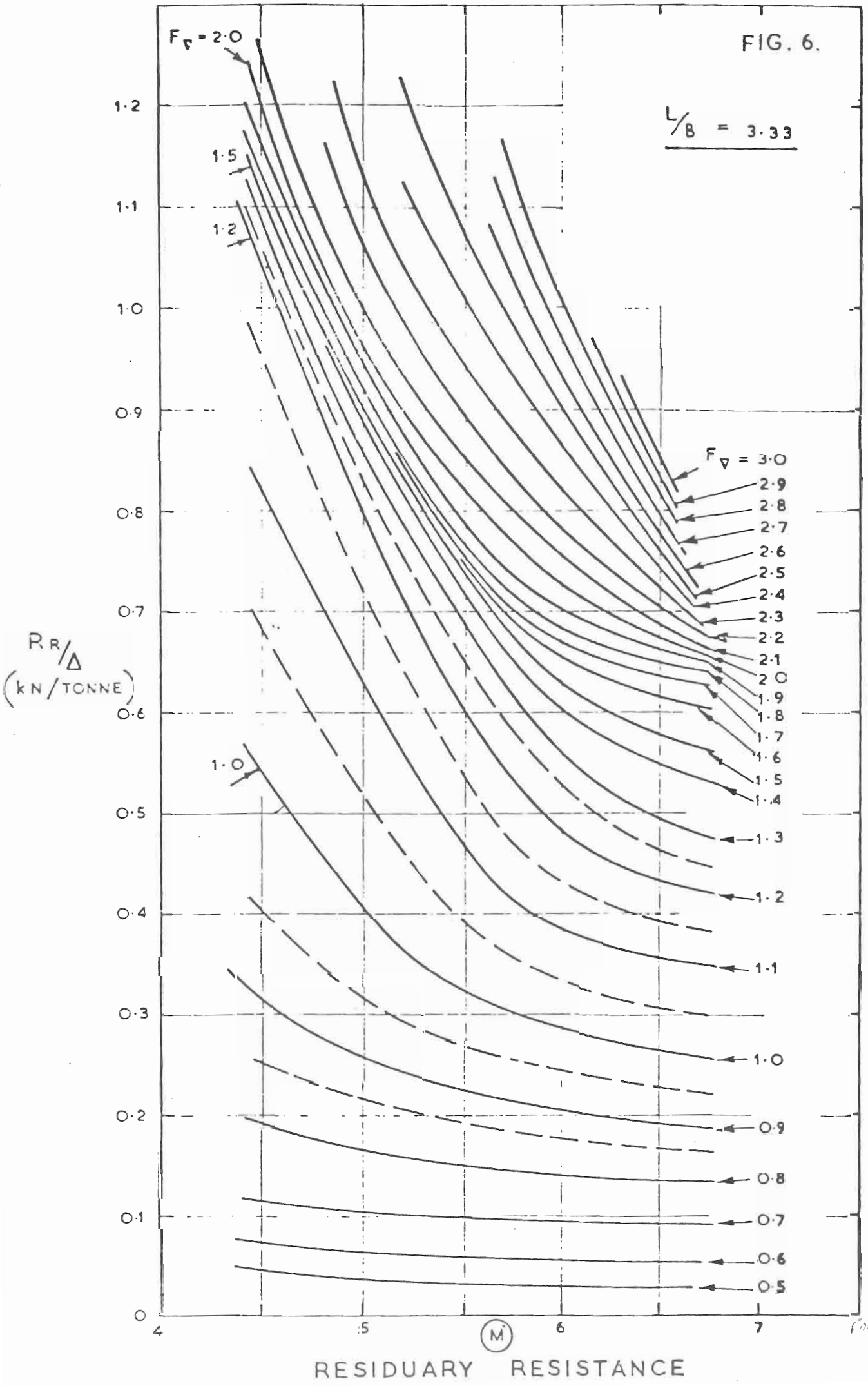
FIG. 6.
L/B = 3·33
F∇ = 2·0
1·5
1·2
1·0
F∇ = 3·0
2·9
2·8
2·7
2·6
2·5
2·4
2·3
2·2
2·1
2·0
1·9
1·8
1·7
1·6
1·5
1·4
1·3
1·2
1·1
1·0
0·9
0·8
0·7
0·6
0·5
RR/Δ (kN/TONNE)
0
0·1
0·2
0·3
0·4
0·5
0·6
0·7
0·8
0·9
1·0
1·1
1·2
4
5
6
7
M
RESIDUARY RESISTANCE

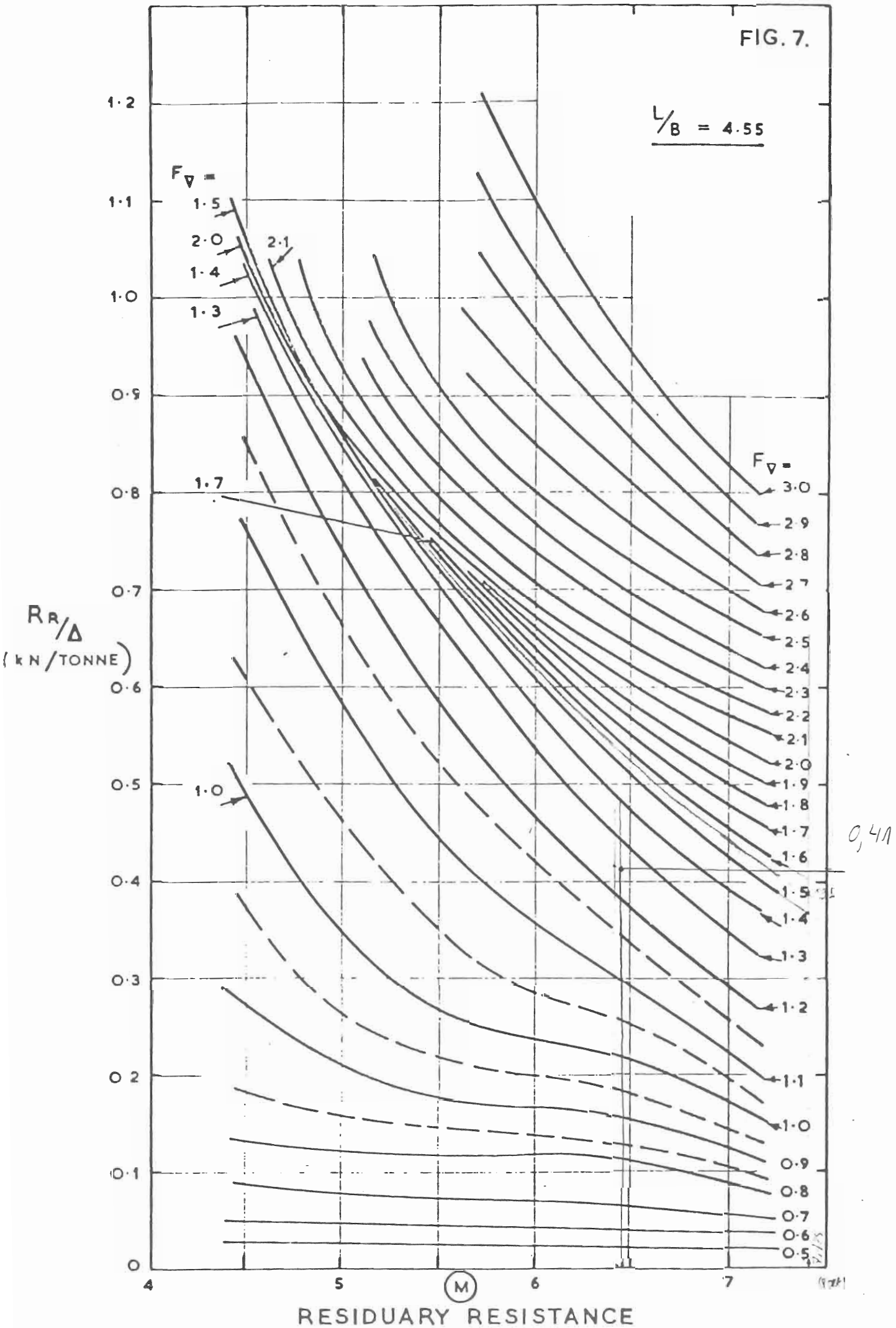
FIG. 7.
L/B = 4.55
F∇ =
1·5
2·0
2·1
1·4
1·3
1·7
1·0
F∇ =
3·0
2·9
2·8
2·7
2·6
2·5
2·4
2·3
2·2
2·1
2·0
1·9
1·8
1·7
1·6
1·5
1·4
1·3
1·2
1·1
1·0
0·9
0·8
0·7
0·6
0·5
0,41
RR/Δ
(kN/TONNE)
1·2
1·1
1·0
0·9
0·8
0·7
0·6
0·5
0·4
0·3
0 2
0·1
0
4
5
M
6
7
RESIDUARY RESISTANCE

FIG. 8.

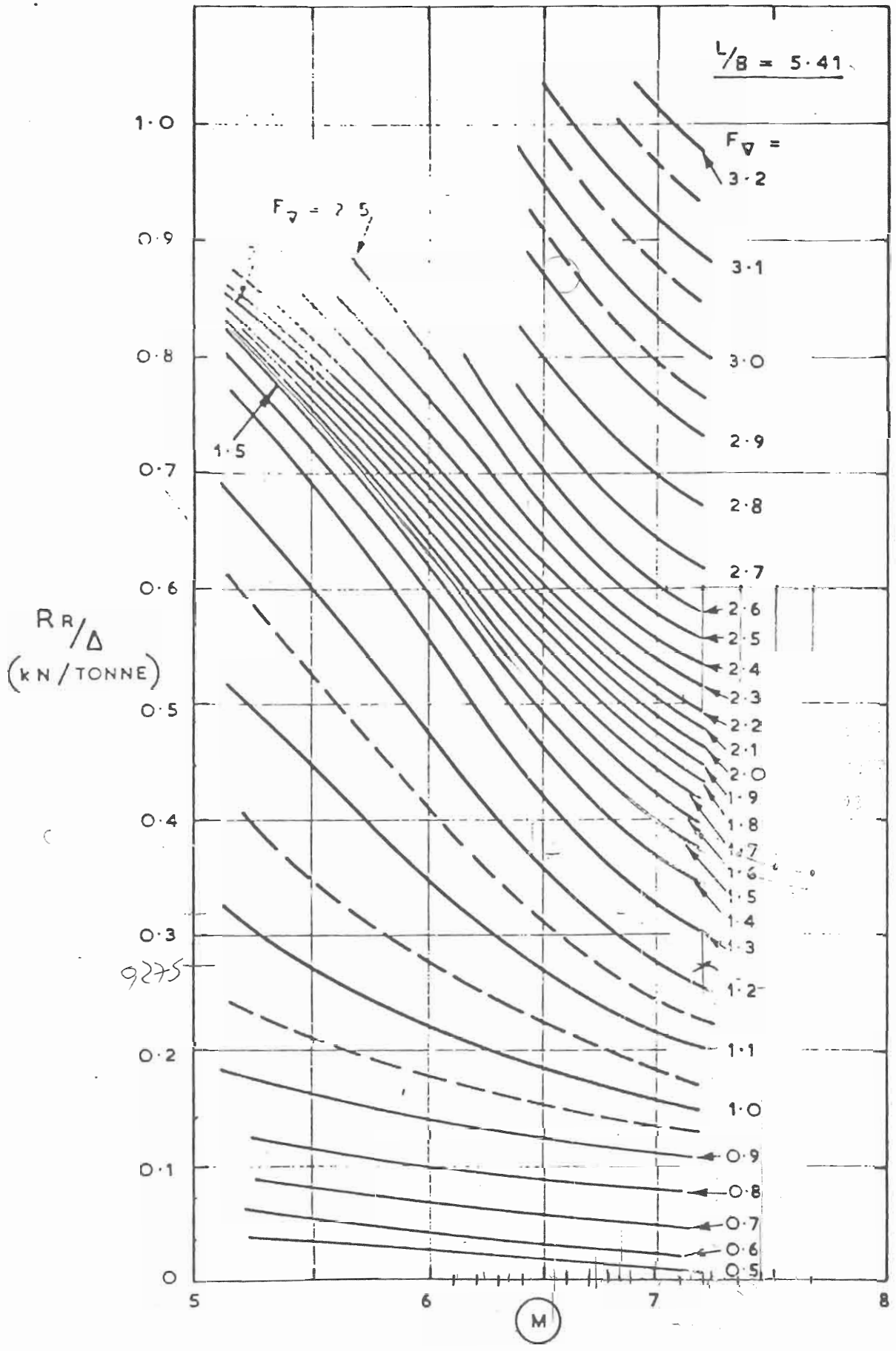

RESIDUARY RESISTANCE

L/B 5,68

0,25

FIG. 9.

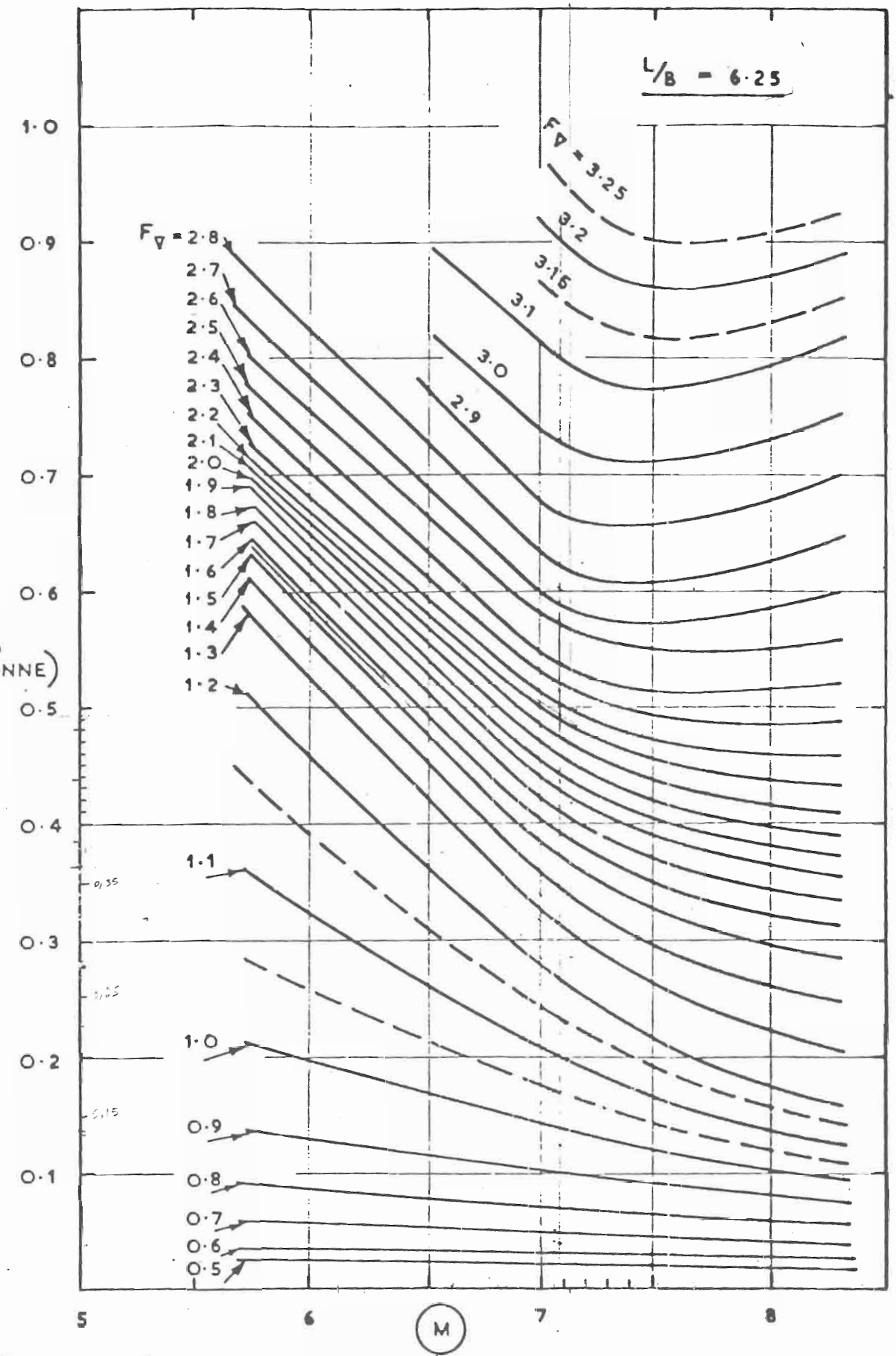

$\frac{R_R}{\Delta} = 0,48$

RESIDUARY RESISTANCE

$\rightarrow R_R = 153,6$ kN

FIG.10.

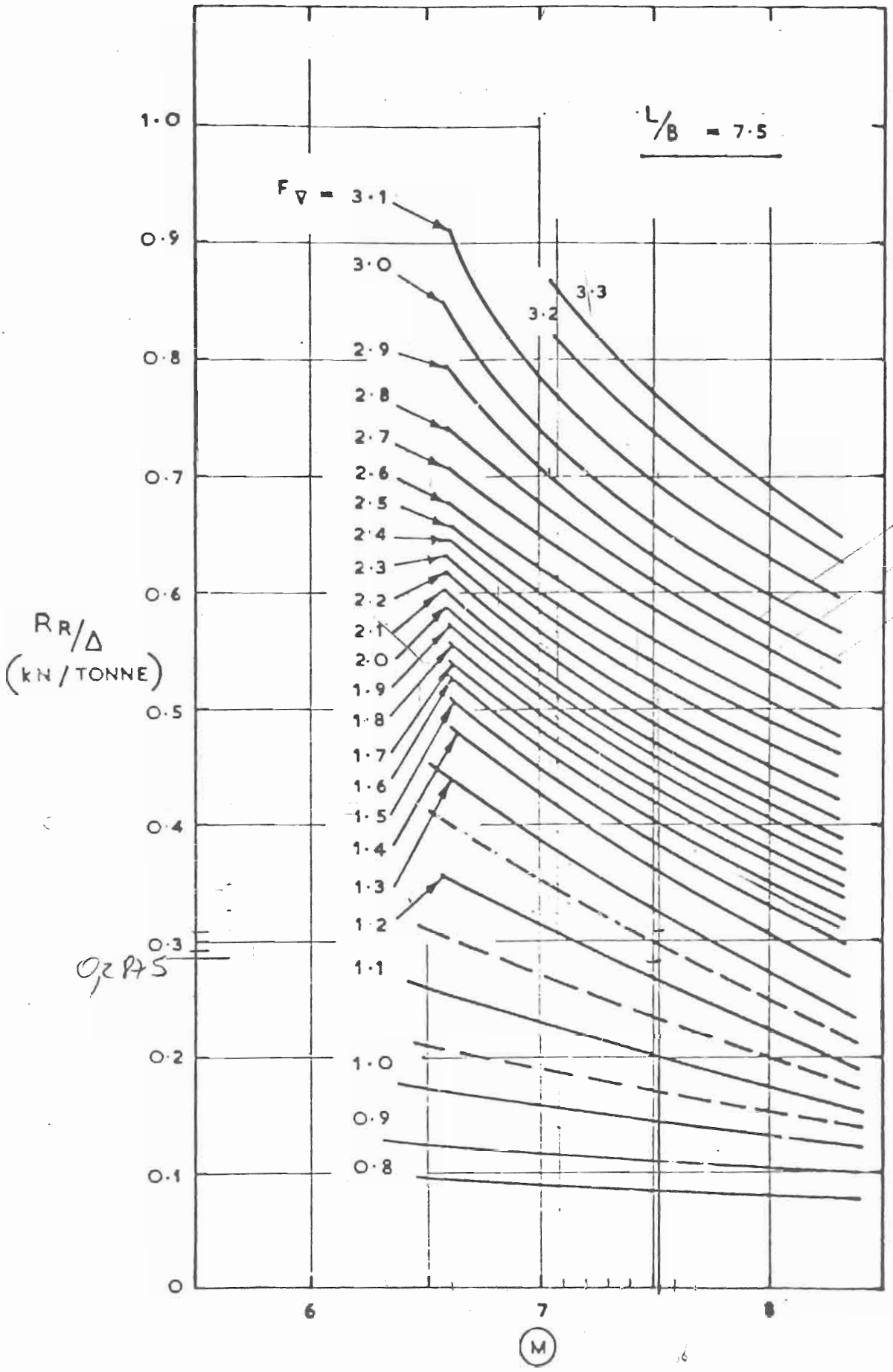

RESIDUARY RESISTANCE

FIG. 11.

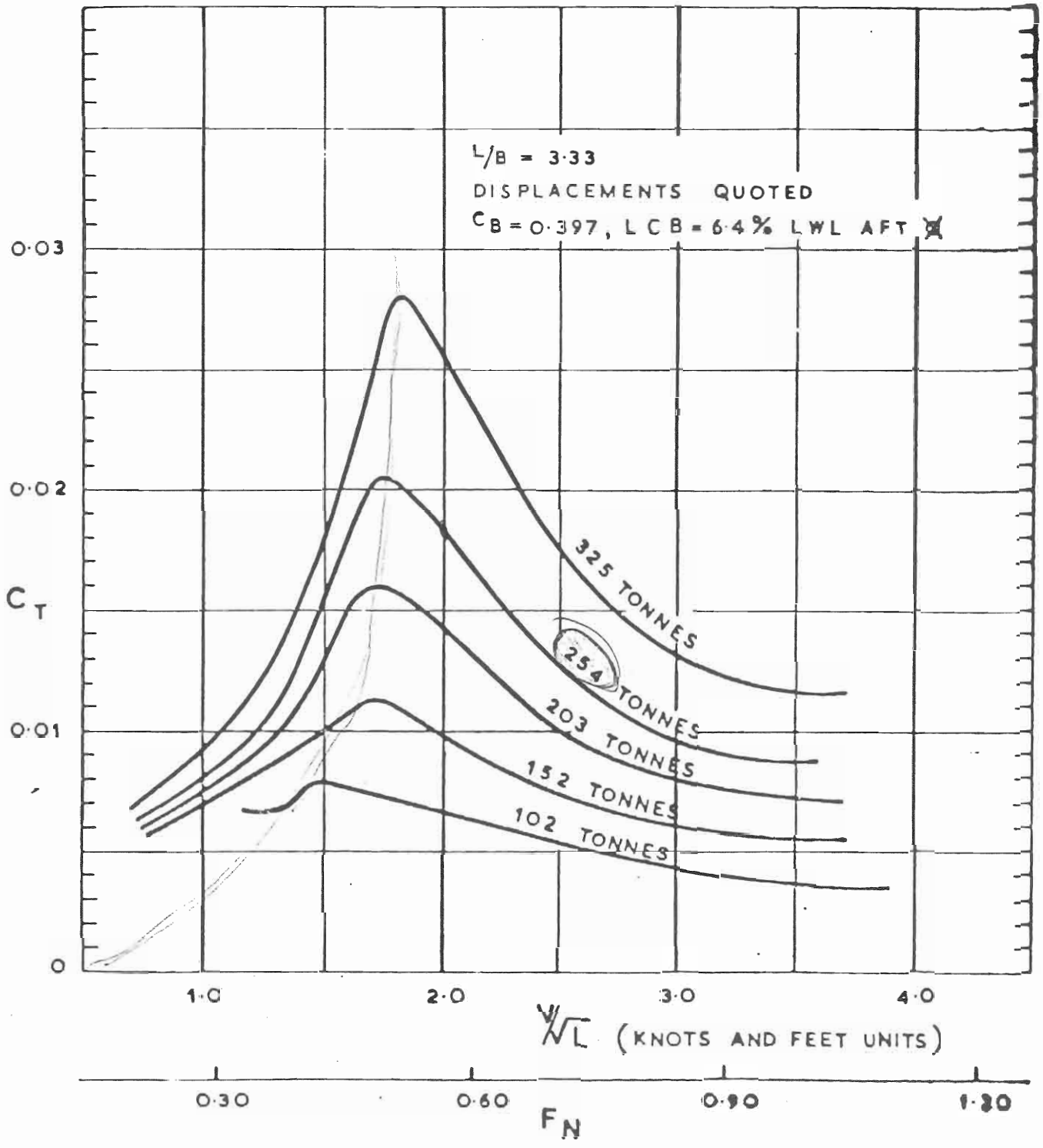

SPECIFIC RESISTANCE COEFFICIENT, C_T

VALUES OF C_T FOR BARE HULL 30·5m LONG

(ZERO ROUGHNESS ALLOWANCE)

FIG. 12.

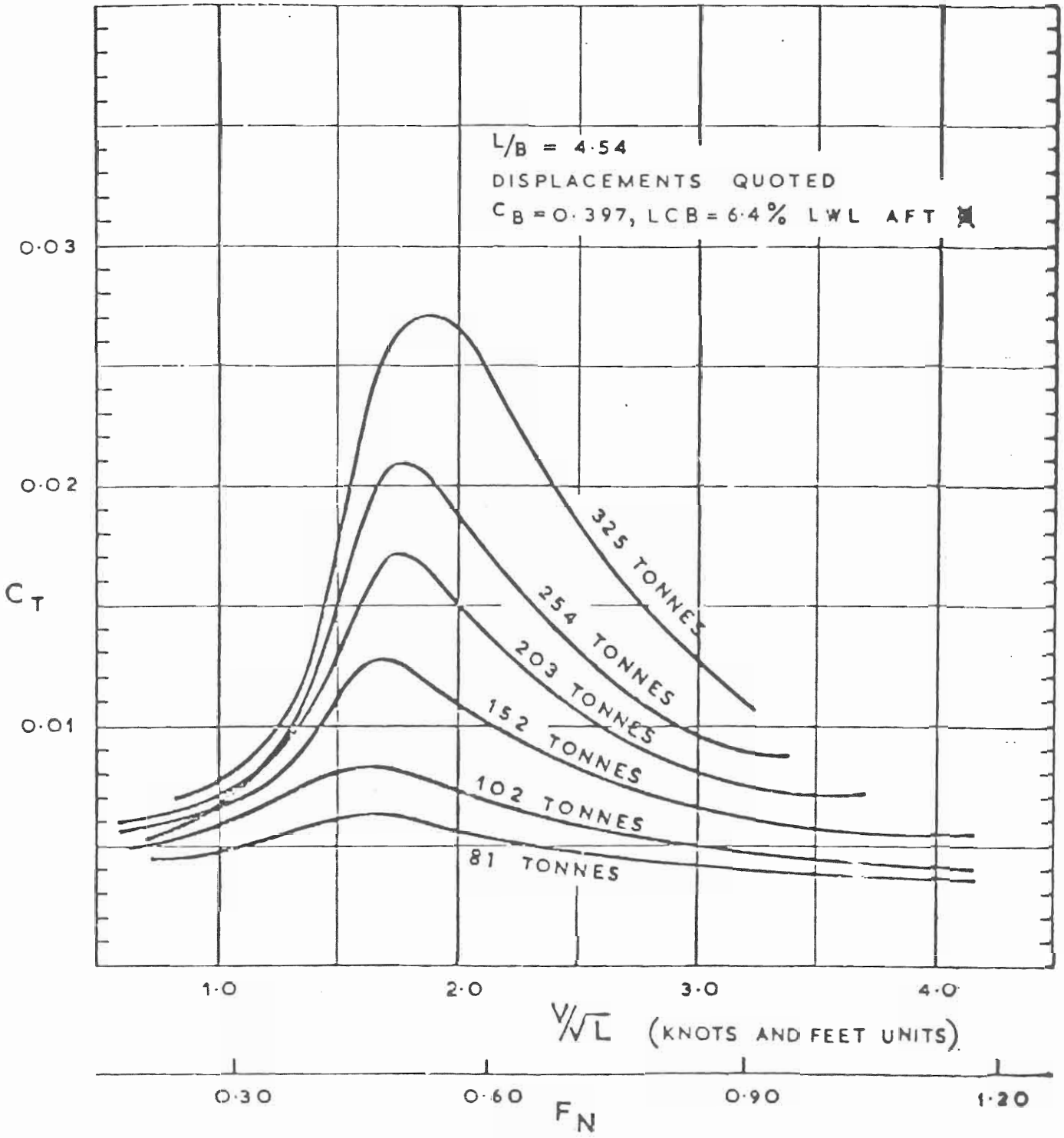

SPECIFIC RESISTANCE COEFFICIENT, C_T

VALUES OF C_T FOR BARE HULL 30·5m LONG

(ZERO ROUGHNESS ALLOWANCE)

FIG.13.

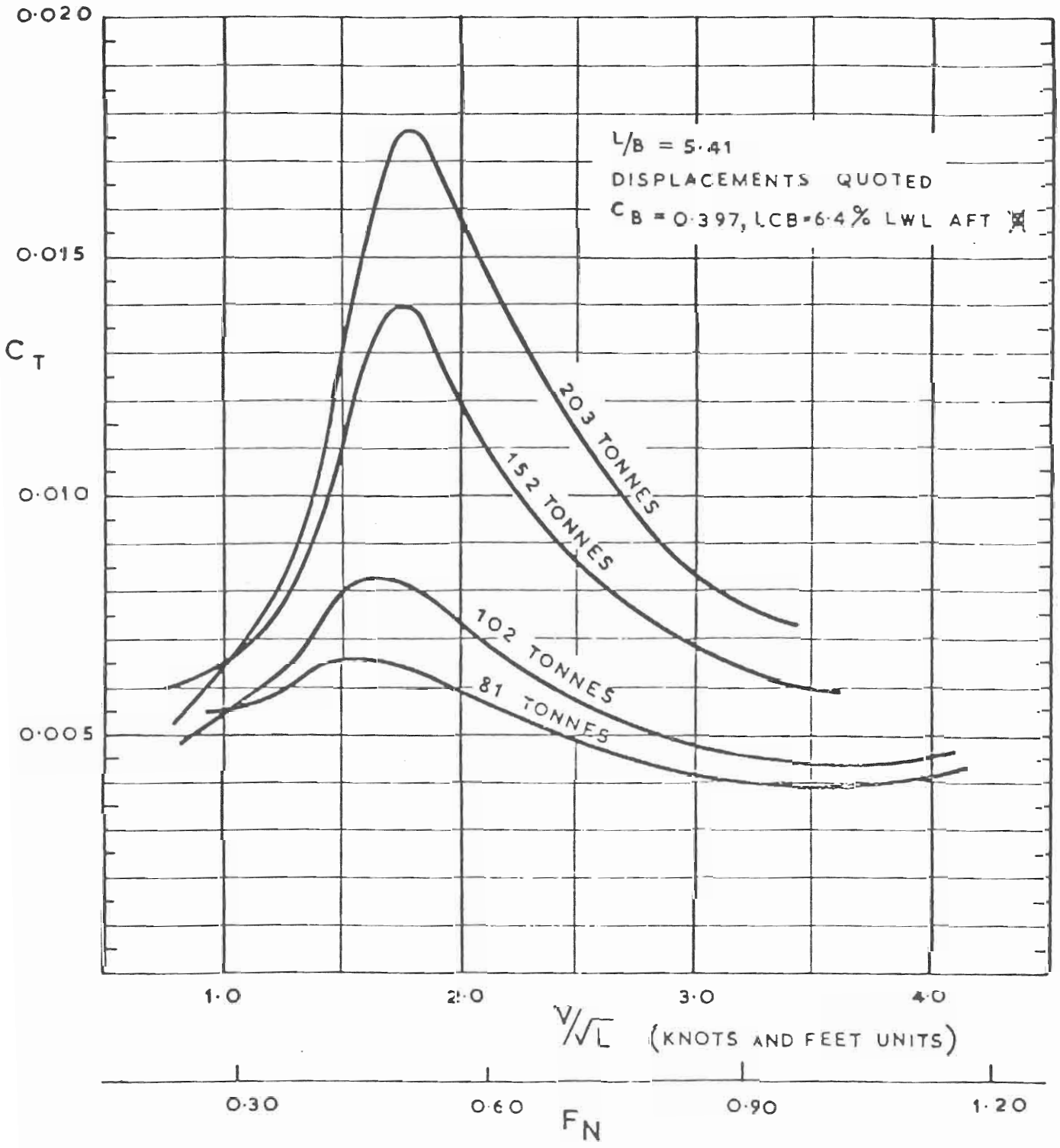

SPECIFIC RESISTANCE COEFFICIENT, C_T

VALUES OF C_T FOR BARE HULL 30·5m LONG

(ZERO ROUGHNESS ALLOWANCE)

FIG. 14

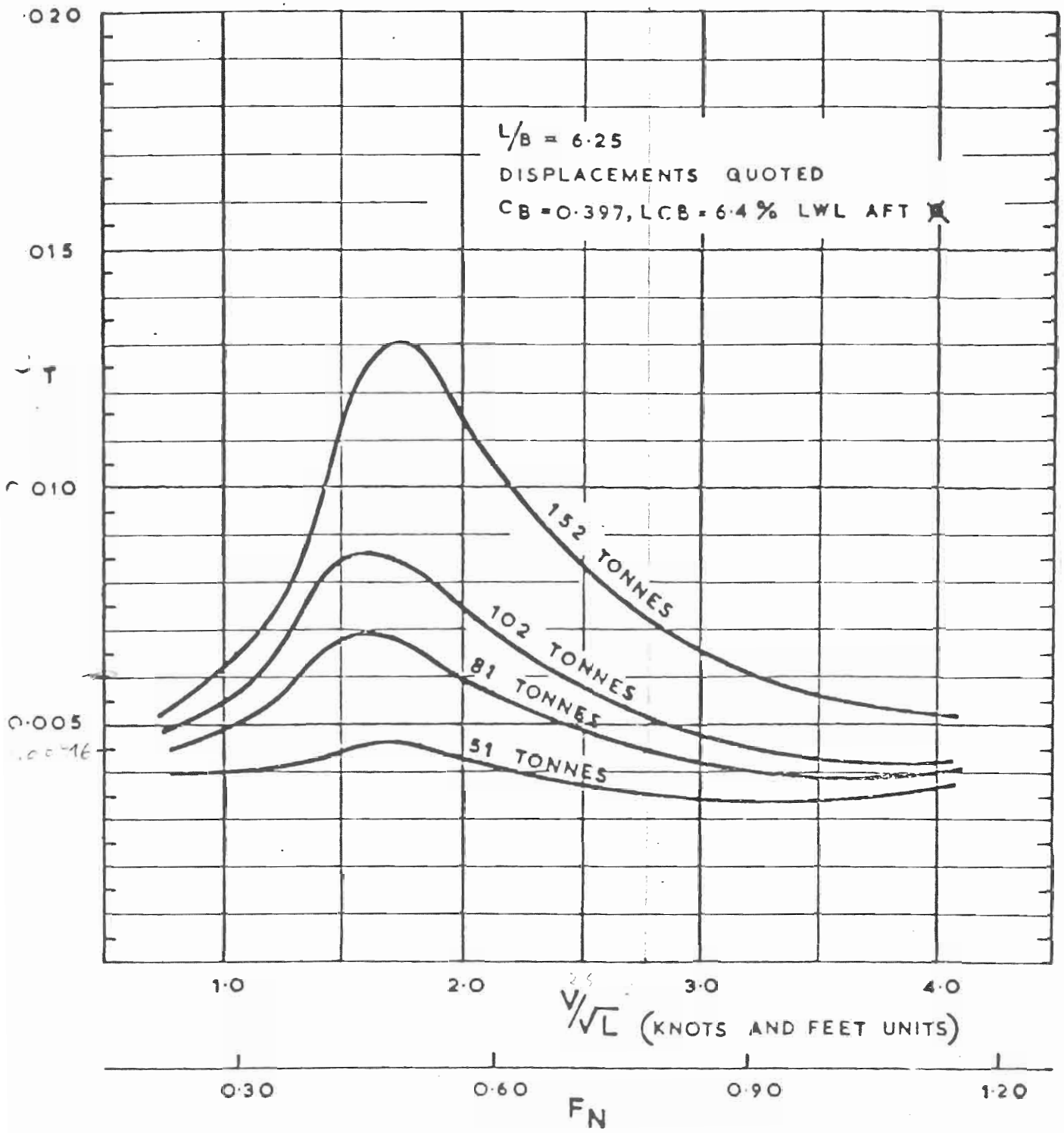

SPECIFIC RESISTANCE COEFFICIENT, C_T

VALUES OF C_T FOR BARE HULL 30·5 m LONG

(ZERO ROUGHNESS ALLOWANCE)

FIG. 15.

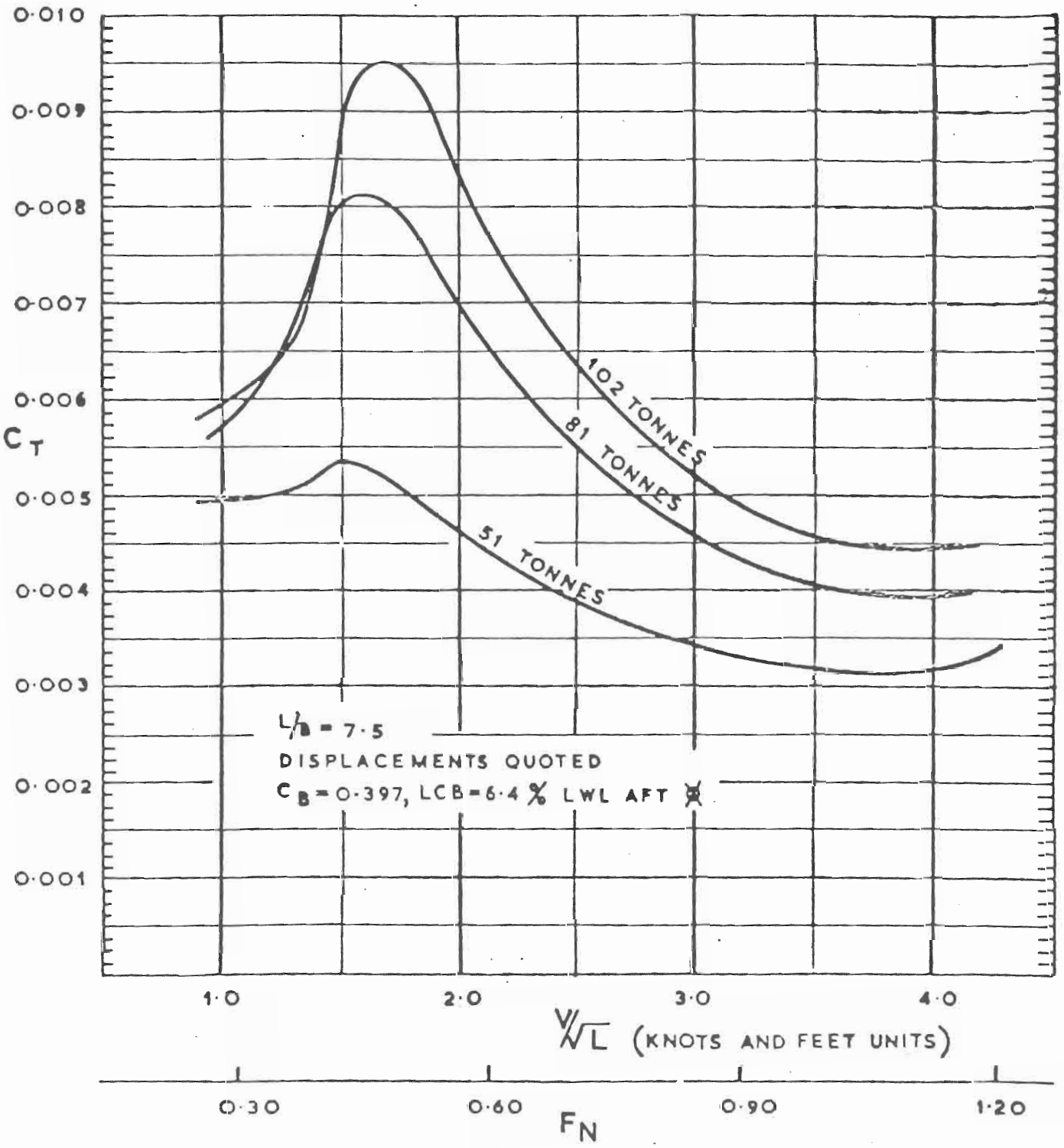

SPECIFIC RESISTANCE COEFFICIENT C_T

VALUES OF C_T FOR BARE HULL 30·5m LONG

(ZERO ROUGHNESS ALLOWANCE)

FIG. 16.

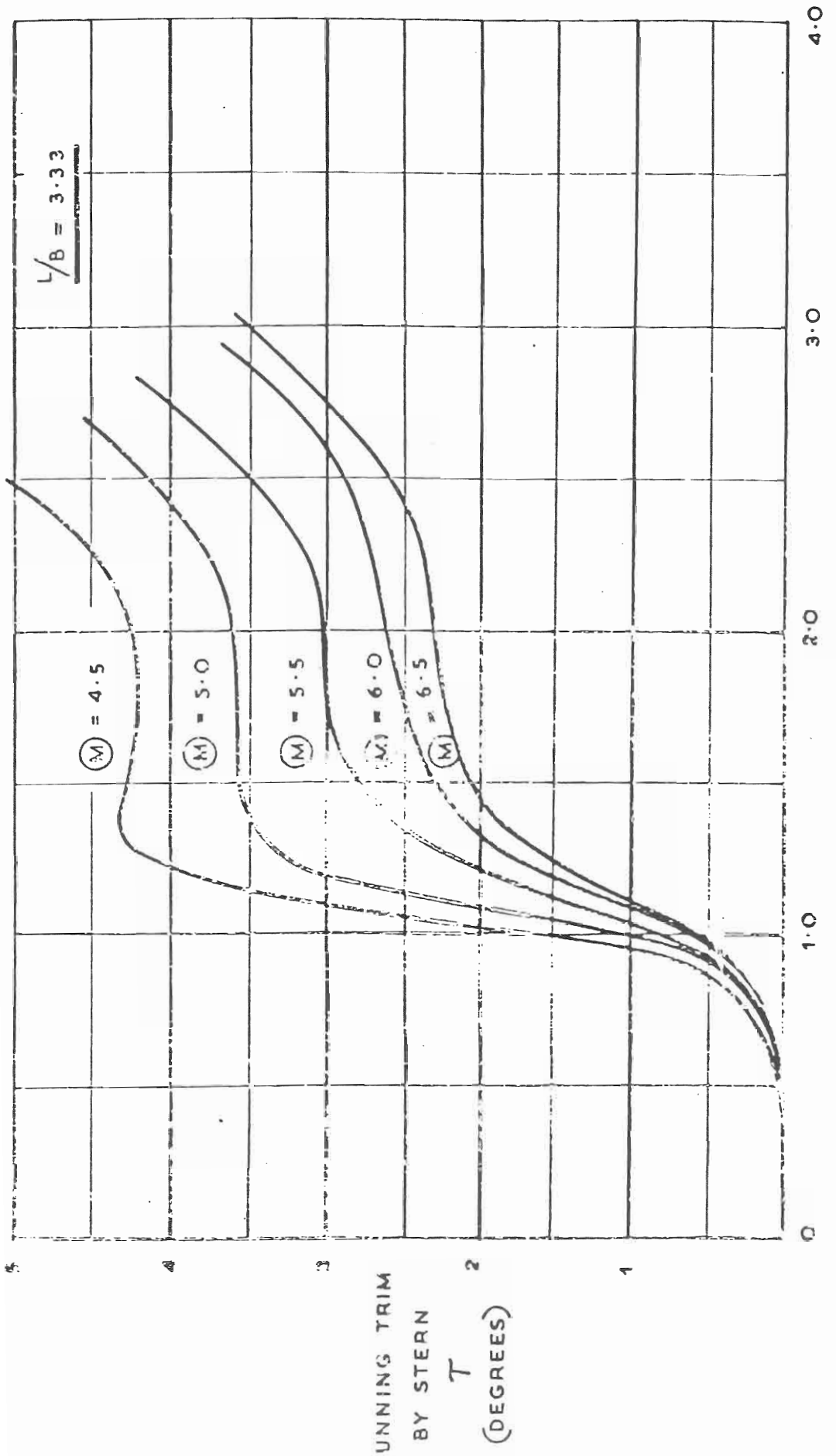

RUNNING TRIM

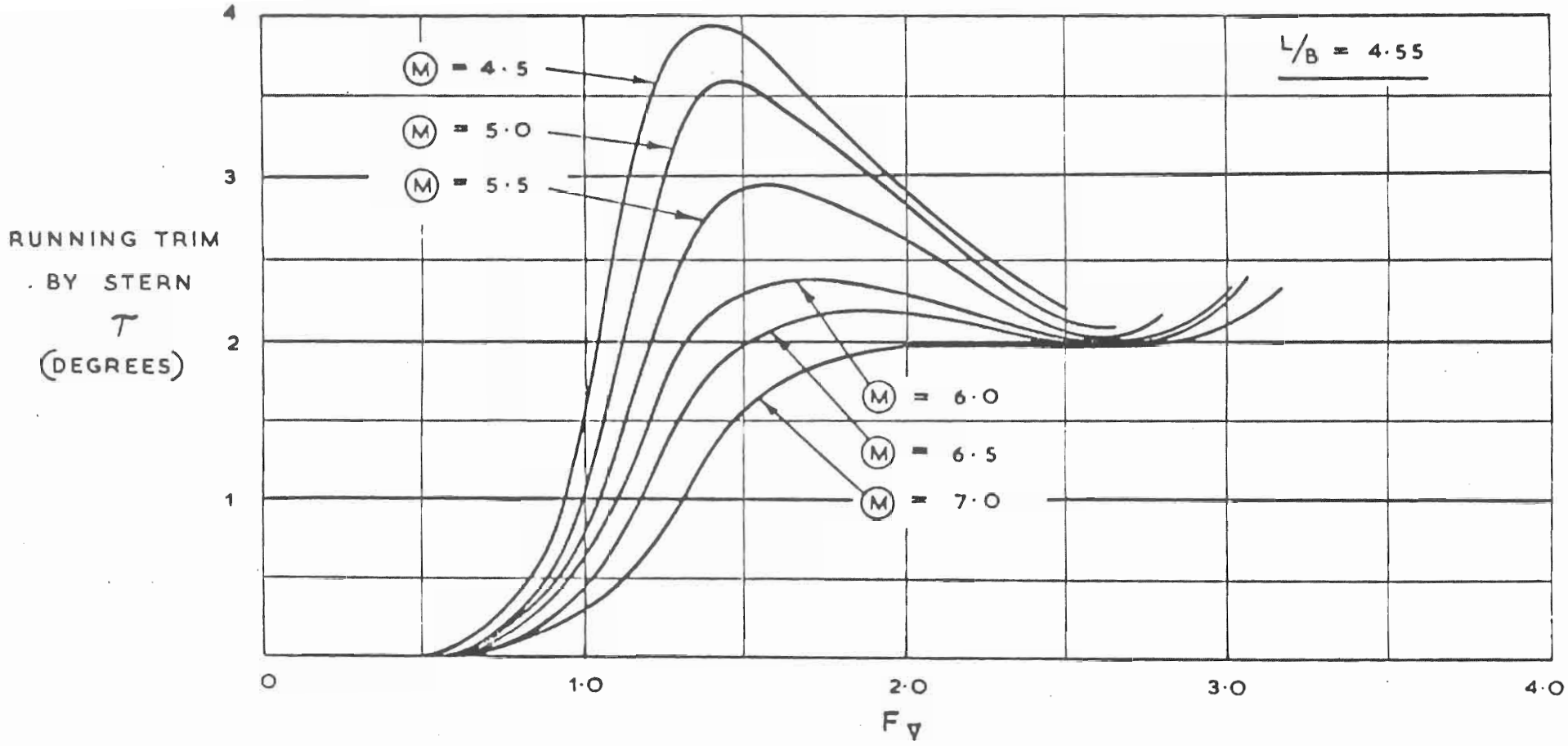

RUNNING TRIM

FIG.17.

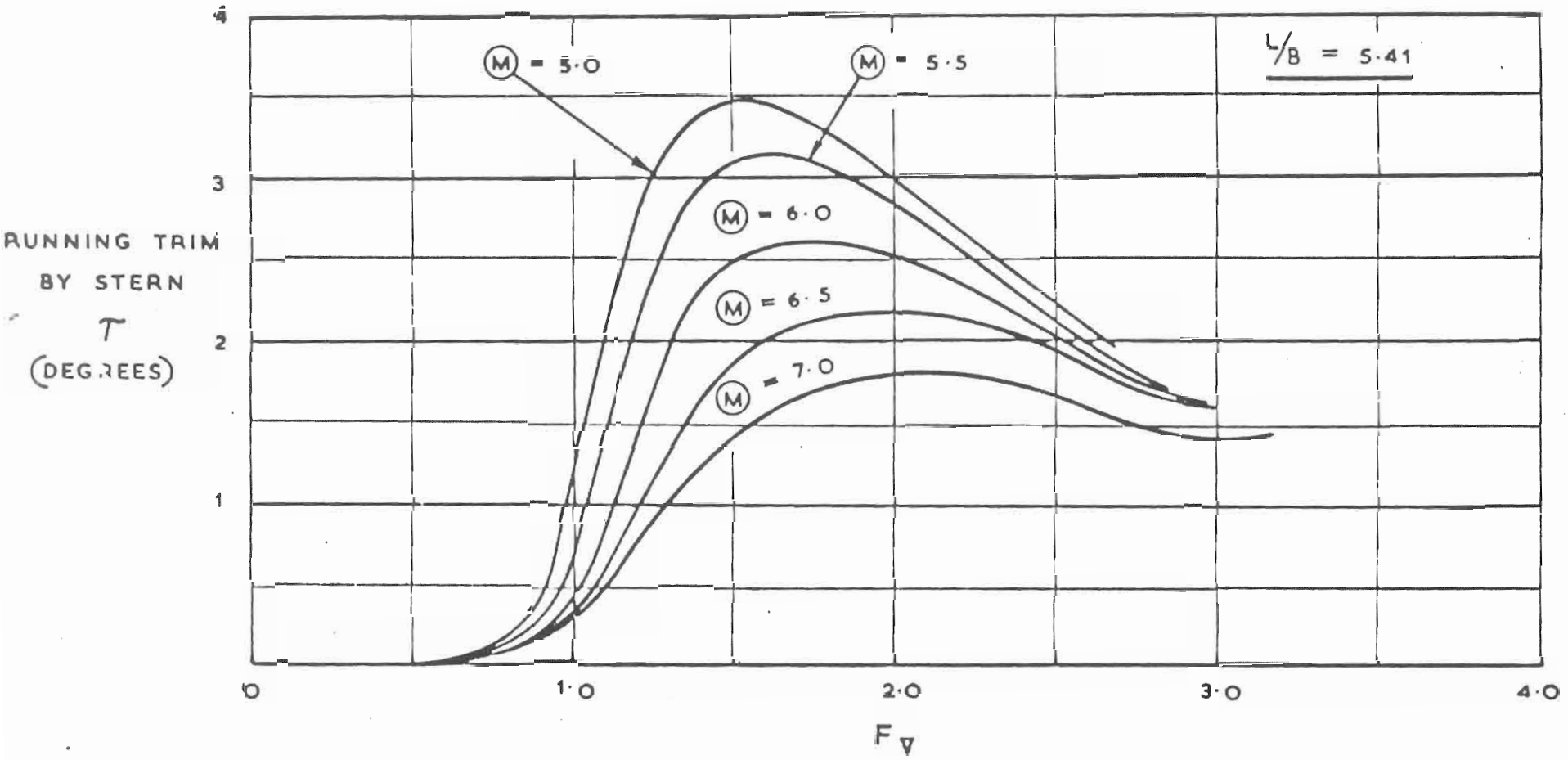

RUNNING TRIM

FIG.18.

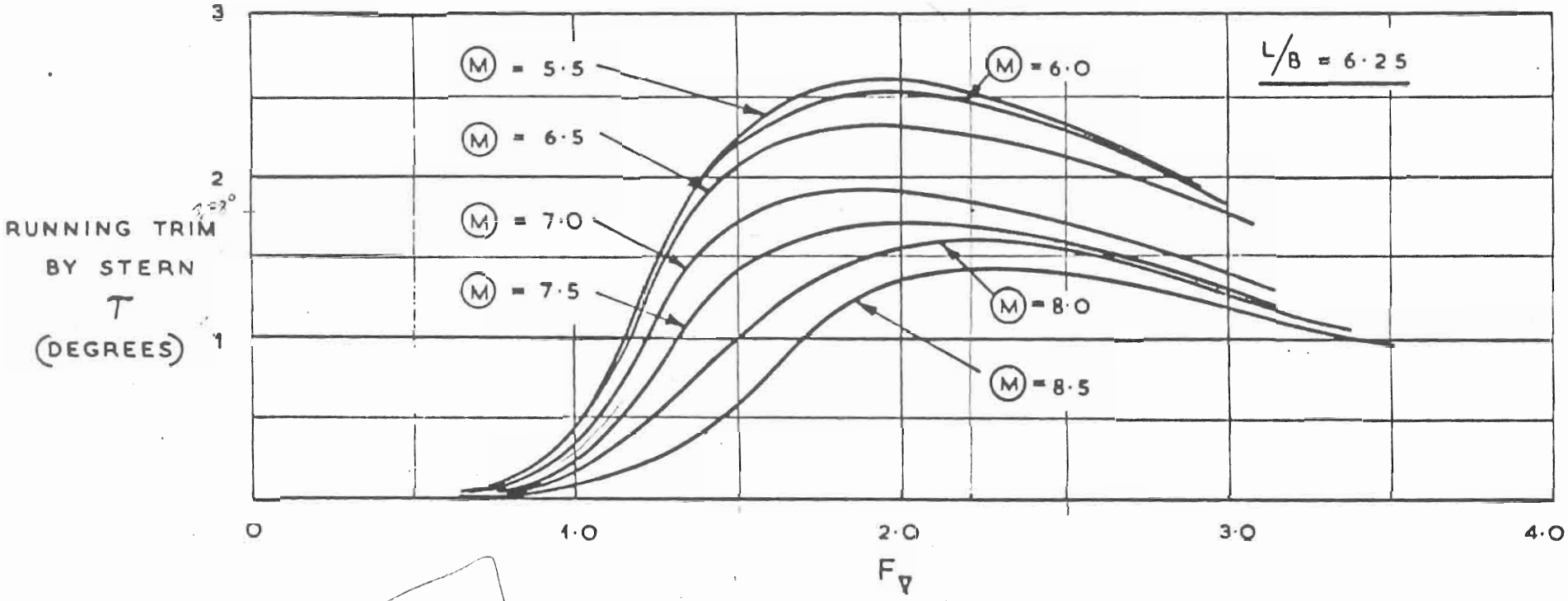

RUNNING TRIM

FIG. 19.

FIG. 20.

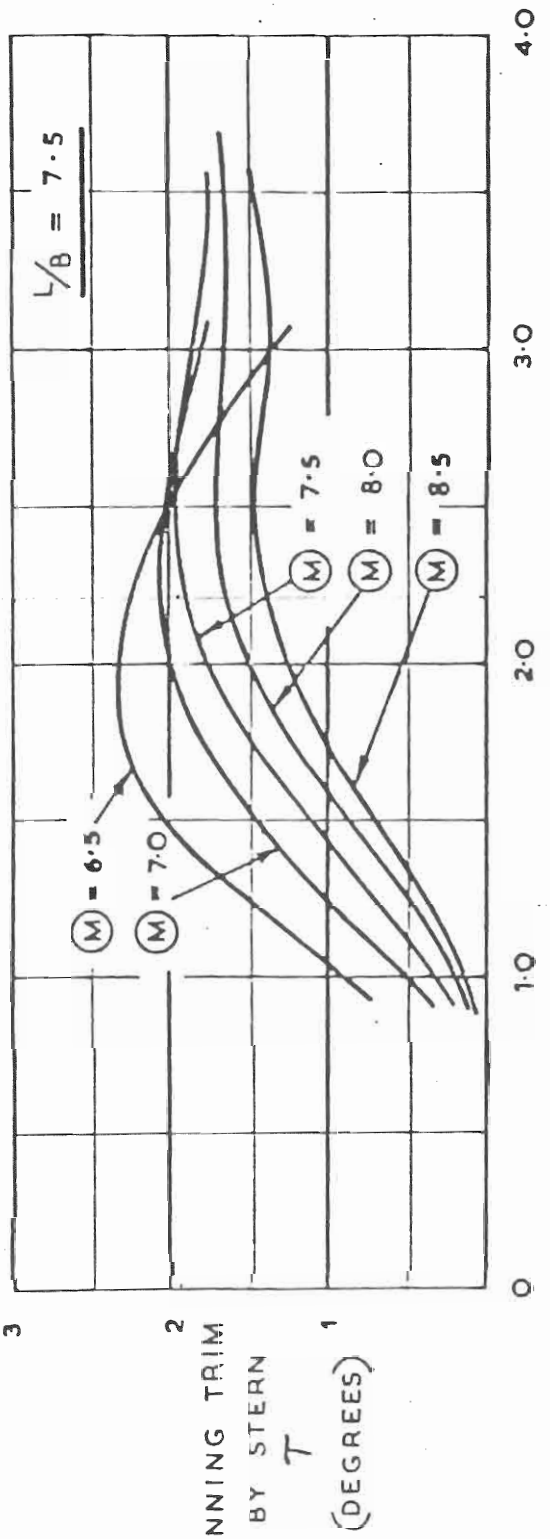

RUNNING TRIM

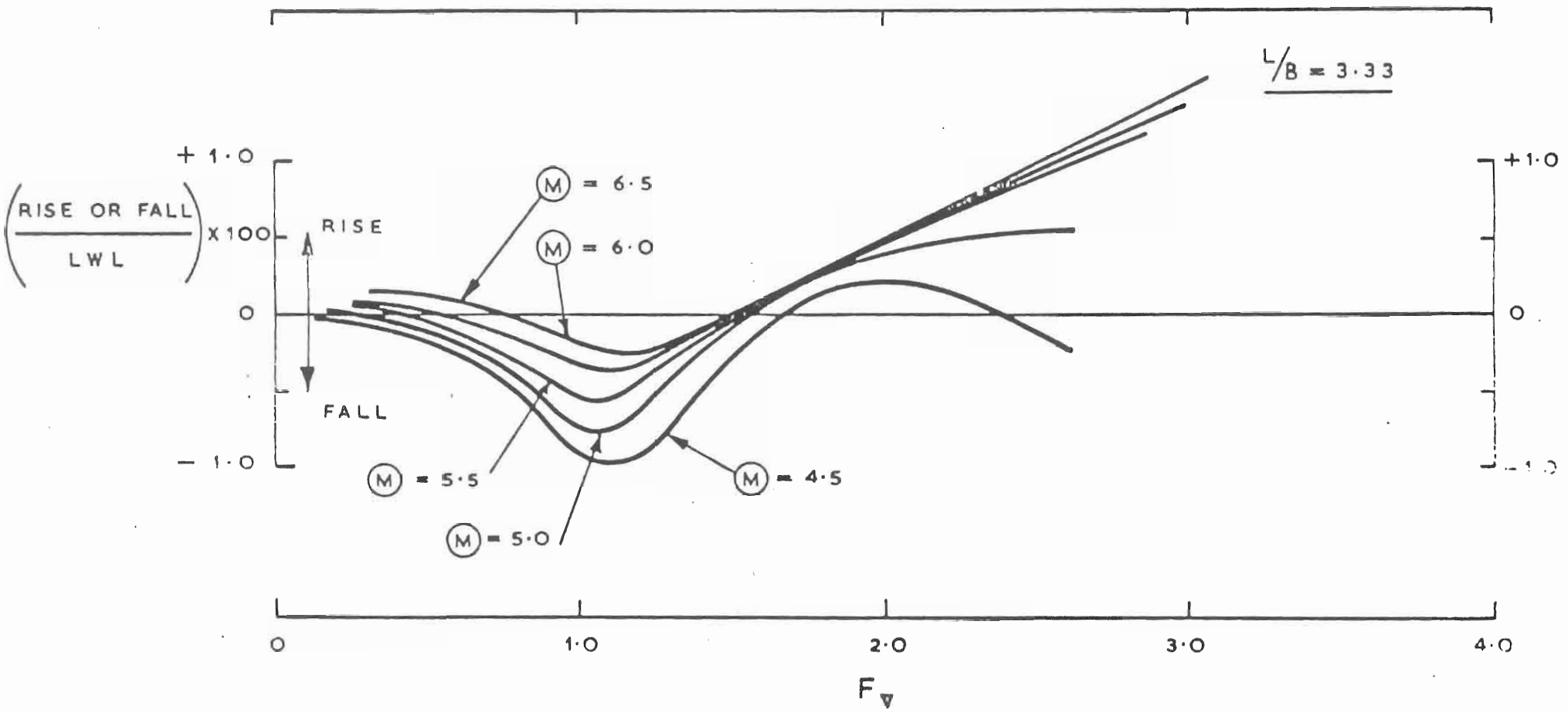

RISE OR FALL OF HULL AT ITS LCG

LCG IS 43·6 % LWL FORWARD OF THE TRANSOM, FOR LEVEL TRIM AT REST

FIG. 21.

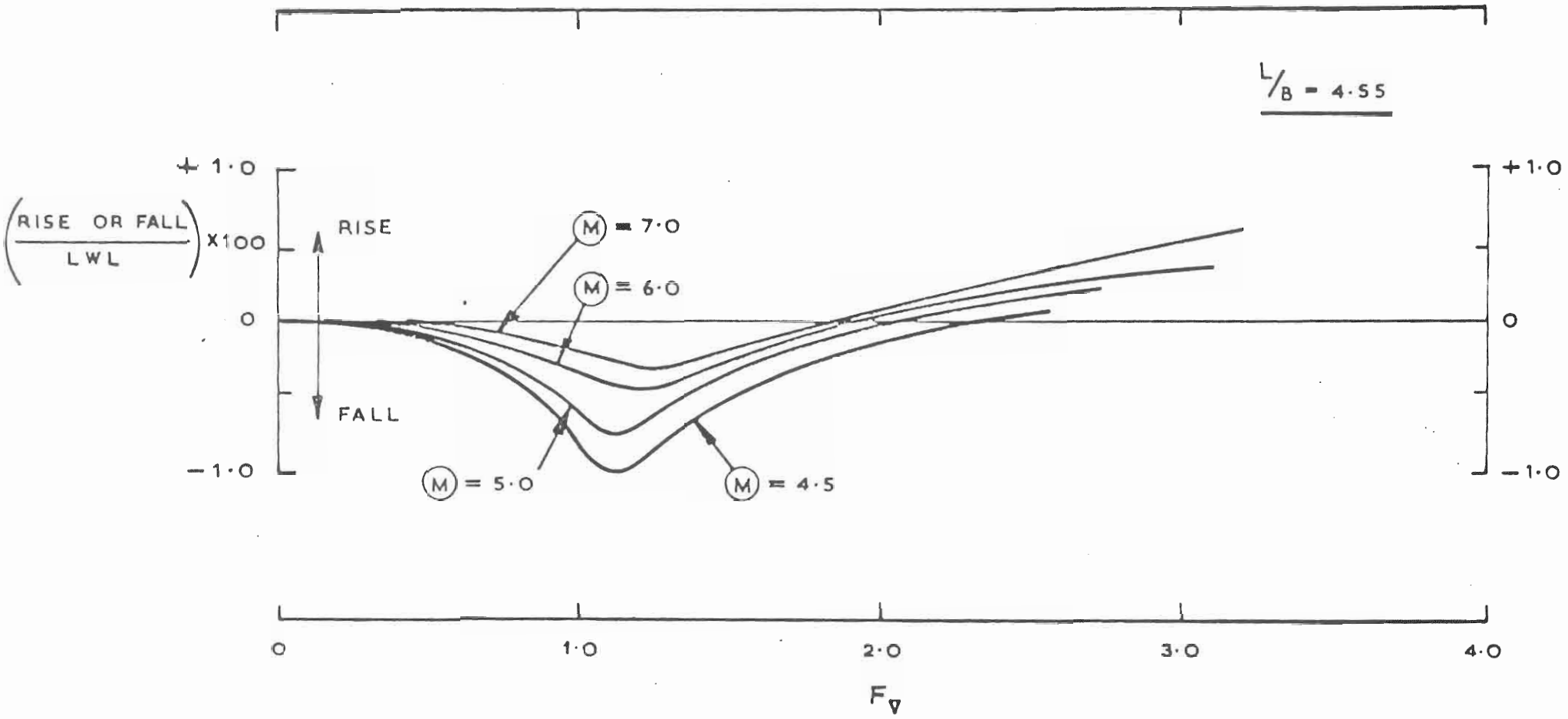

RISE OR FALL OF HULL AT ITS LCG

LCG IS 43·6 % LWL FORWARD OF THE TRANSOM, FOR LEVEL TRIM AT REST

FIG.22.

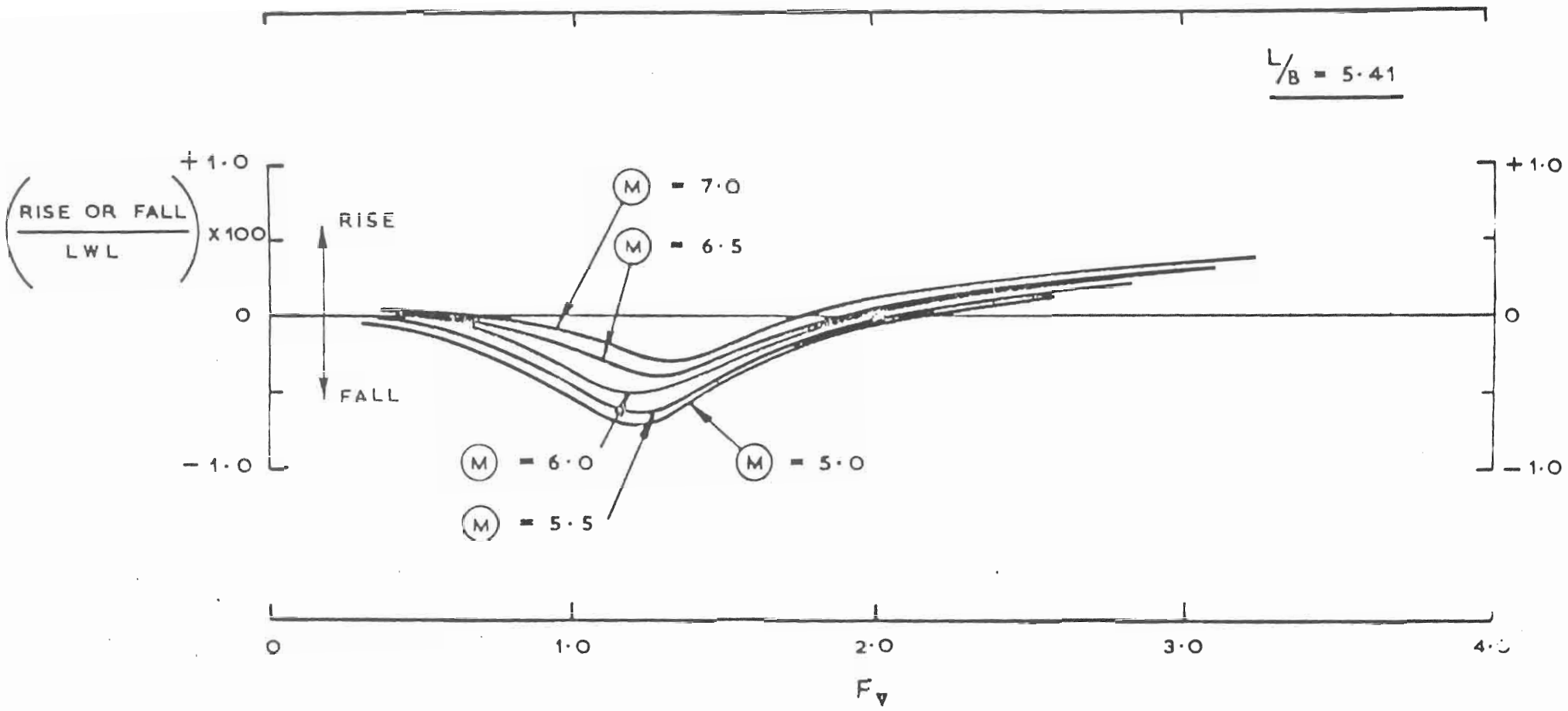

RISE OR FALL OF HULL AT ITS LCG

LCG IS 43·6 % LWL FORWARD OF THE TRANSOM , FOR LEVEL TRIM AT REST

FIG. 23.

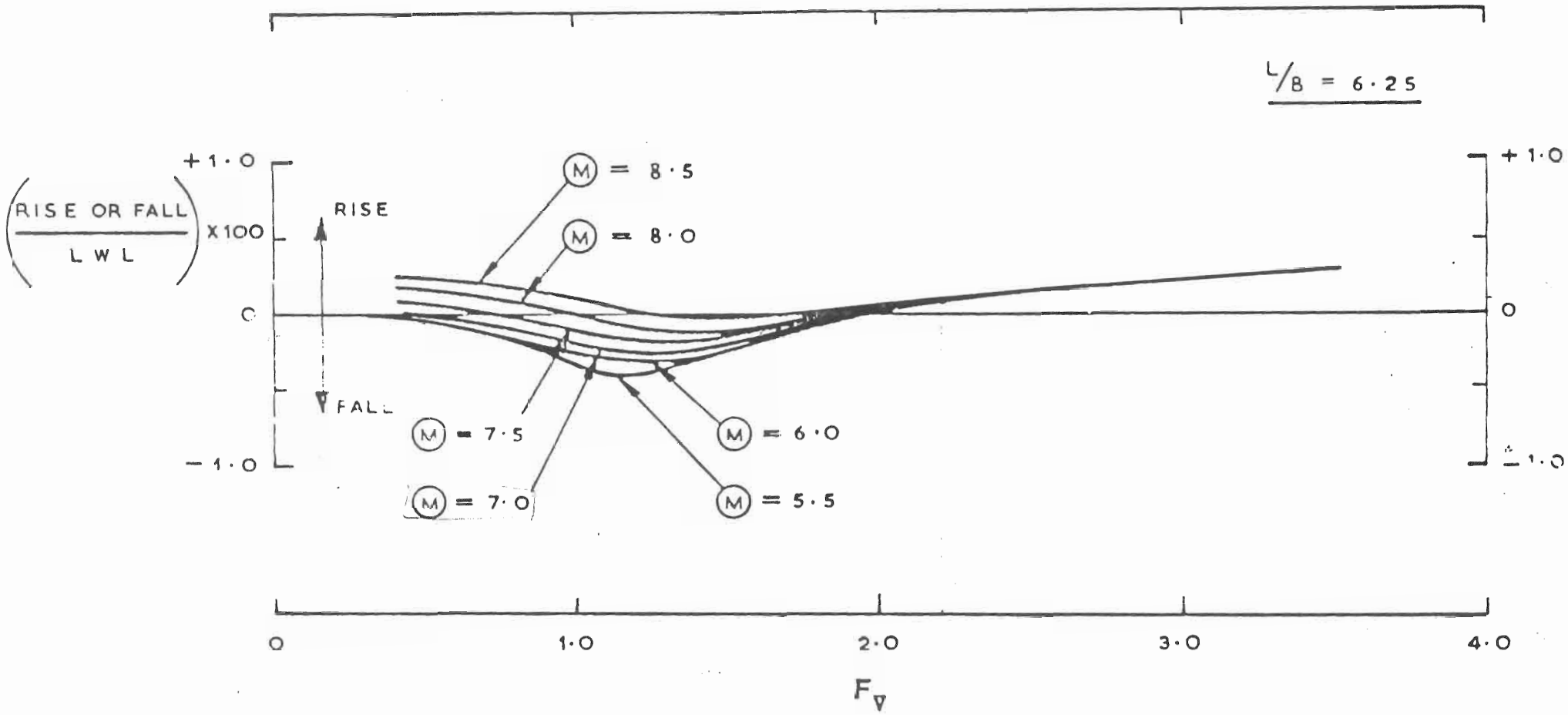

RISE OR FALL OF HULL AT ITS LCG

LCG IS 43·6% LWL FORWARD OF THE TRANSOM, FOR LEVEL TRIM AT REST

FIG.24.

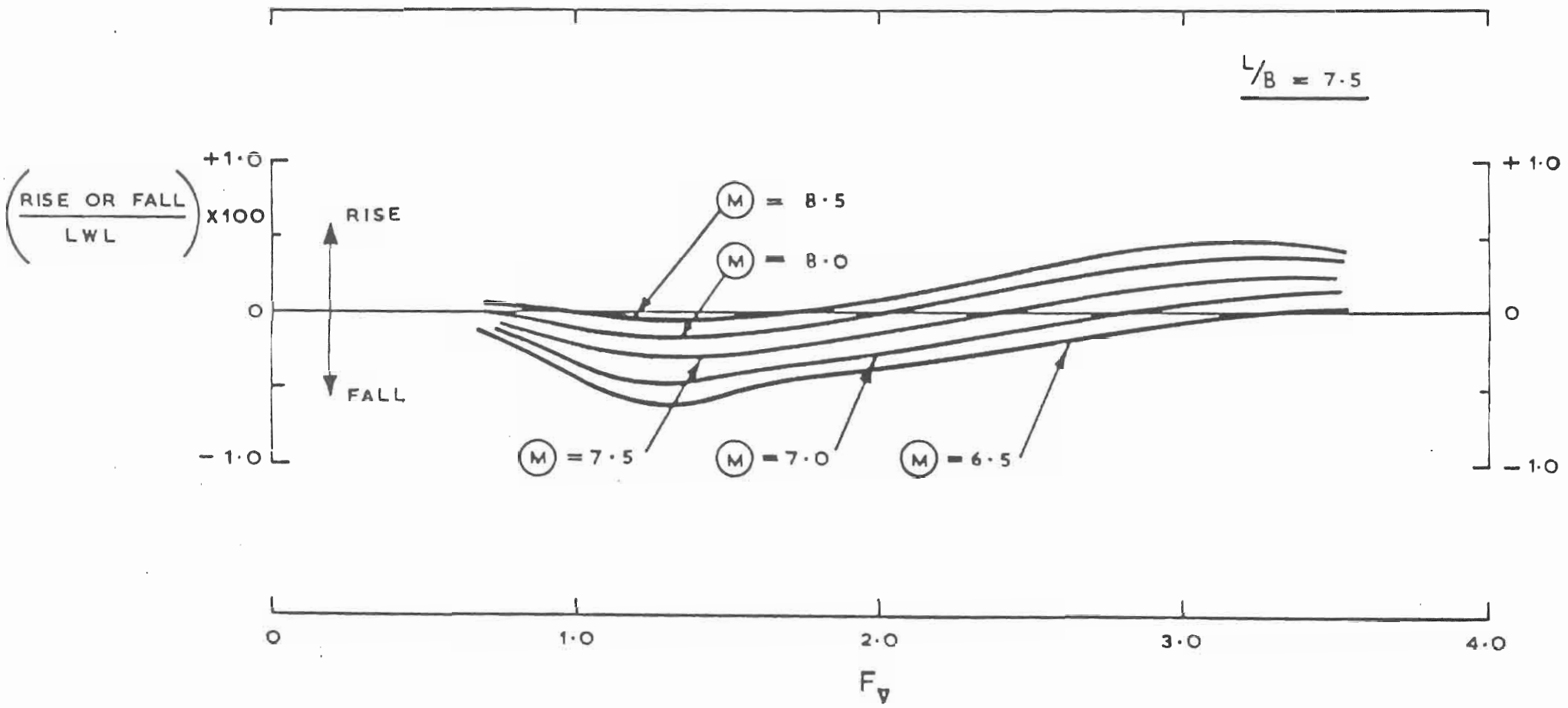

RISE OR FALL OF HULL AT ITS LCG

LCG IS 43·6 % LWL FORWARD OF THE TRANSOM, FOR LEVEL TRIM AT REST

FIG. 25.

FIG.26.

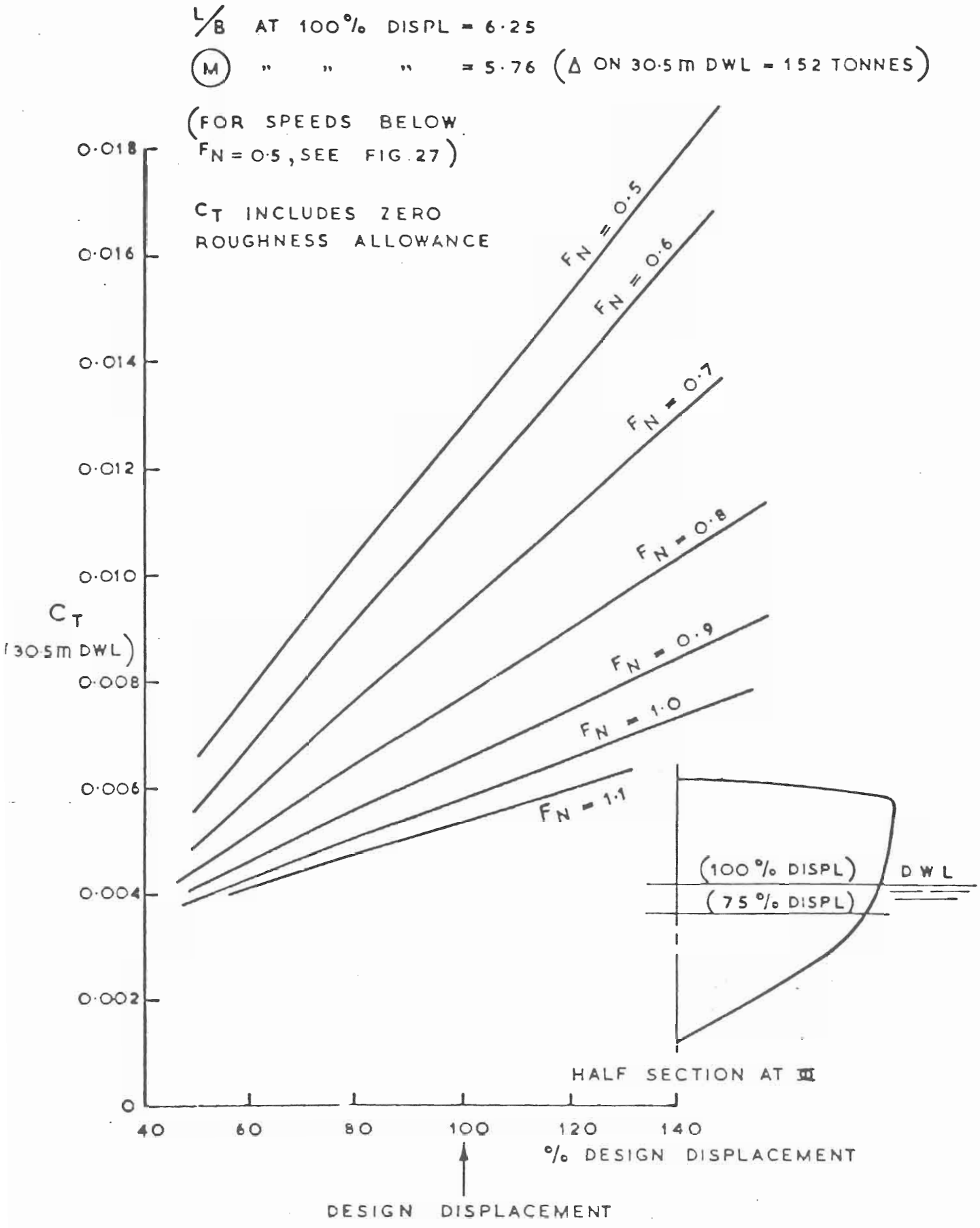

EFFECT OF DISPLACEMENT ON RESISTANCE OF GIVEN HULL FORM

L/B AT 100% DISPL = 6·25

(M) " " " = 5·76

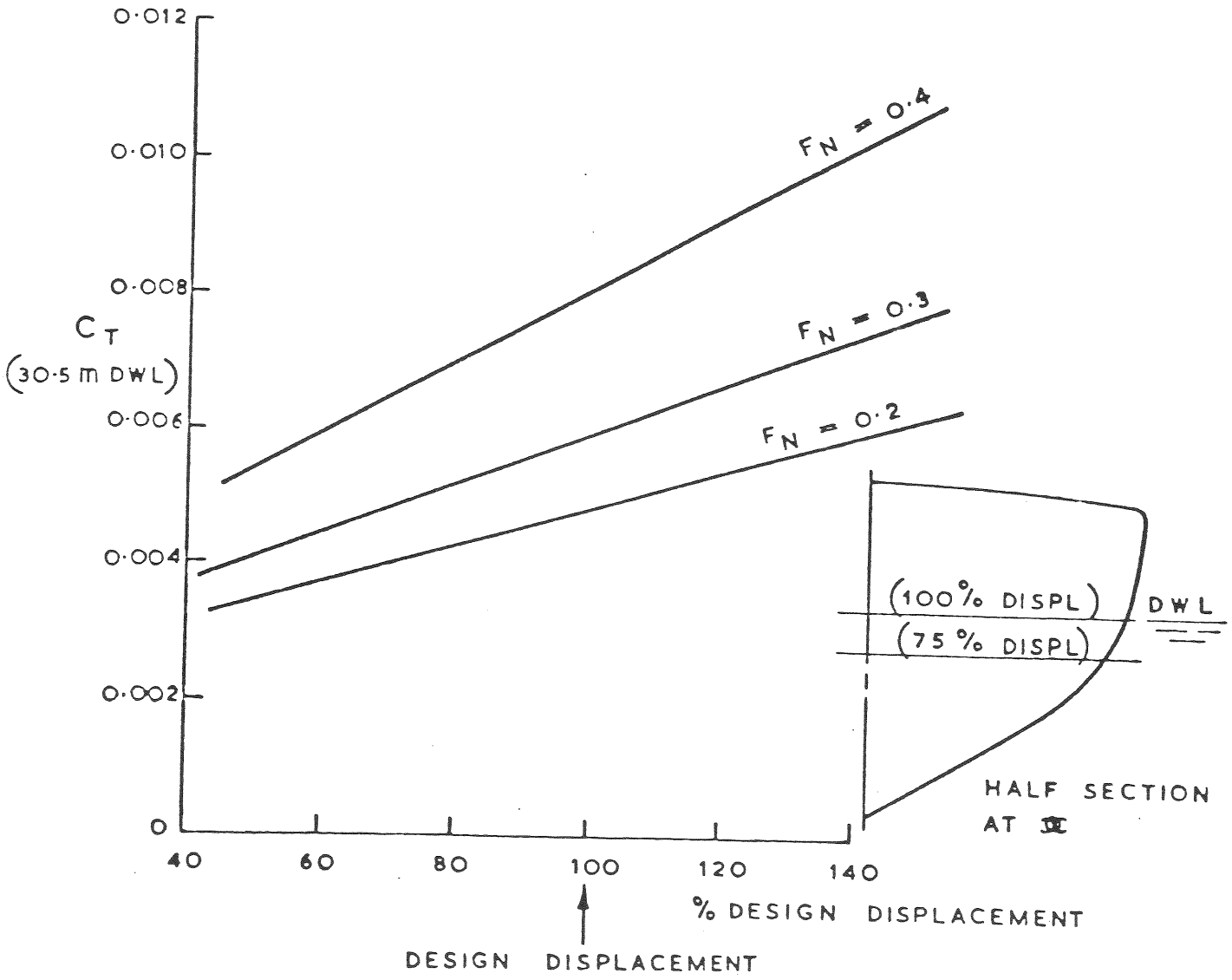

EFFECT OF DISPLACEMENT ON RESISTANCE OF GIVEN HULL FORM

FIG. 28.

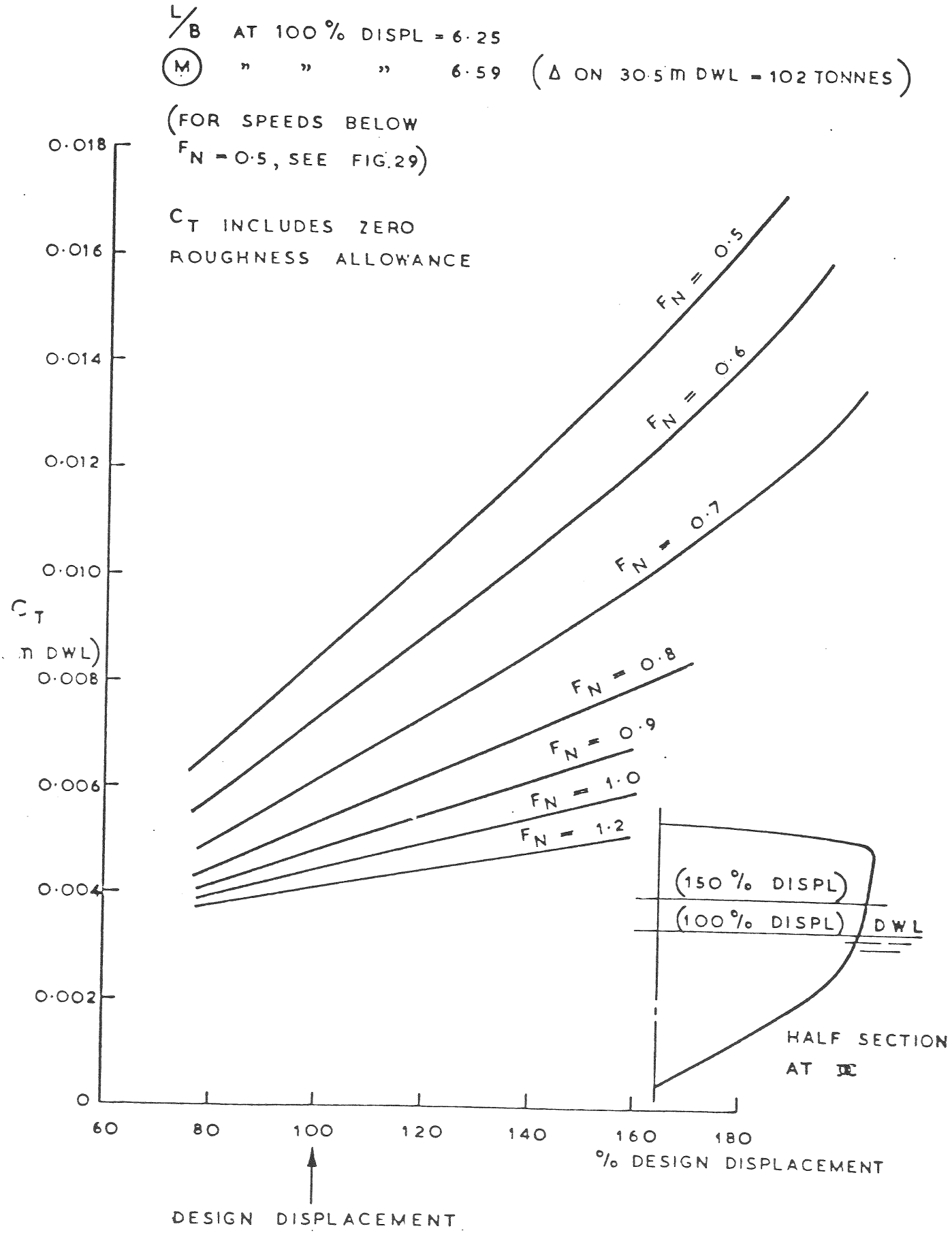

EFFECT OF DISPLACEMENT ON RESISTANCE OF GIVEN HULL FORM

FIG. 29.

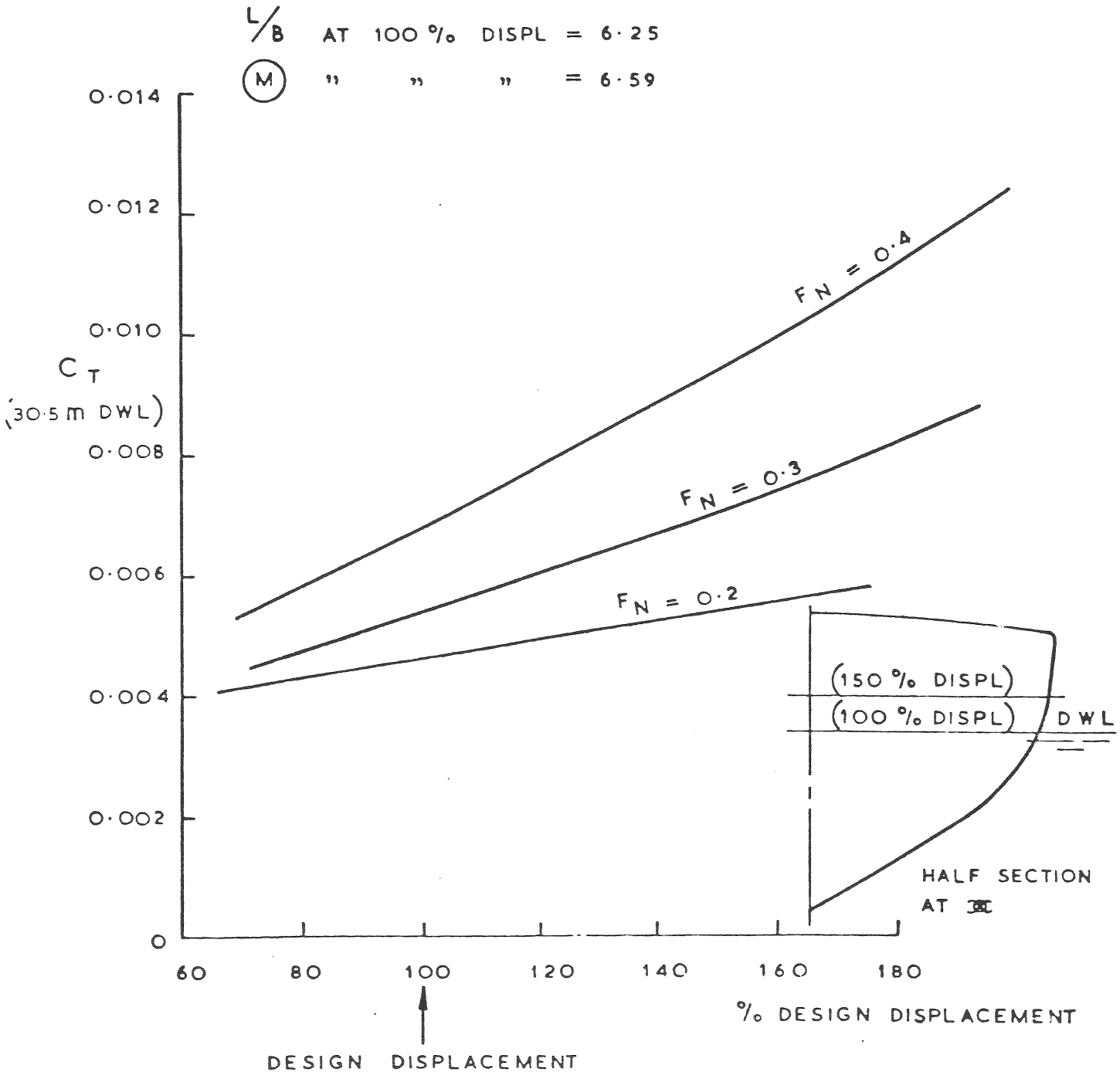

EFFECT OF DISPLACEMENT ON RESISTANCE OF GIVEN HULL FORM

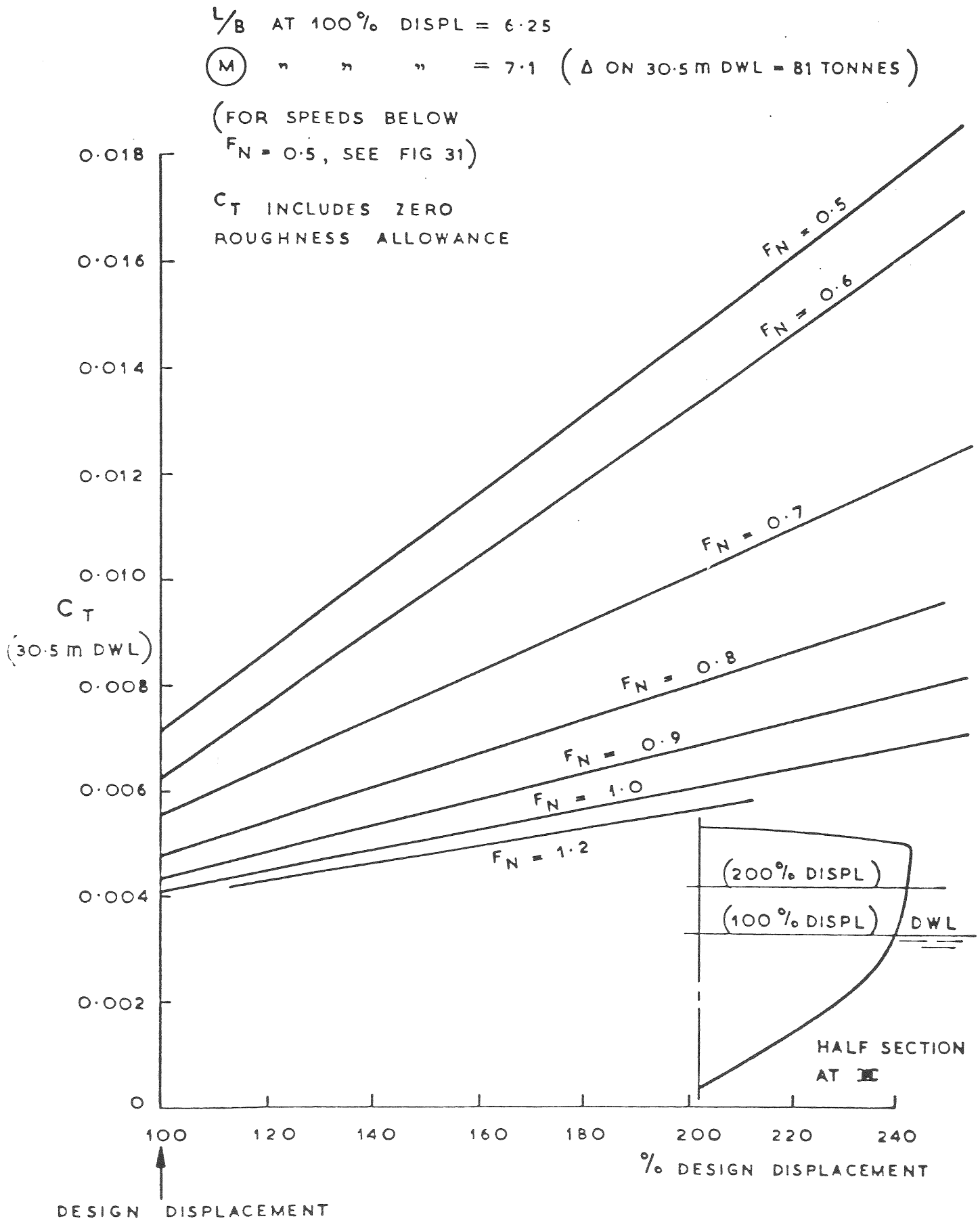

EFFECT OF DISPLACEMENT ON RESISTANCE OF GIVEN HULL FORM

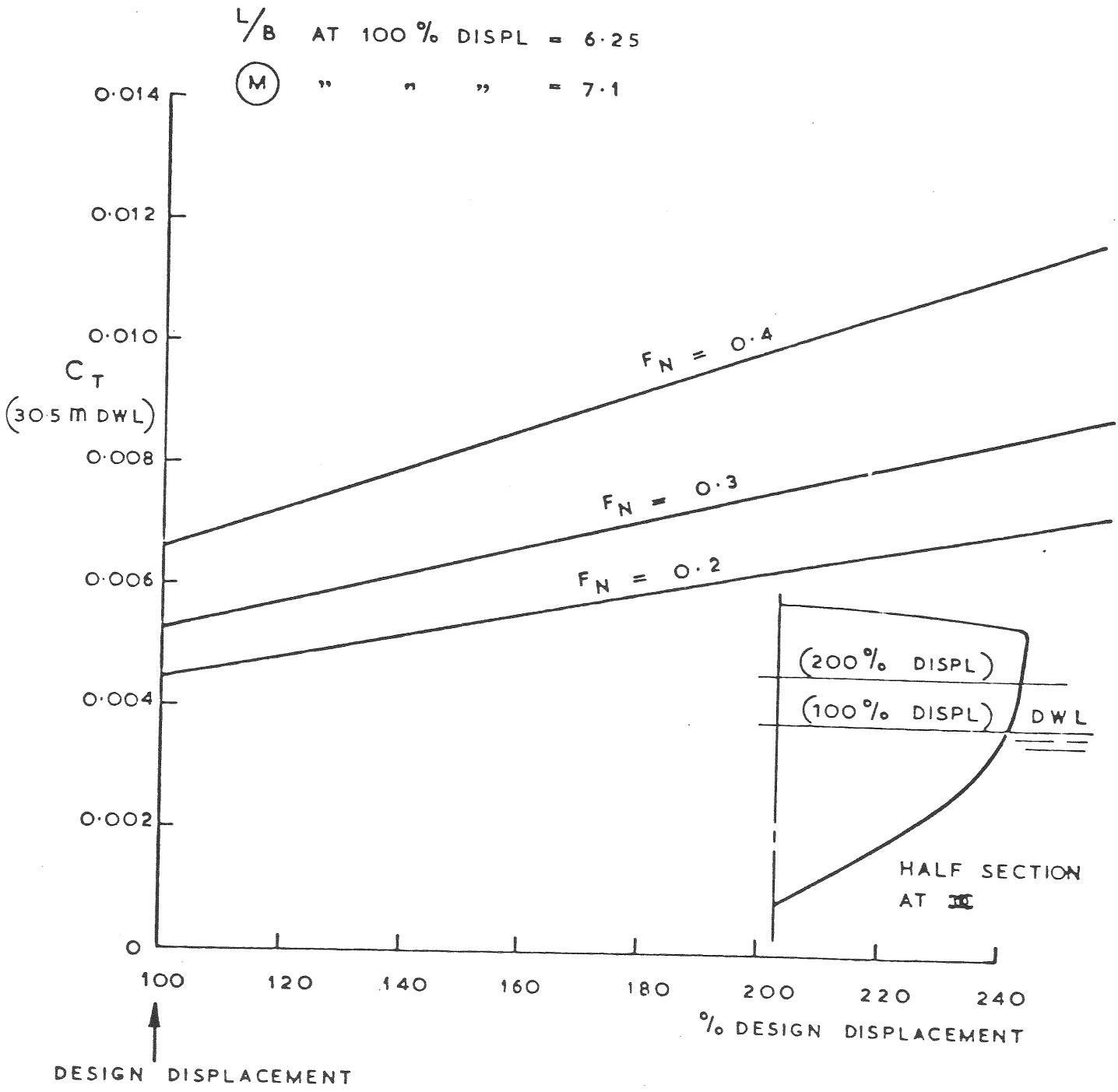

EFFECT OF DISPLACEMENT ON RESISTANCE OF GIVEN HULL FORM

FIG. 32.

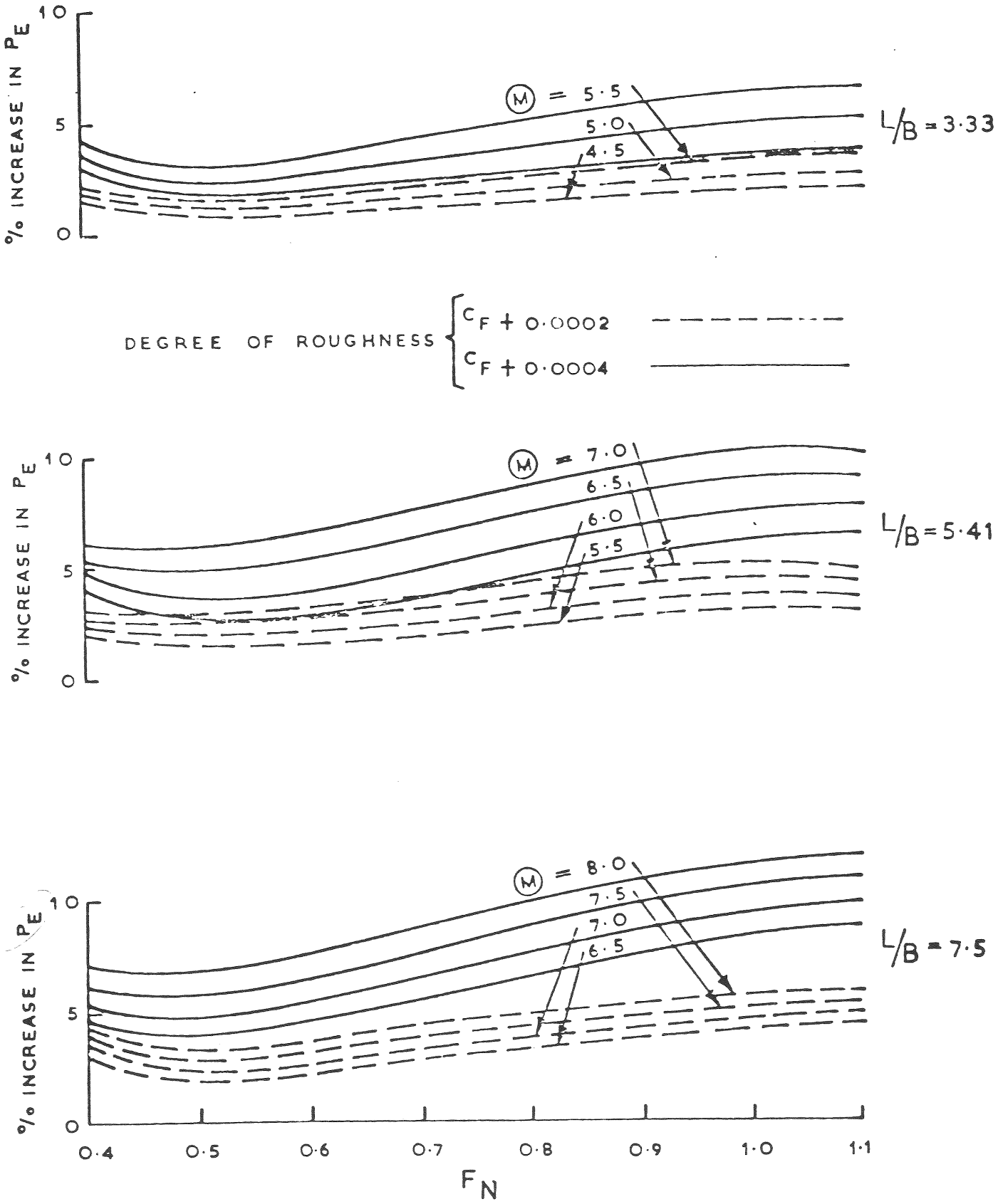

EFFECT OF HULL ROUGHNESS ON EFFECTIVE POWER

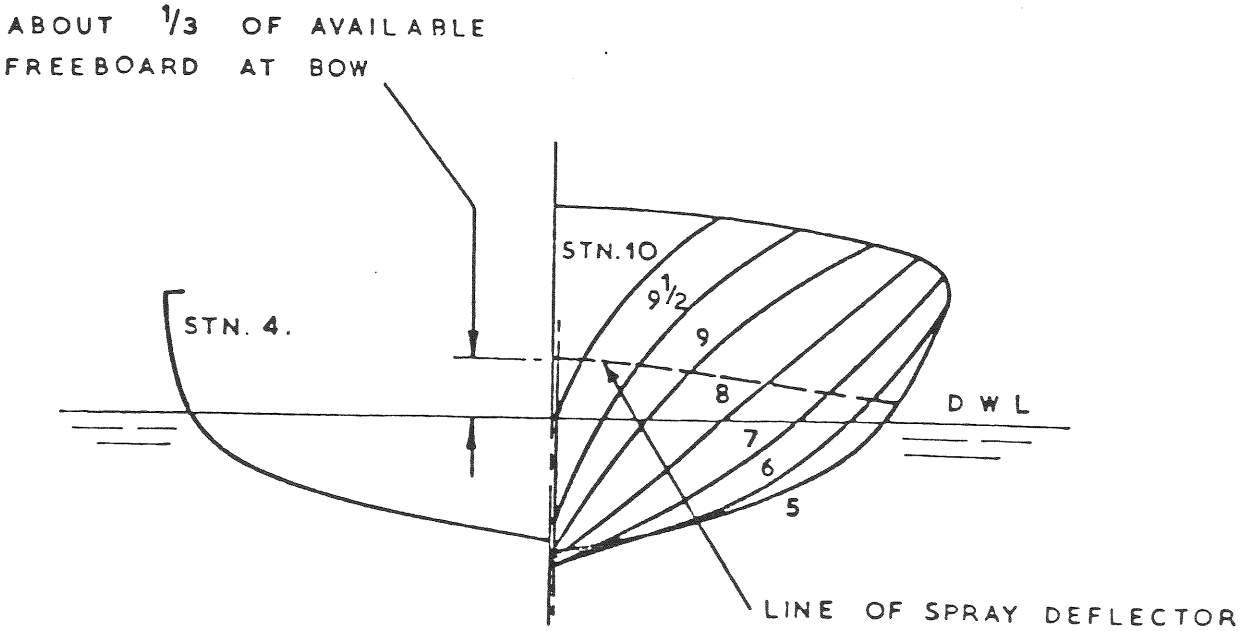

SPRAY DEFLECTOR CAN EITHER BE :

(A) A SPRAY RAIL ADDED TO HULL FORWARD AND TERMINATED AT STATION . 4 .

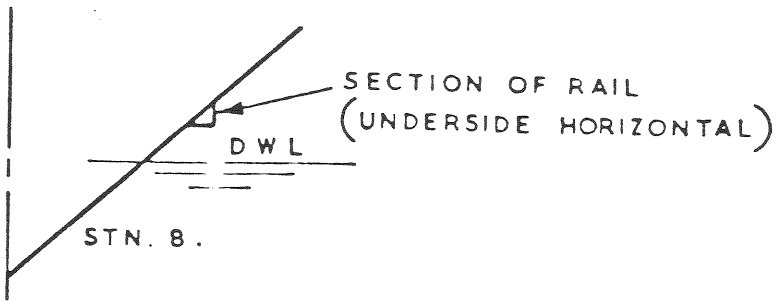

OR (B) INCLUDED IN SECTION SHAPE AT BOW

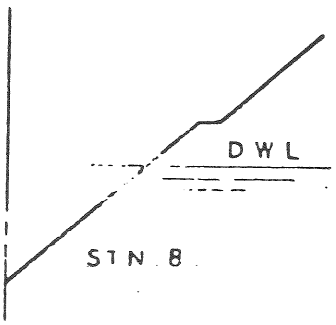

DISPOSITION OF SPRAY DEFLECTOR

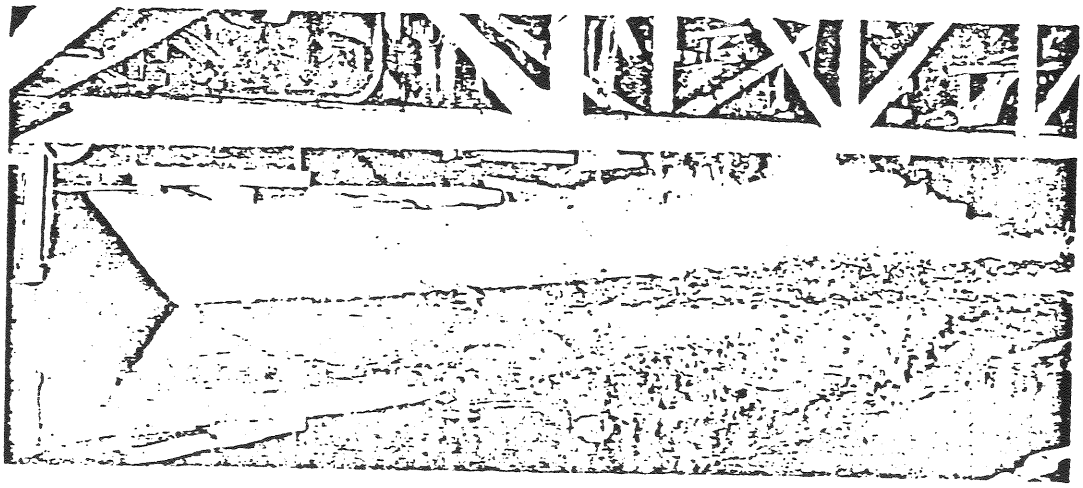

RAIL NOT FITTED

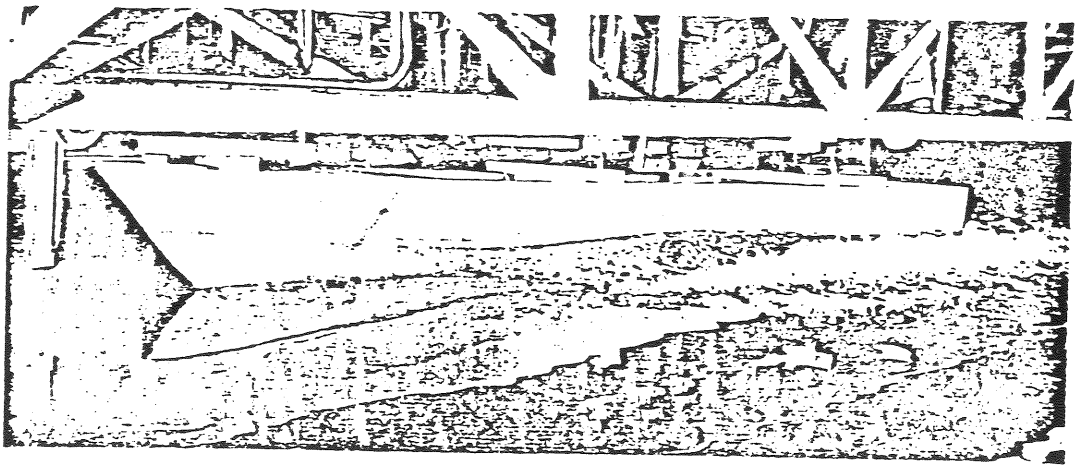

RAIL FITTED

HULL PARTICULARS :— $L/B = 5 \cdot 5$

$\textcircled{M} = 6 \cdot 8$

$F_N = 1 \cdot 0$

EFFECT OF SPRAY RAIL ON WETNESS

FIG. 35.

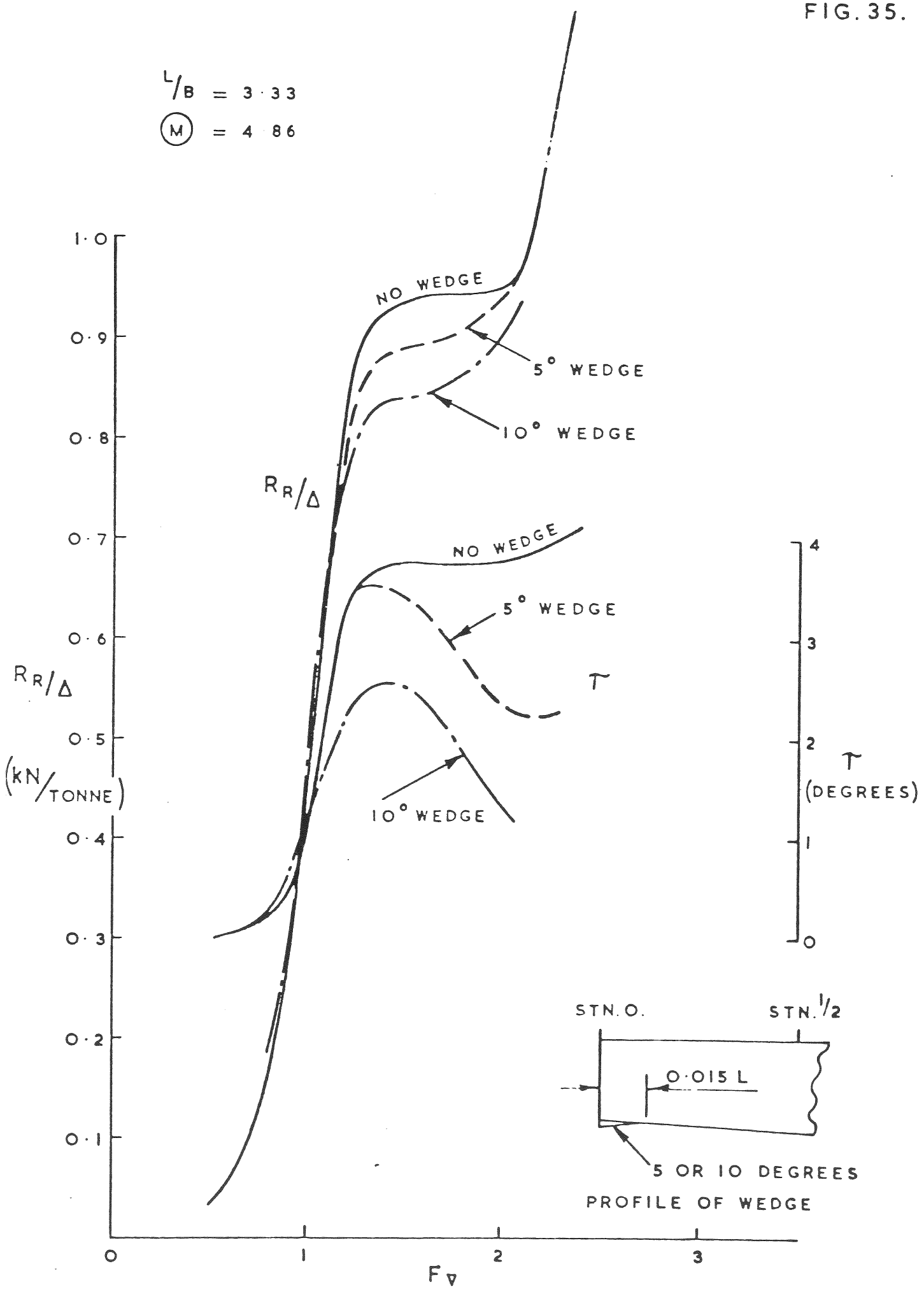

EFFECT OF WEDGE FITTED UNDER TRANSOM

FIG. 36.

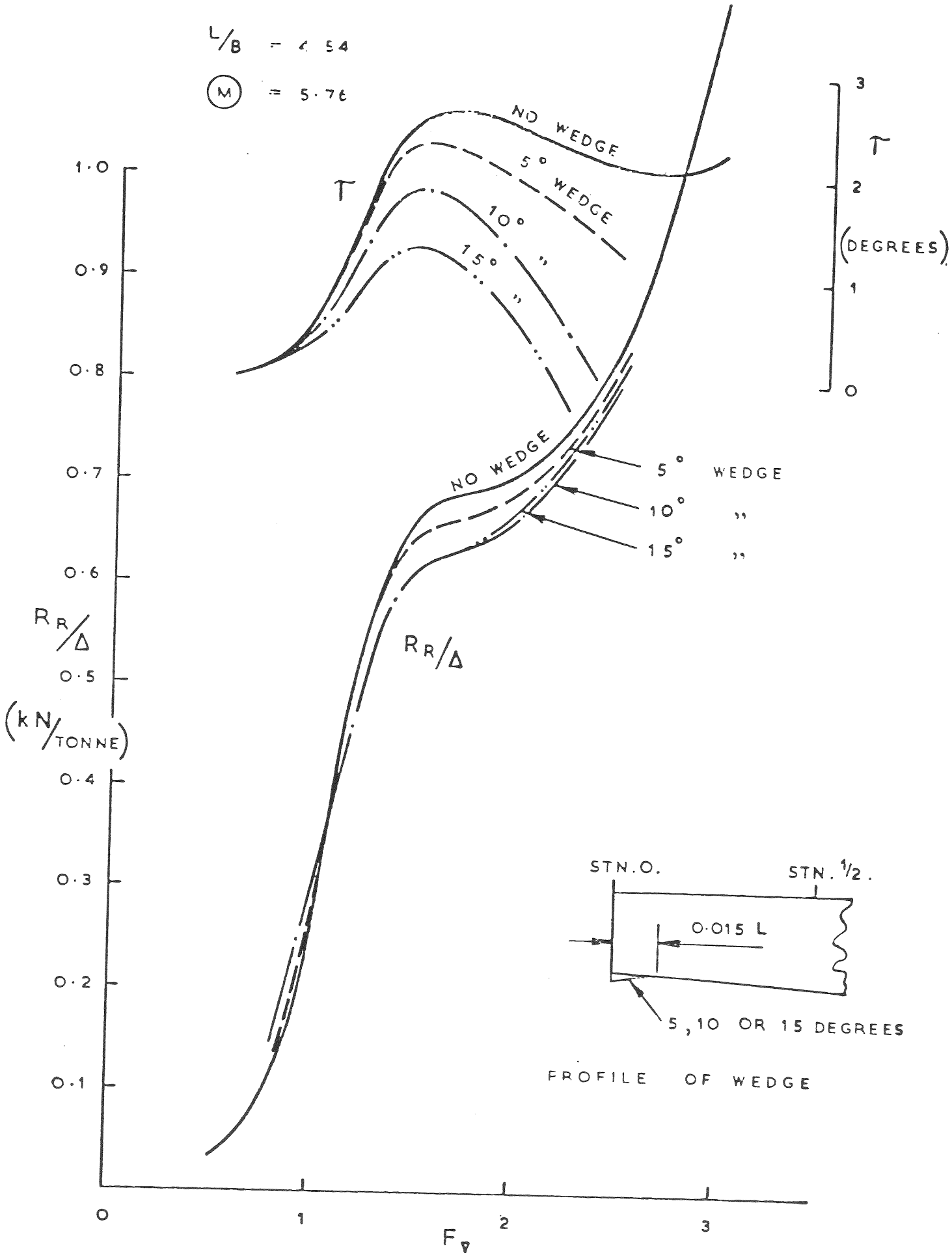

EFFECT OF WEDGE FITTED UNDER TRANSOM

FIG. 37.

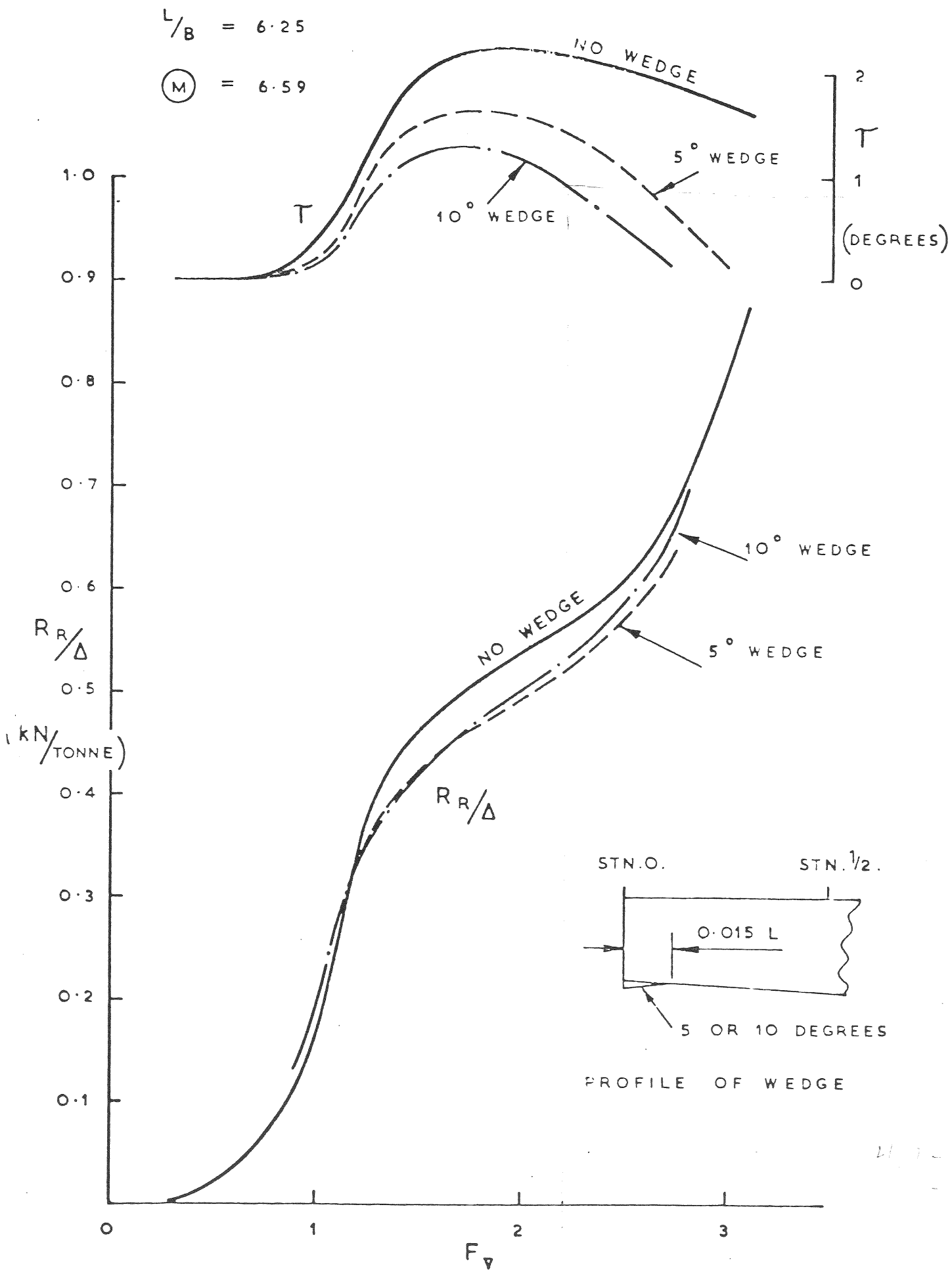

EFFECT OF WEDGE FITTED UNDER TRANSOM

FIG. 38.

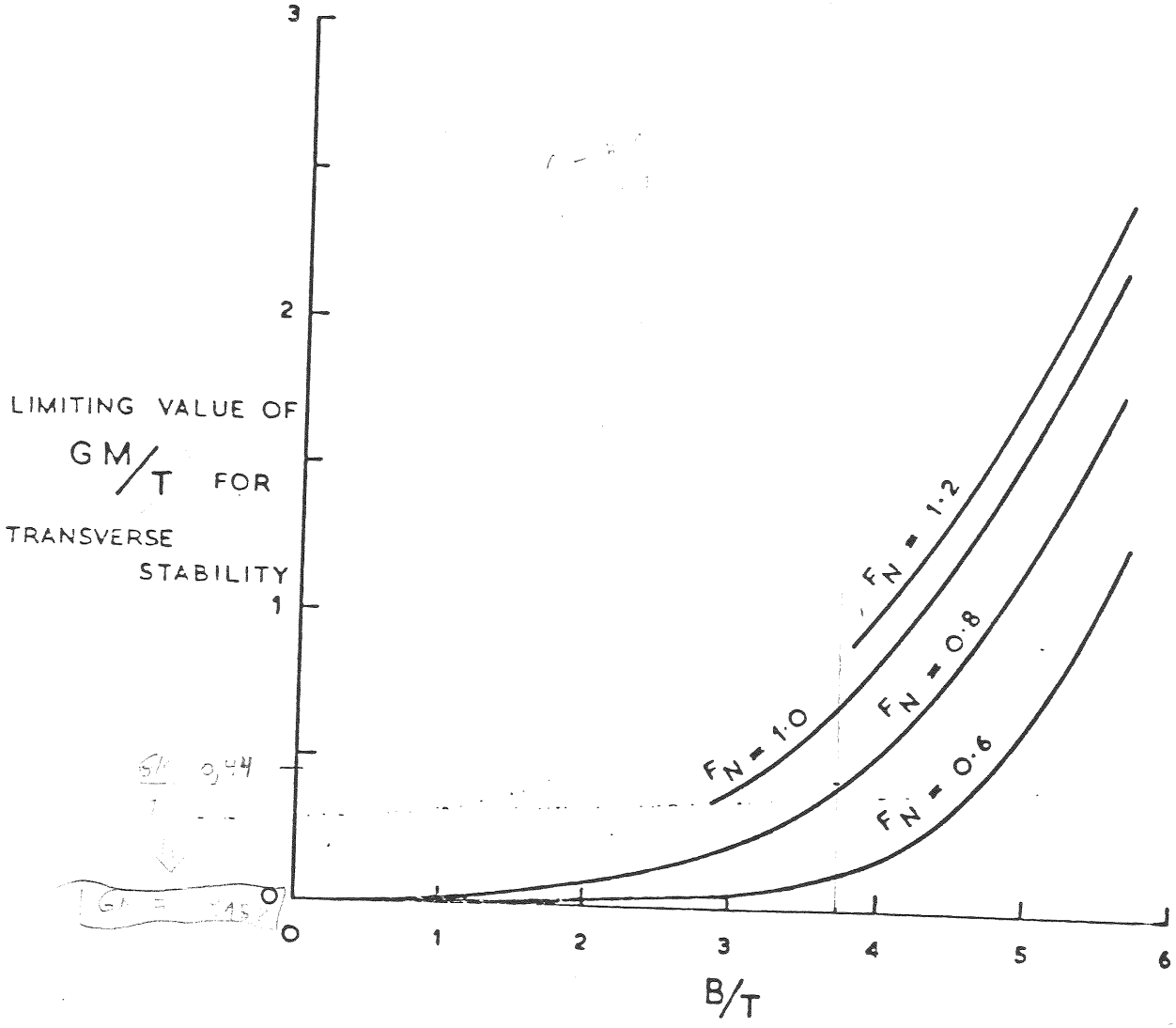

HULL STABILITY AT SPEED

IN CALM WATER

FIG. 39.

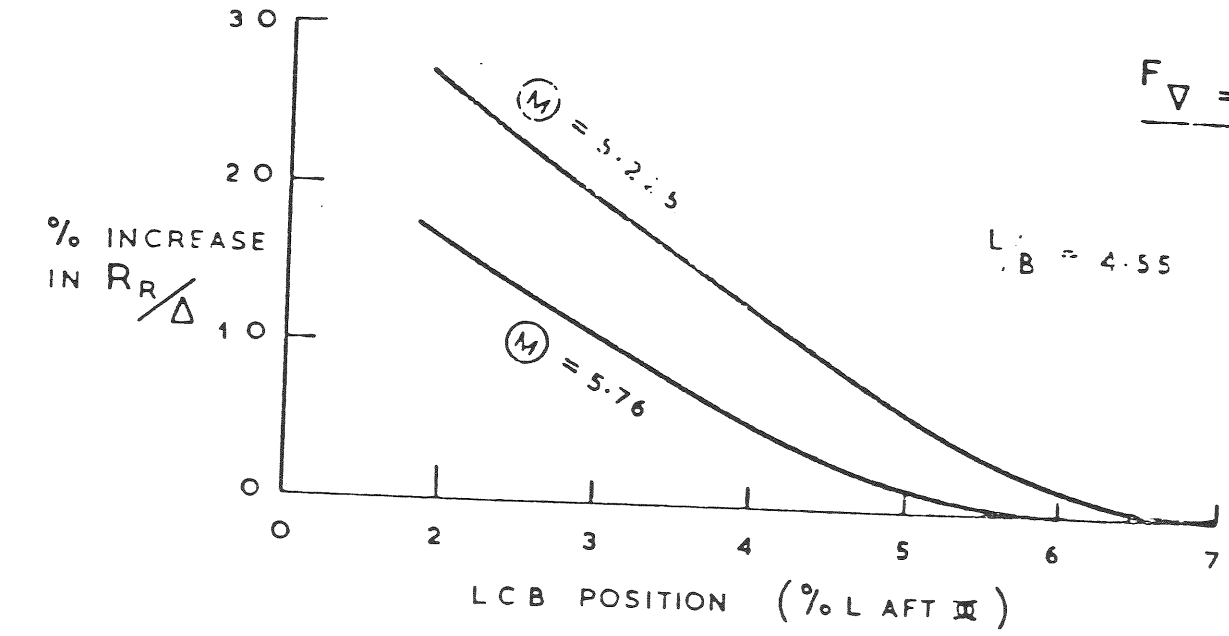

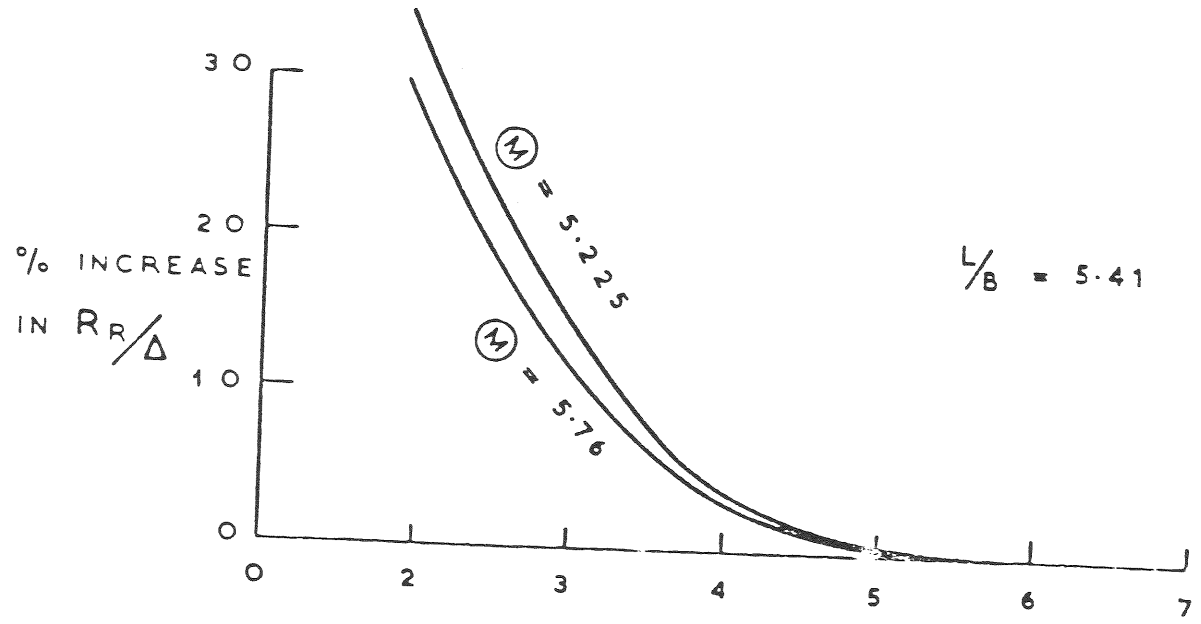

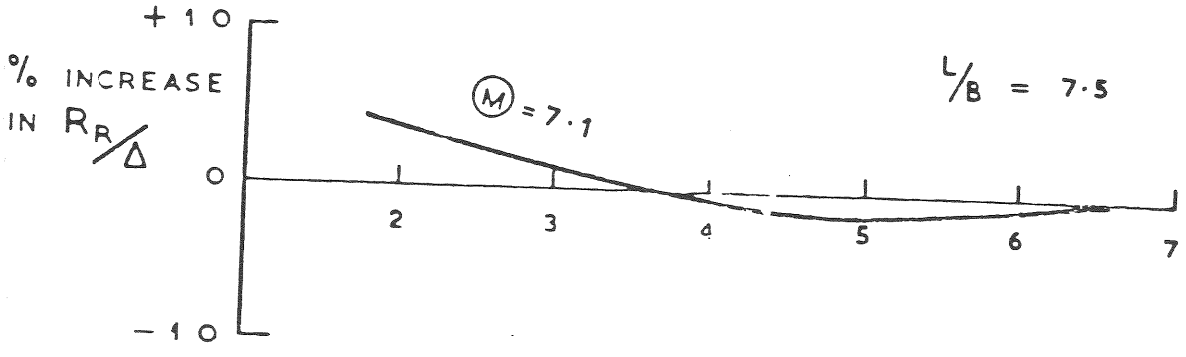

EFFECT OF POSITION OF LCB ON RESISTANCE

FIG. 40.

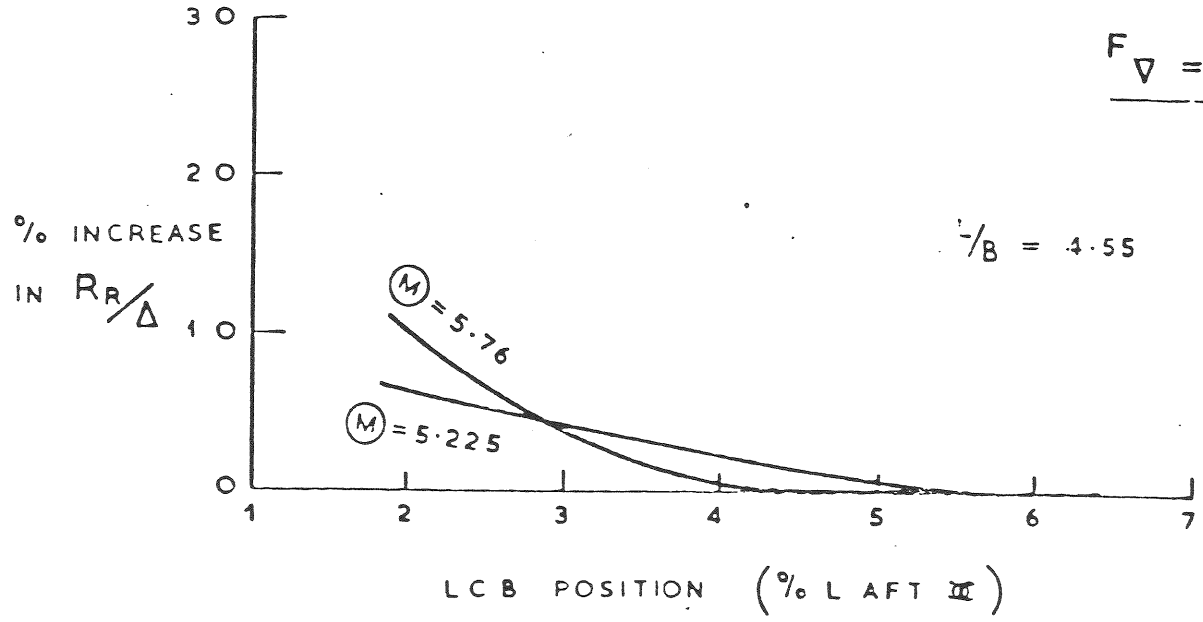

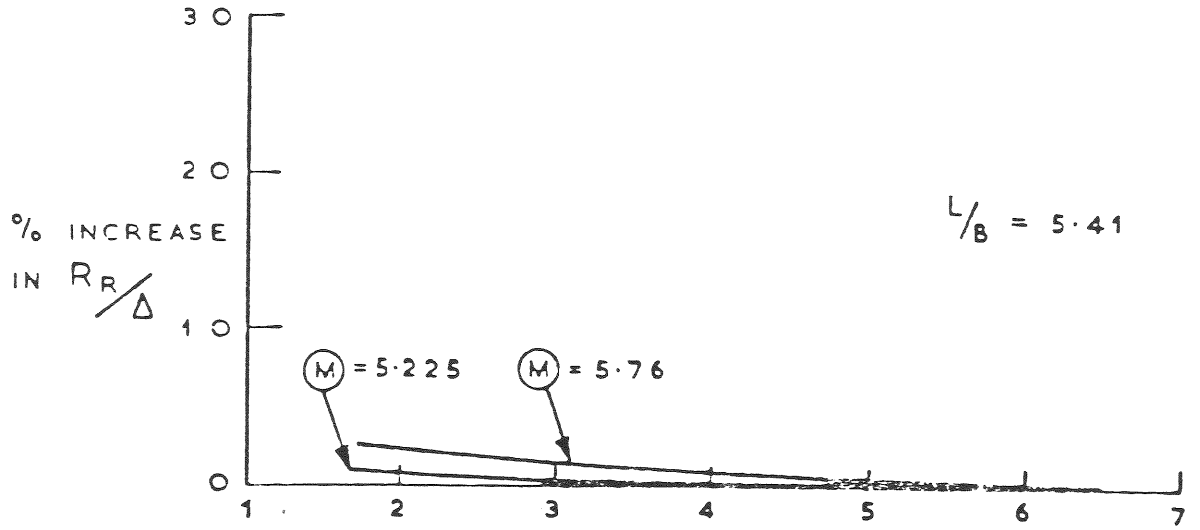

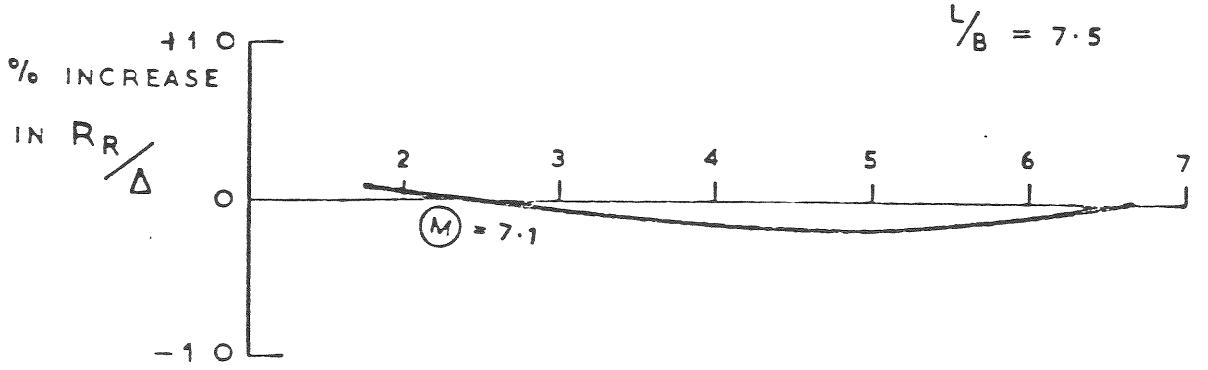

EFFECT OF POSITION OF LCB ON RESISTANCE

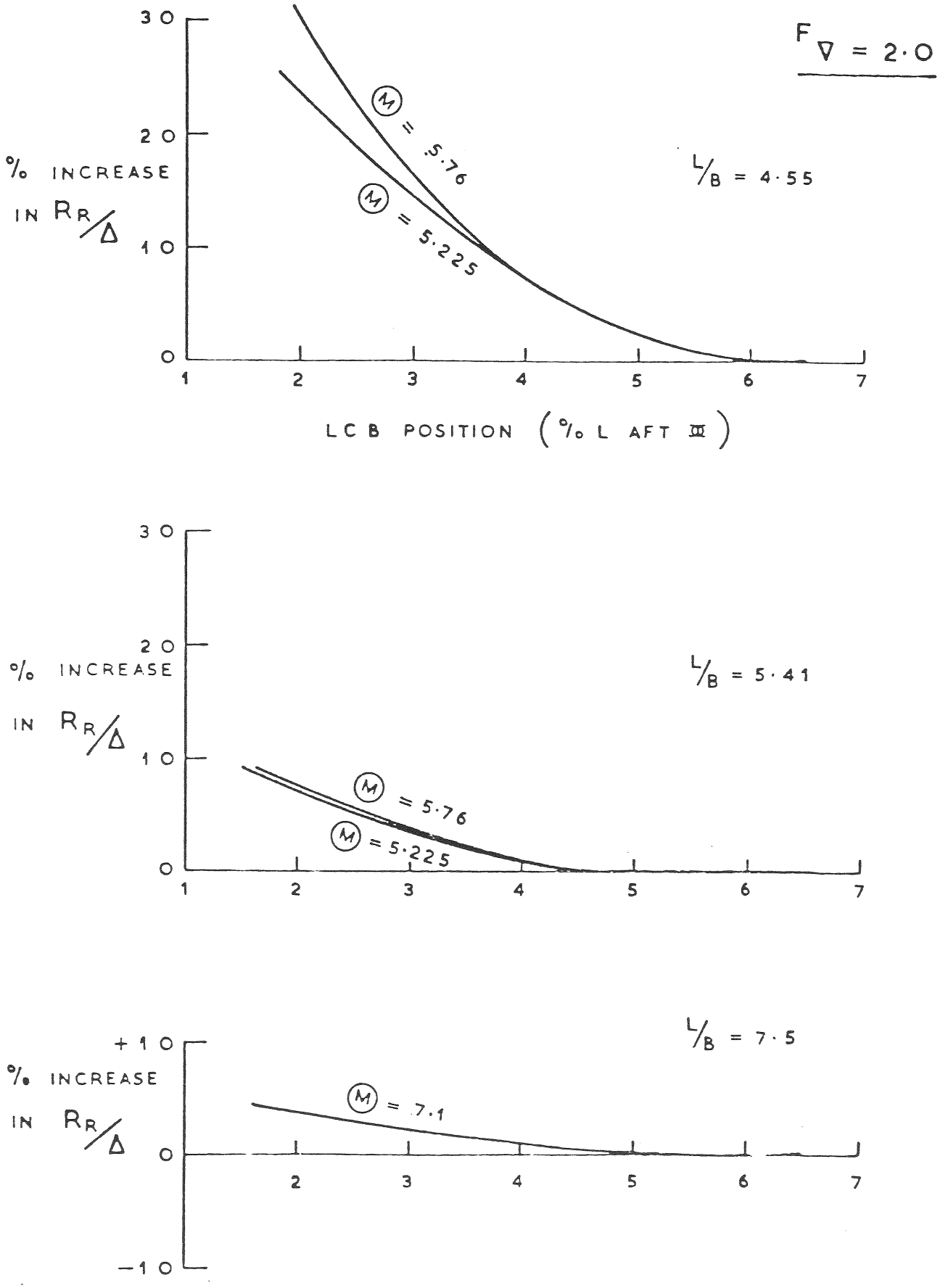

EFFECT OF POSITION OF LCB ON RESISTANCE

FIG. 42.

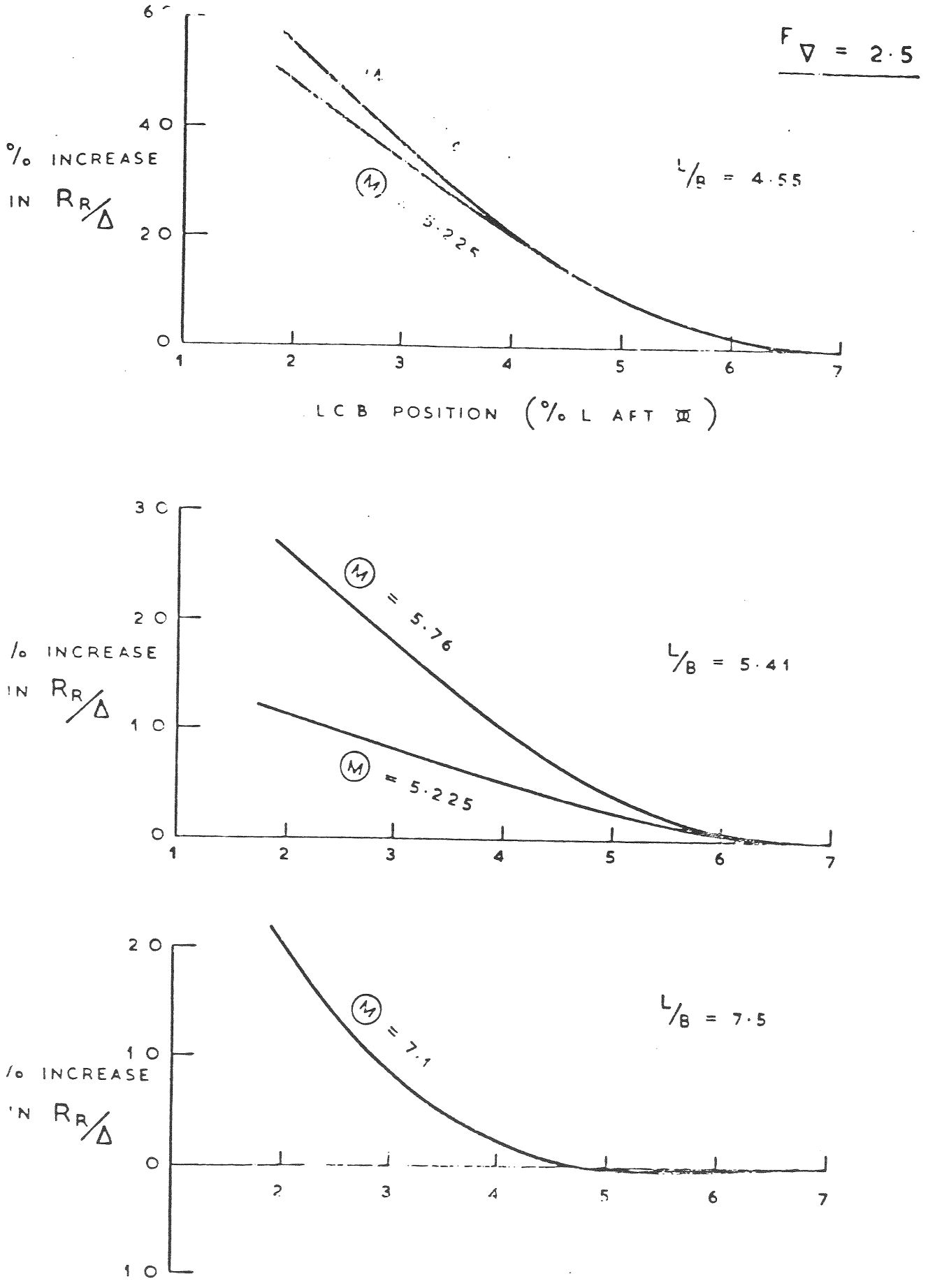

EFFECT OF POSITION OF LCB ON RESISTANCE

FIG. 43.

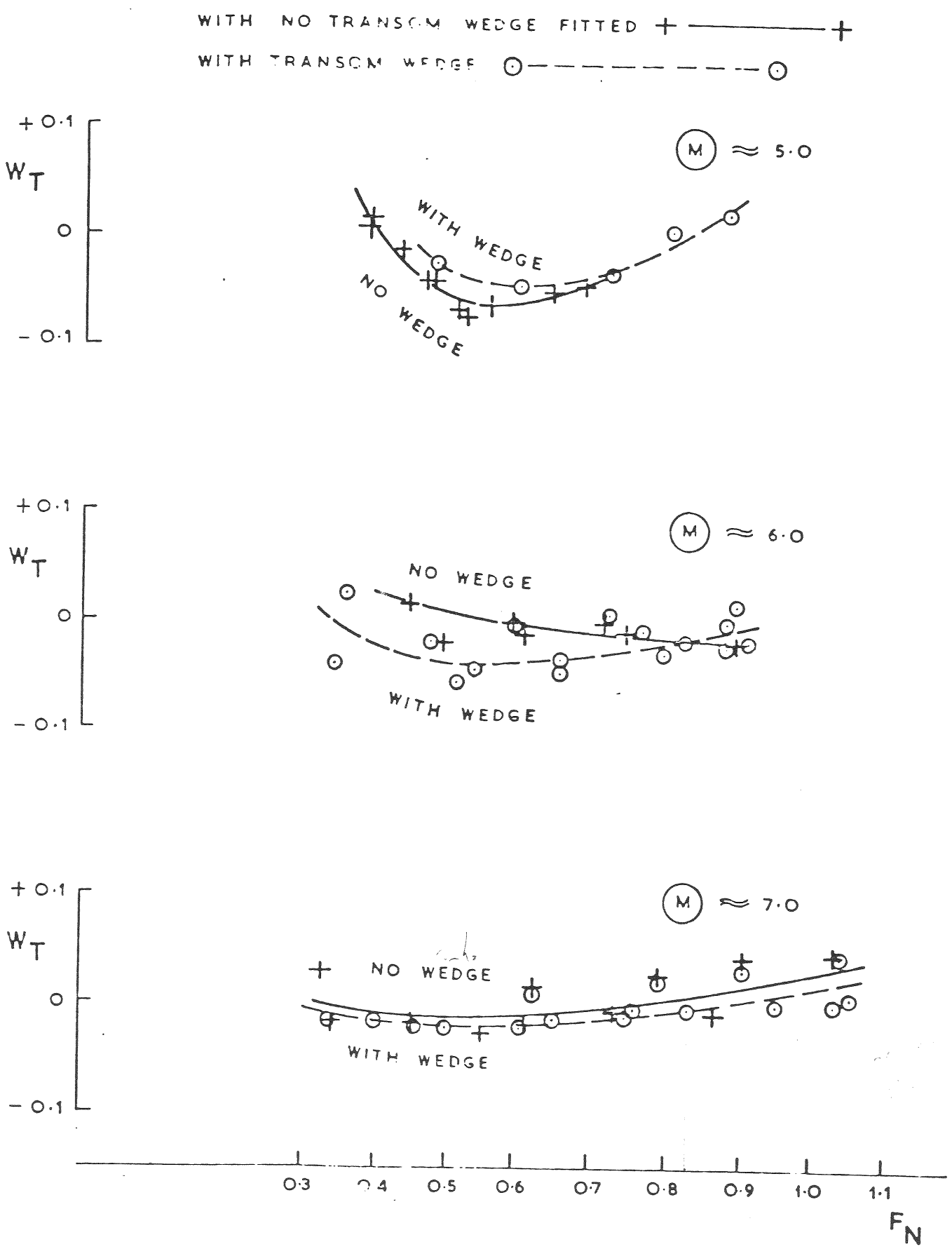

TAYLOR WAKE FRACTION, W_T

FIG. 44.

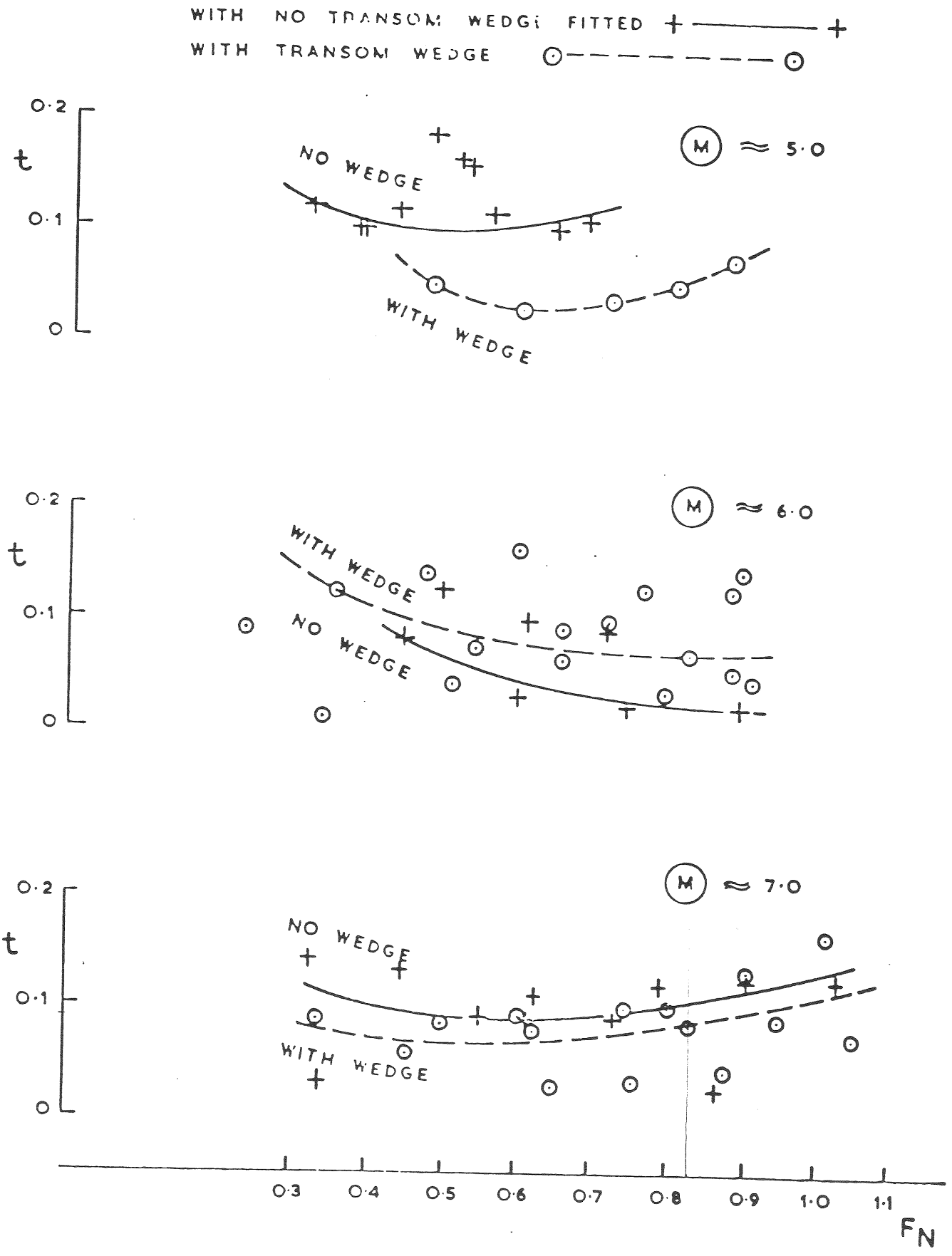

THRUST DEDUCTION, t

FIG. 45.

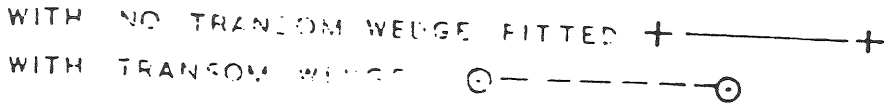

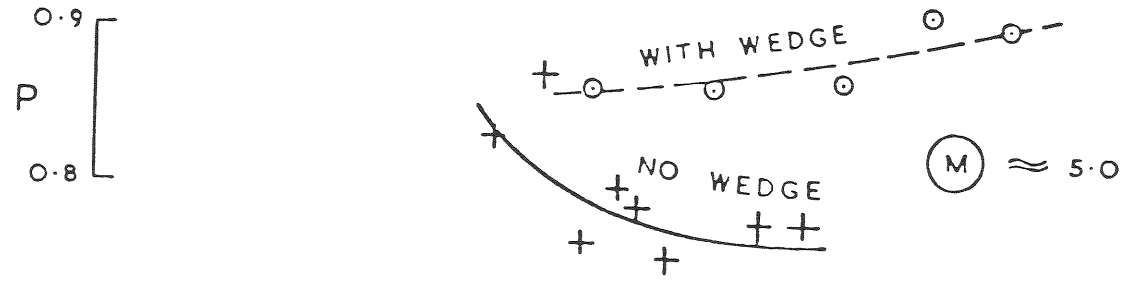

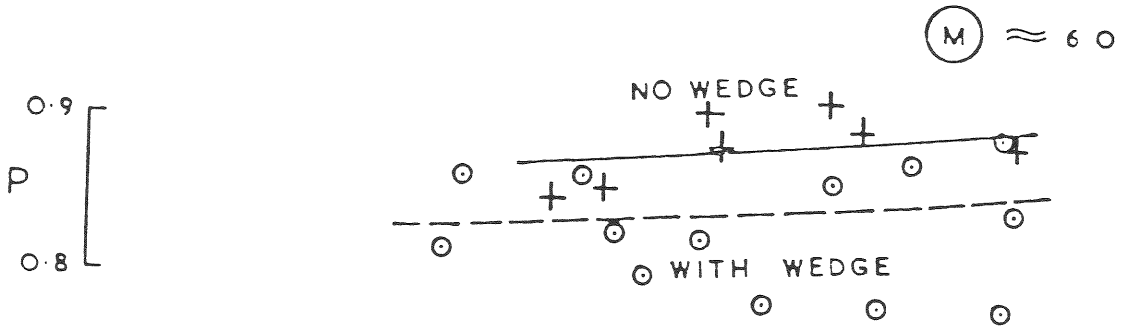

$P = \eta_H \times \eta_R$ WHERE η_H IS HULL EFFICIENCY AND η_R IS RELATIVE ROTATIVE EFFICIENCY

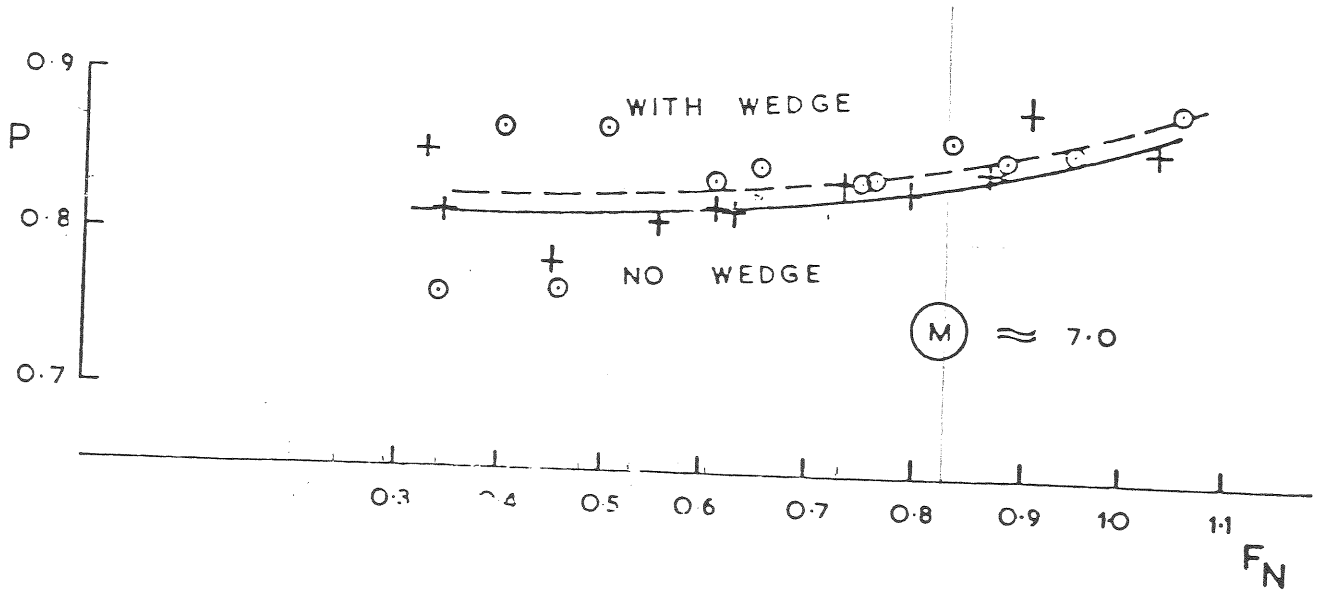

PROPULSIVE FACTOR , P

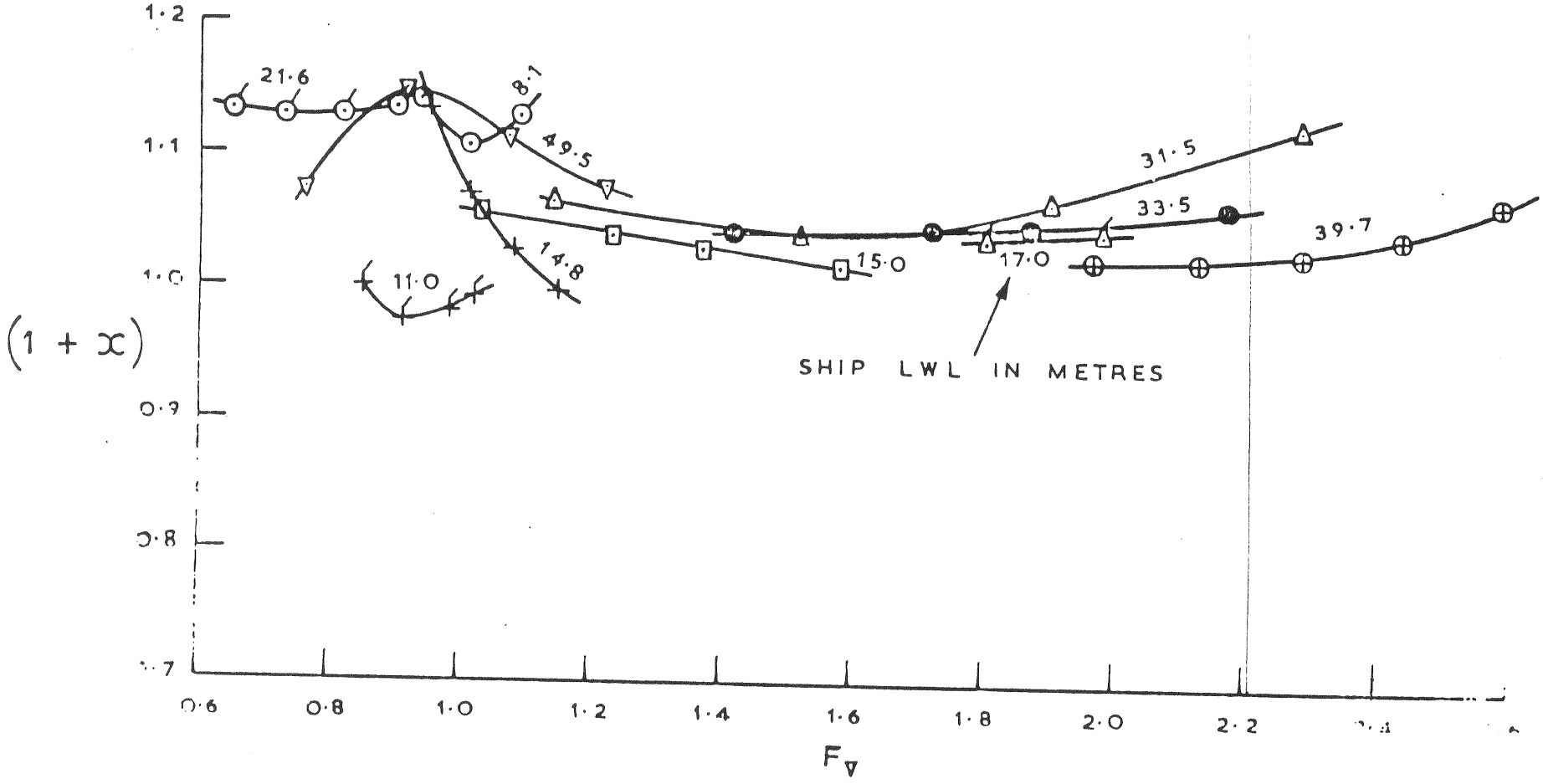

VARIATION OF POWER PREDICTION FACTOR $(1+x)$

FIG. 46.

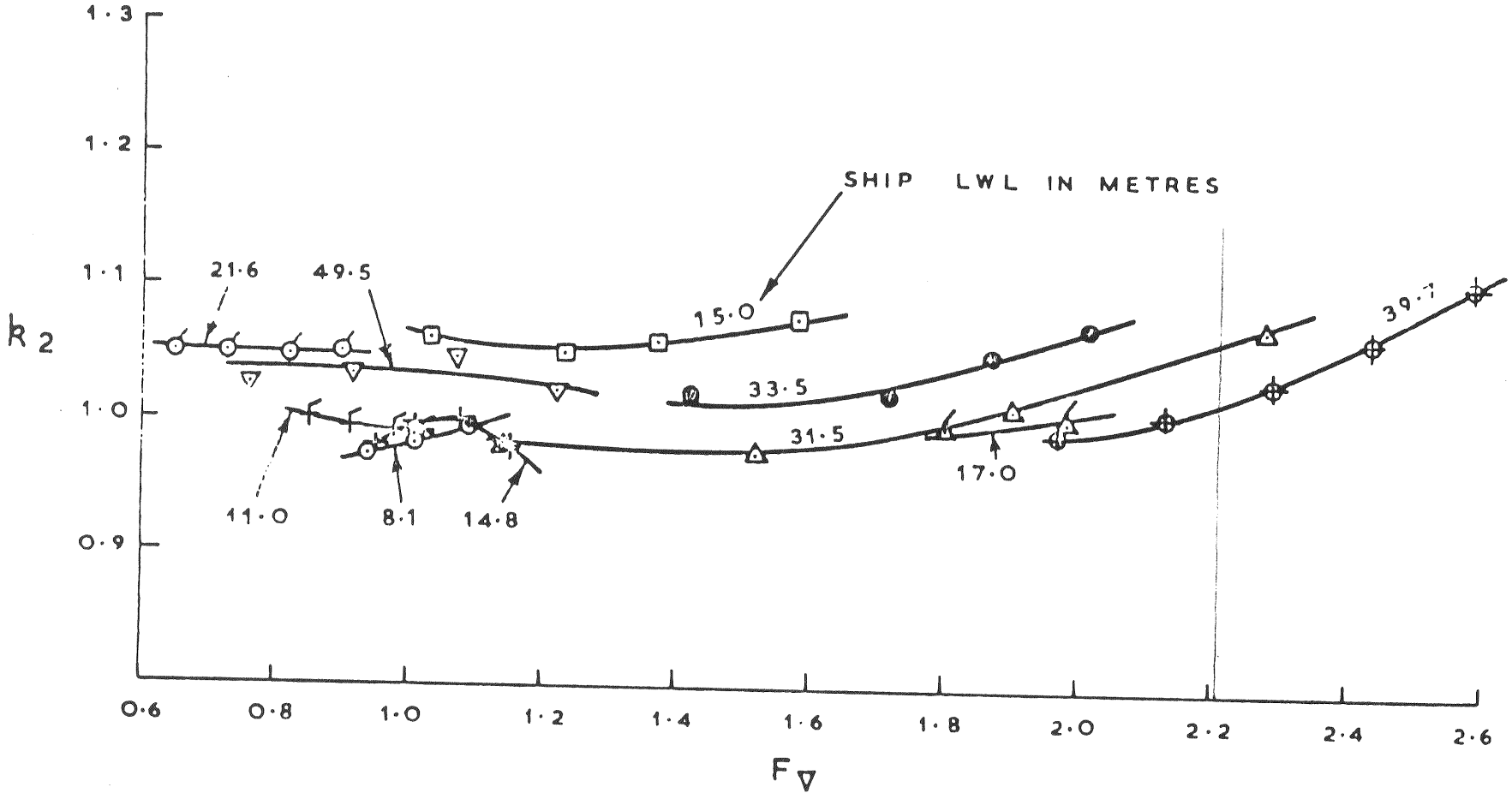

VARIATION OF PROPELLER REVOLUTIONS PREDICTION FACTOR, k_2

FIG. 47.

FIG.48.

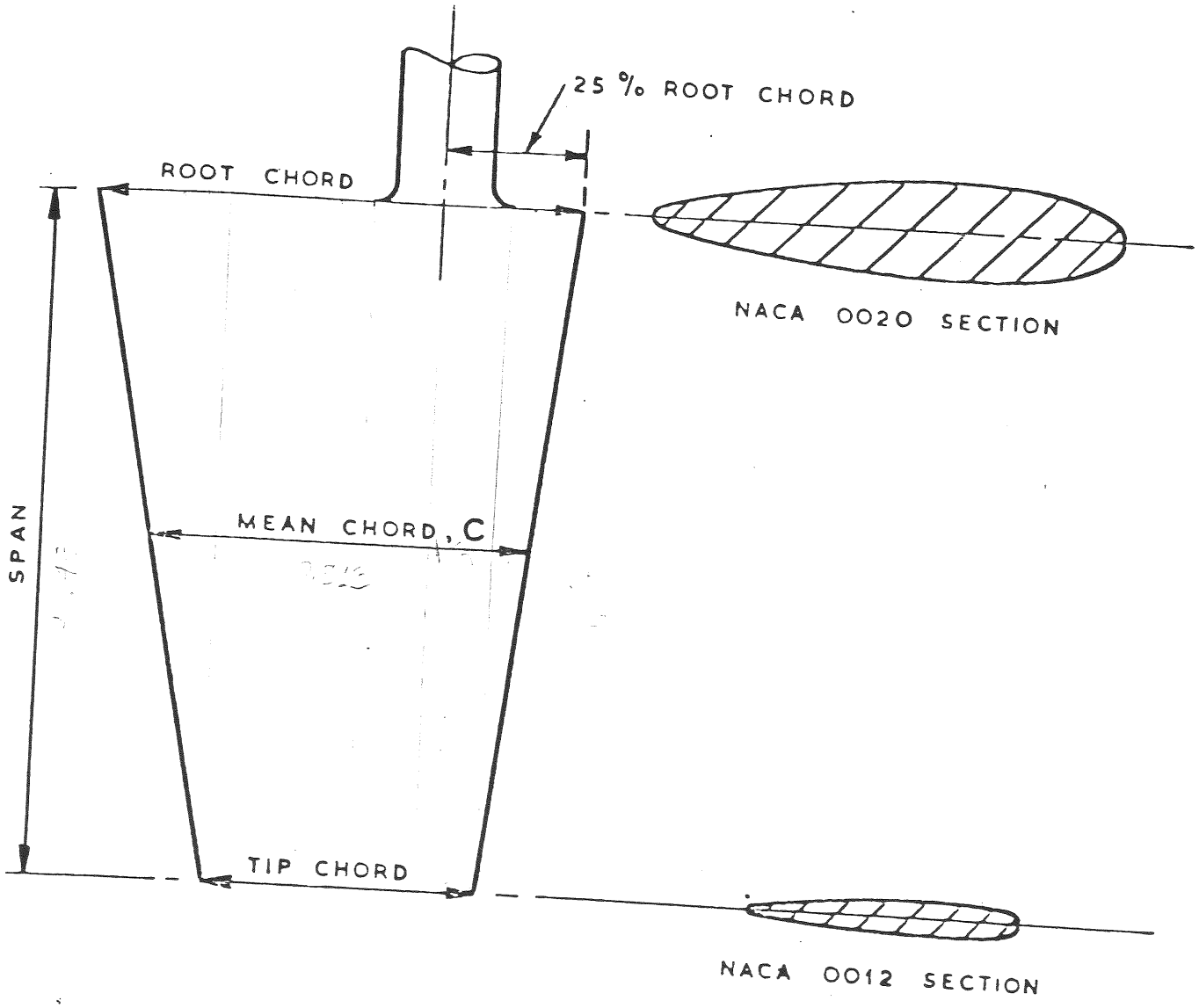

$$\text{GEOMETRIC ASPECT RATIO} = \frac{\text{SPAN}}{\text{MEAN CHORD}} = 1{\cdot}8$$

$$\text{EFFECTIVE ASPECT RATIO} = 3{\cdot}5 \text{ APPROX}$$

$$\text{TAPER RATIO} = \frac{\text{TIP CHORD}}{\text{ROOT CHORD}} = 0{\cdot}6$$

$$\text{RUDDER AREA RATIO} = \frac{\text{TOTAL AREA OF RUDDERS}}{\text{AREA OF HULL PROFILE BELOW WATERLINE}}\ * = \frac{1}{27}$$

* TWIN RUDDERS FITTED

PARTICULARS OF RUDDERS USED IN MANOEUVRING EXP'M'TS

FIG. 49.

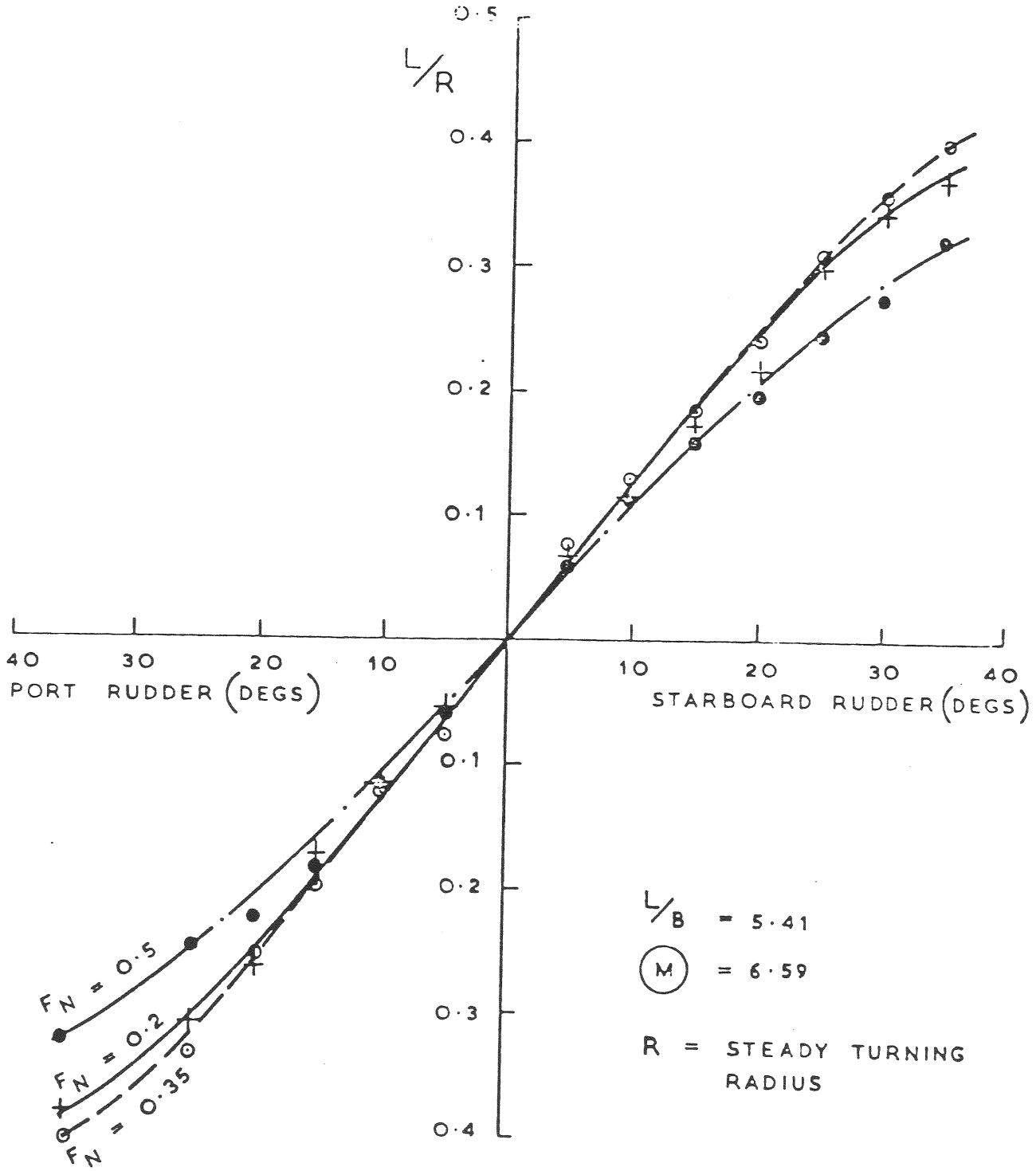

RATIO OF TURNING CIRCLE TO SHIP LENGTH

FIG. 50.

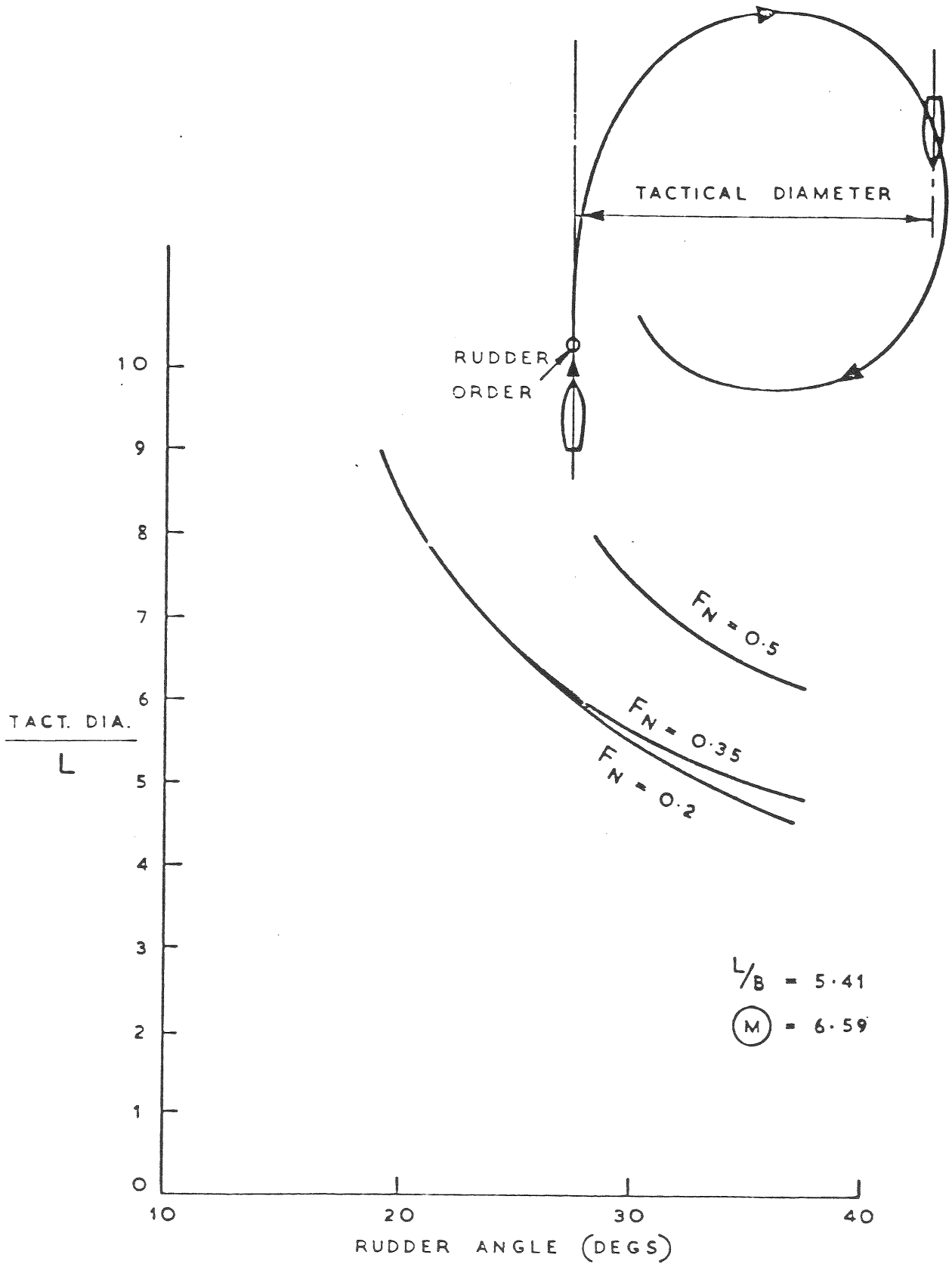

VARIATION OF TACTICAL DIAMETER WITH RUDDER ANGLE

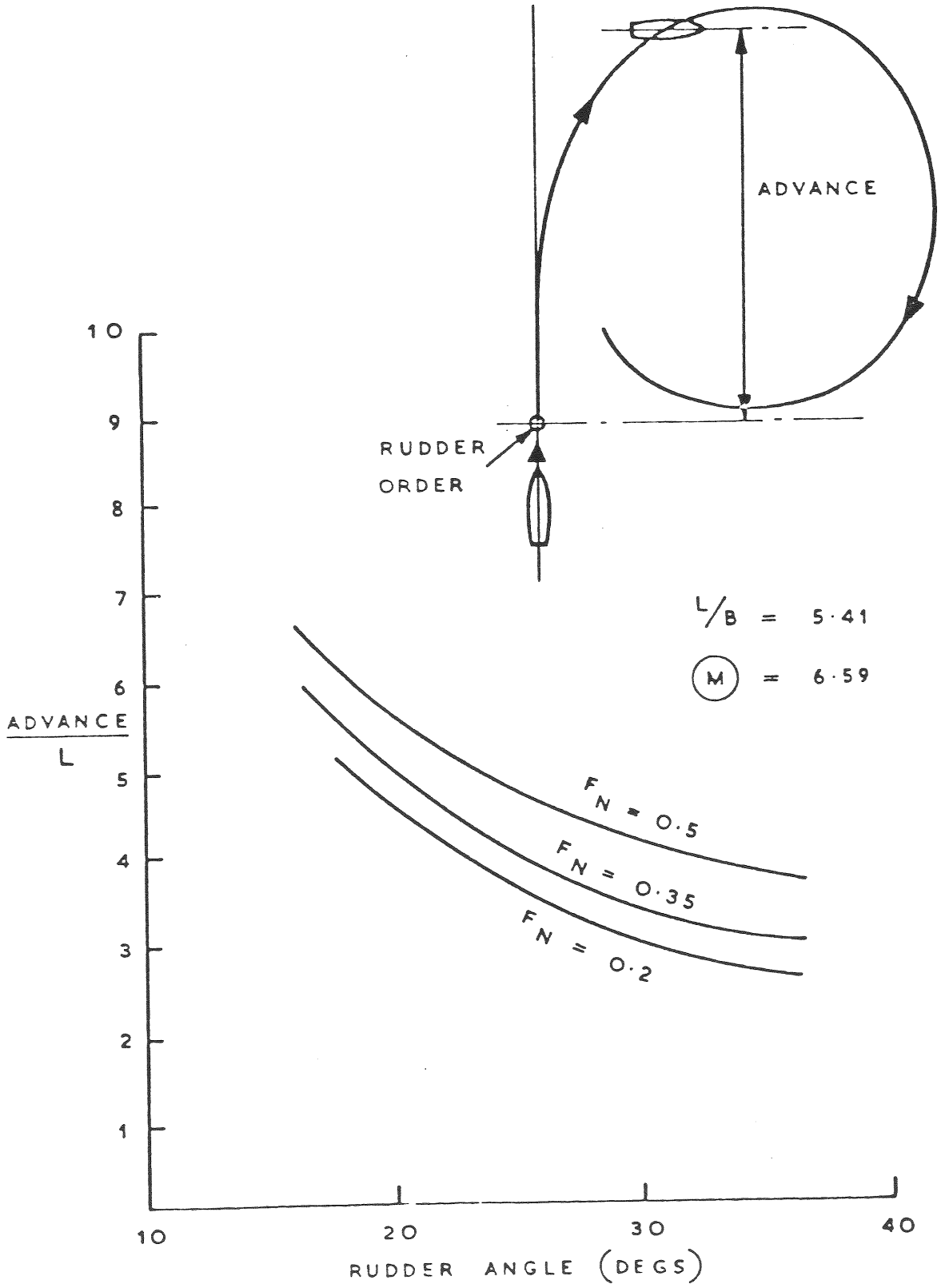

VARIATION OF ADVANCE WITH RUDDER ANGLE

FIG. 52.

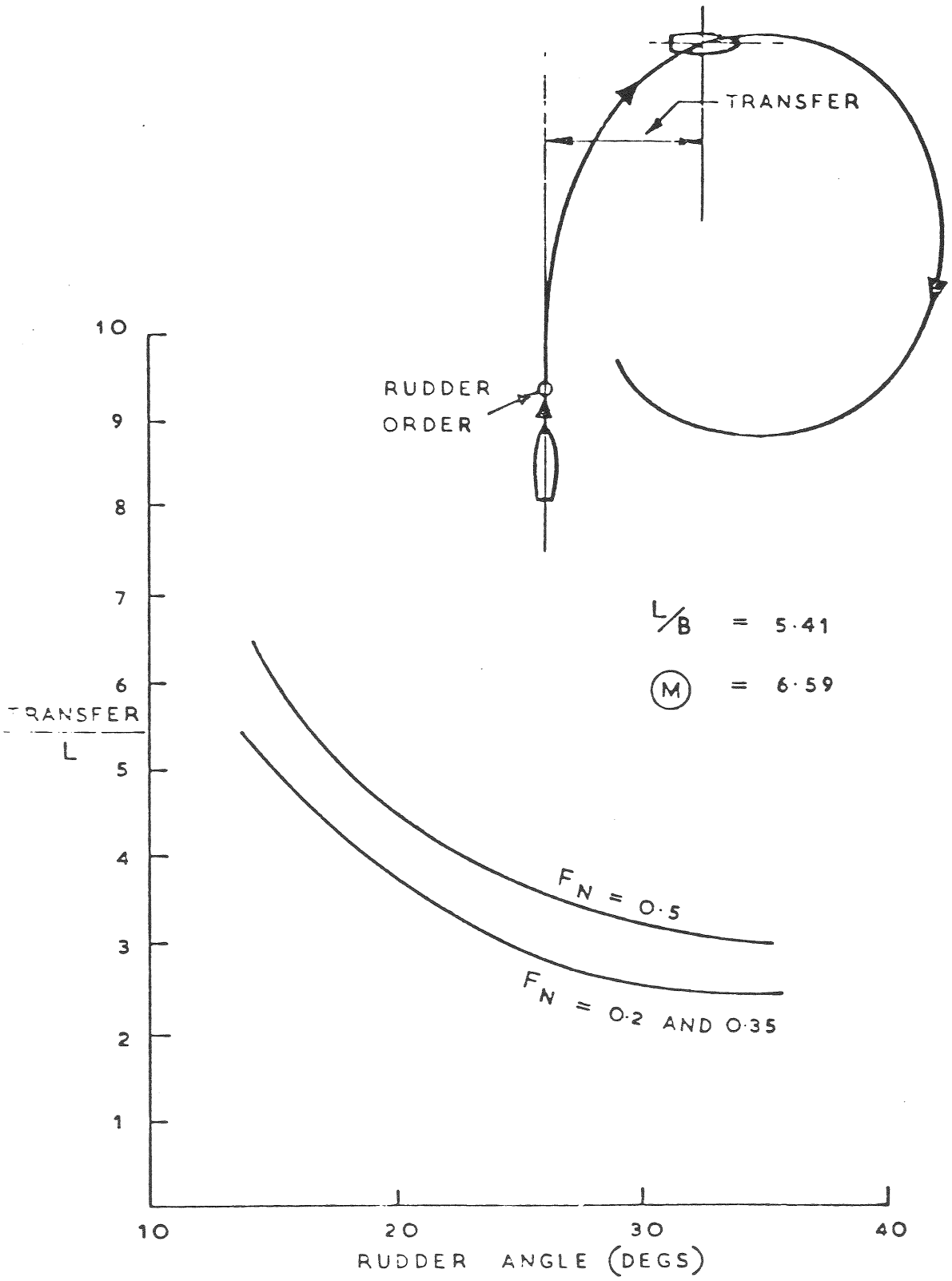

VARIATION OF TRANSFER WITH RUDDER ANGLE

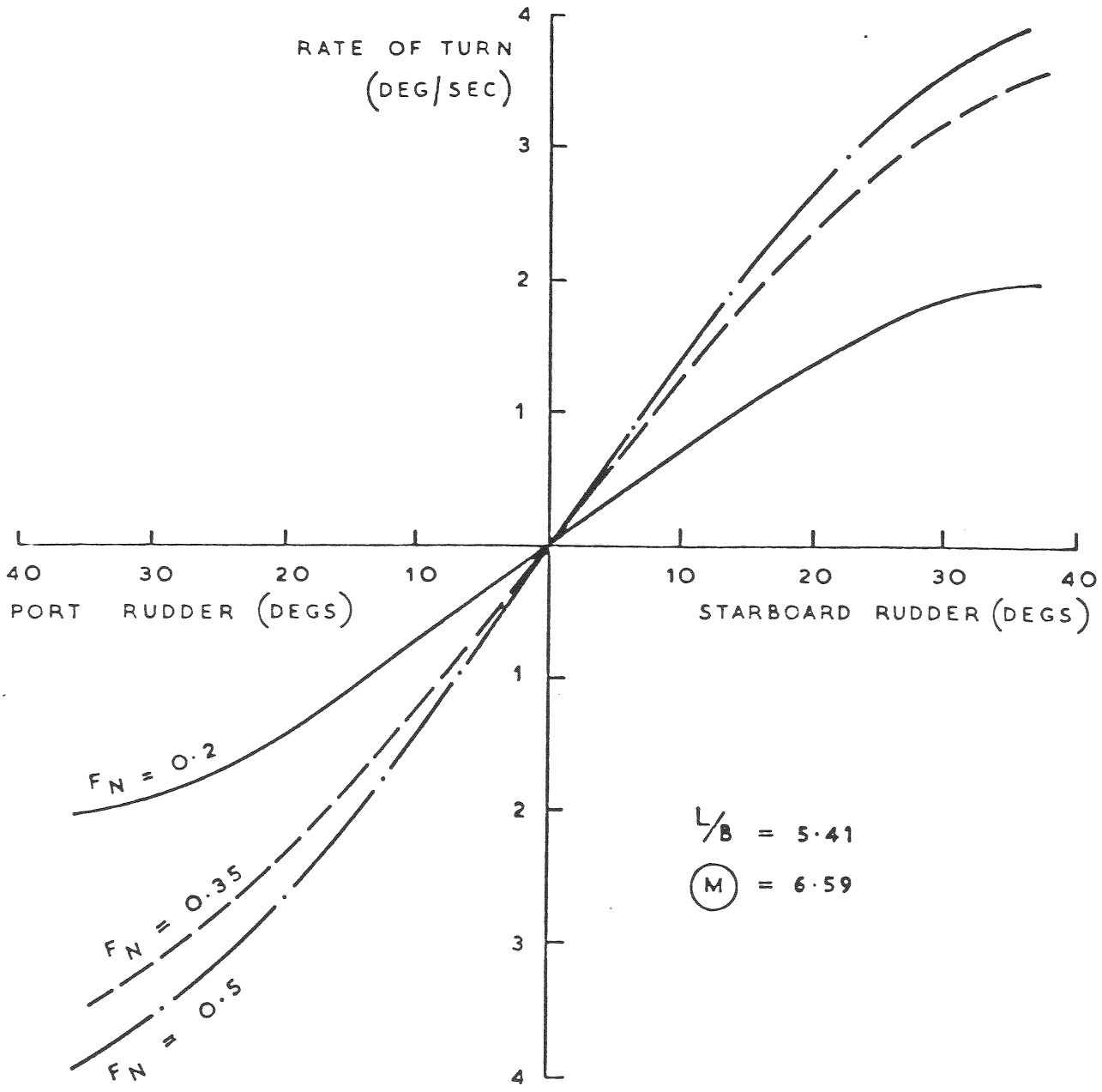

RATE OF TURN
DURING STEADY STATE

FIG. 54.

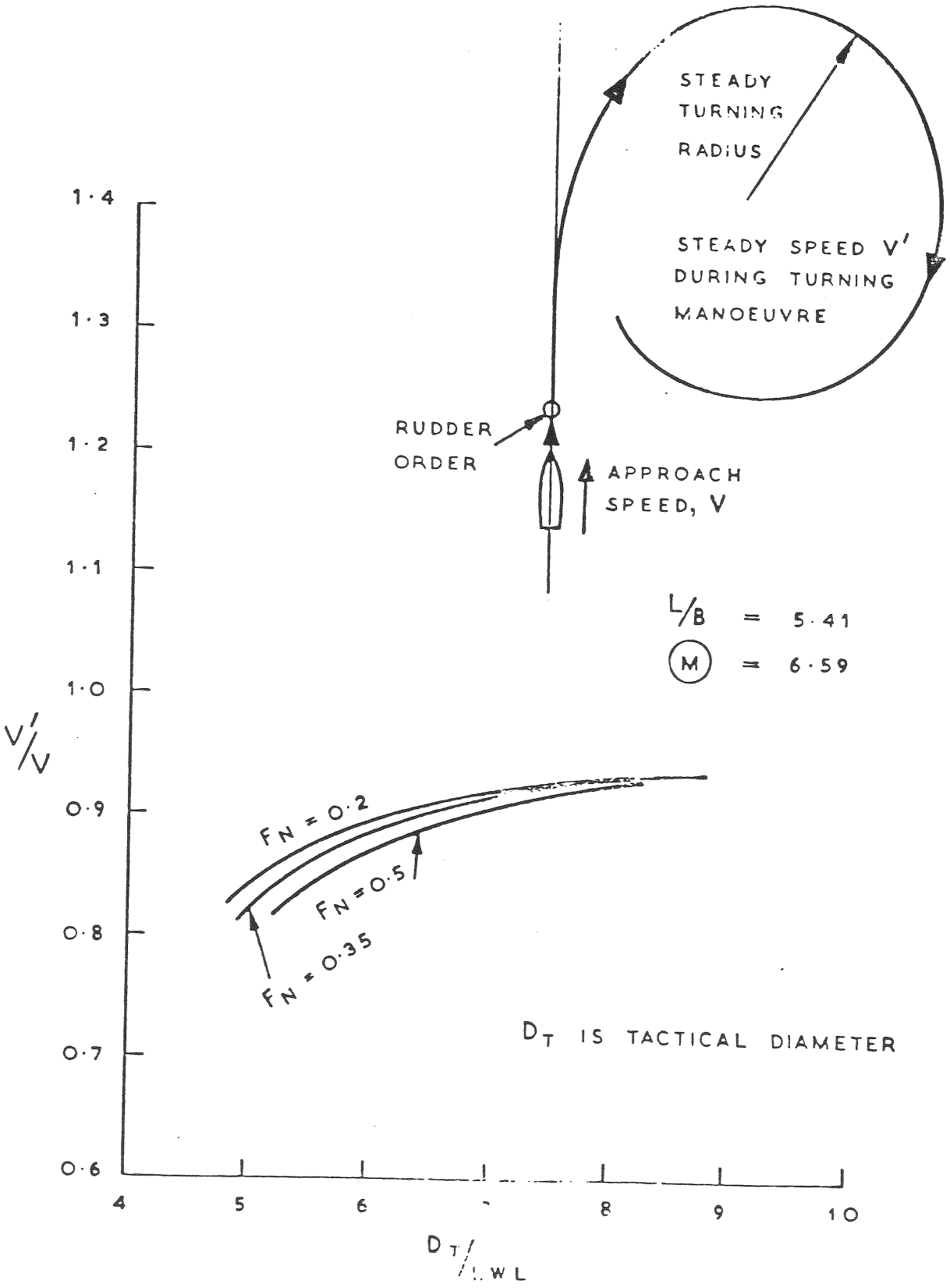

RATIO OF STEADY SPEED IN TURN
TO APPROACH SPEED

FIG. 55.

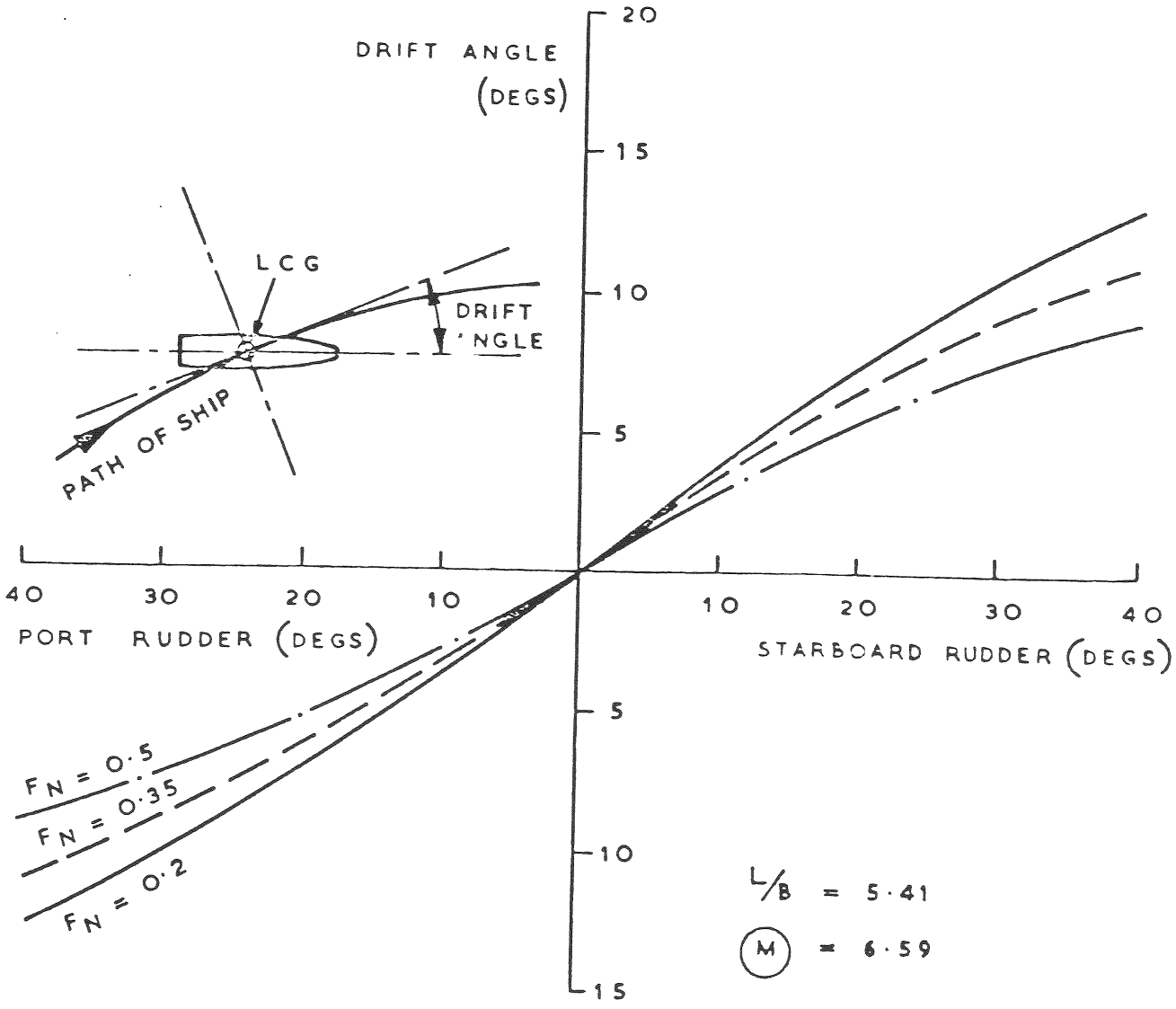

VARIATION OF DRIFT ANGLE WITH RUDDER ANGLE

FIG. 56.

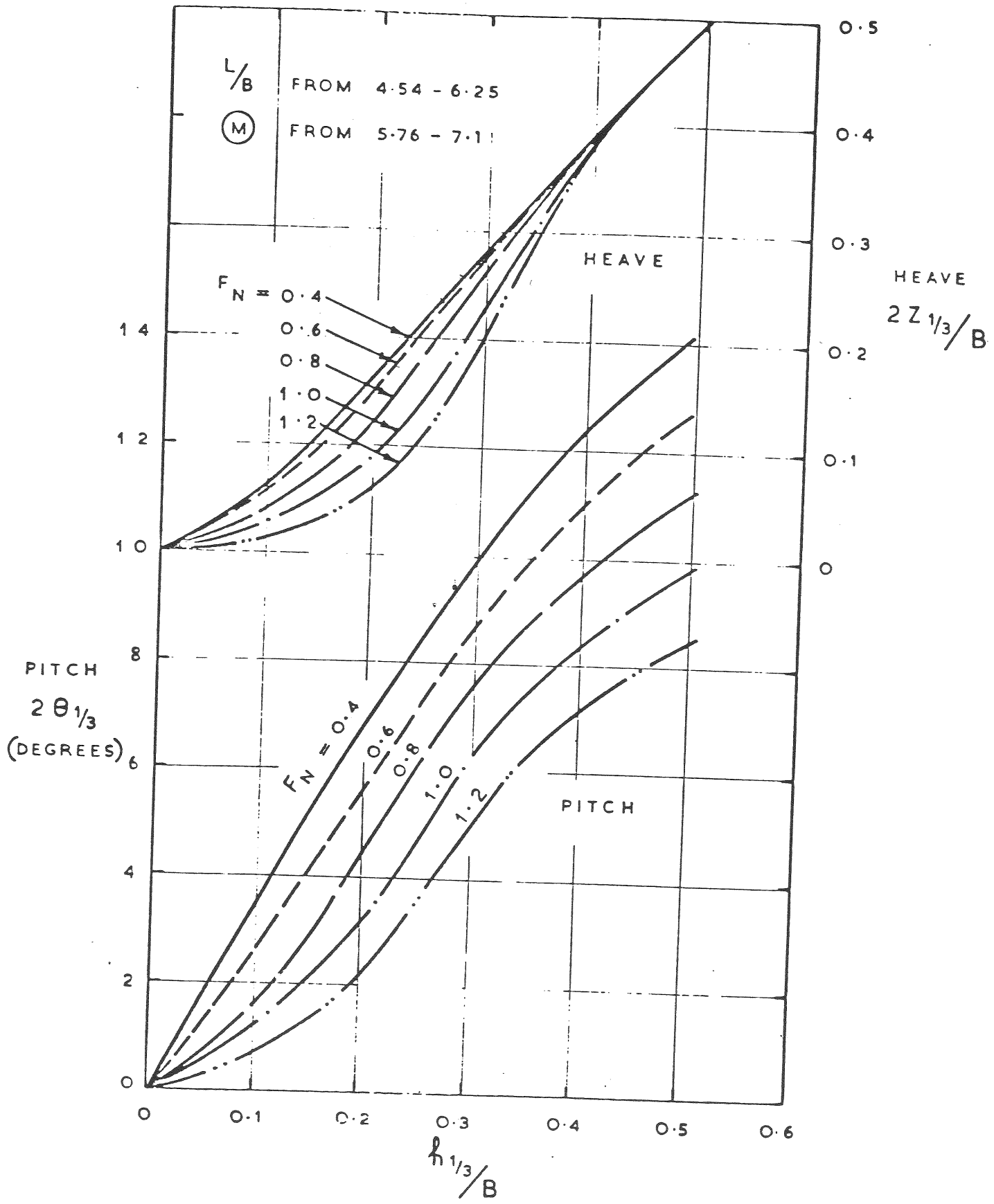

SIGNIFICANT PITCH AND HEAVE AMPLITUDES IN IRREGULAR HEAD SEAS

FIG. 57.

L/B FROM 4·54 – 6·25

(M) FROM 5·76 – 7·1

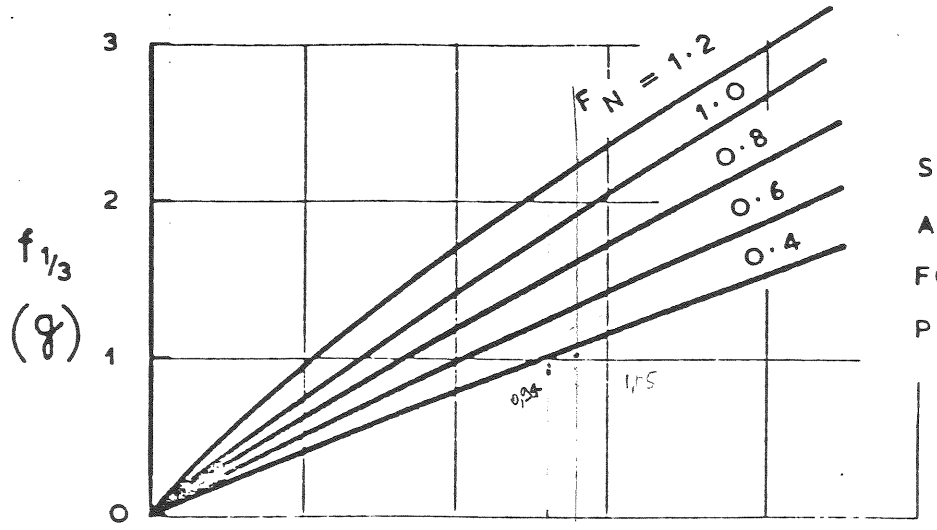

SIGNIFICANT ACCELERATIONS AT FORWARD PERPENDICULAR

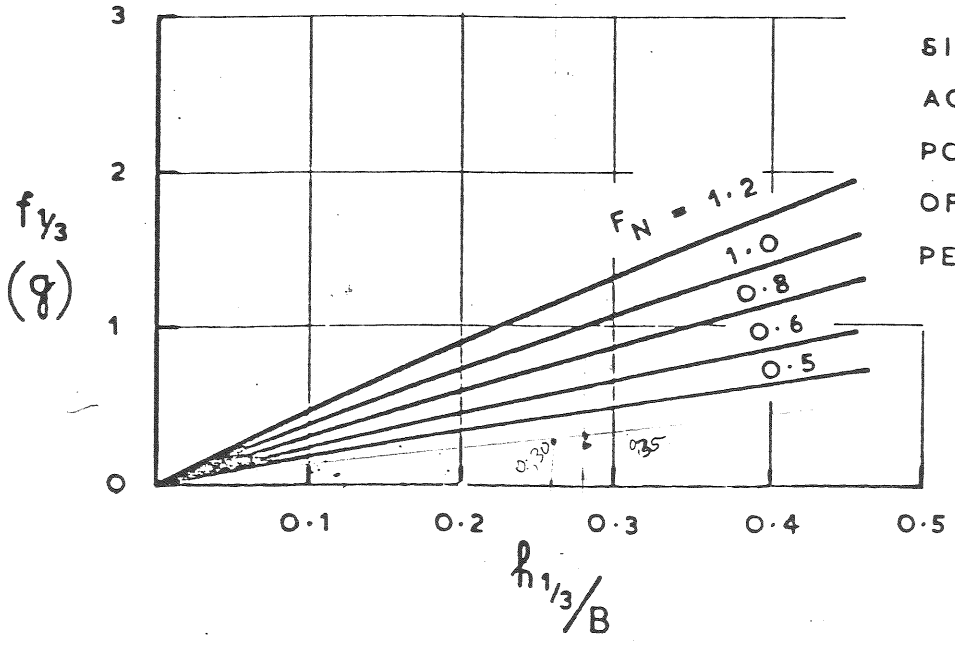

SIGNIFICANT ACCELERATIONS AT POINT 30% L AFT OF FORWARD PERPENDICULAR

SIGNIFICANT ACCELERATIONS IN IRREGULAR HEAD SEAS